AN INTEGRATED MODELLING AND OPTIMIZATION APPROACH FOR HYDROGEN ENERGY NETWORK

A Dissertation

by

CHANGKYU KIM

Submitted to the Office of Graduate and Professional Studies of
Texas A&M University
in partial fulfillment of the requirements for the degree of

MASTER OF SCIENCE

Chair of Committee,	Efstratios N. Pistikopoulos
Committee Members,	Mahmoud El-Halwagi
	Sergiy Butenko
Head of Department,	Efstratios N. Pistikopoulos

August 2017

Major Subject: Energy

ABSTRACT

Issues related to global warming have moved hydrogen into the spotlight as a promising energy carrier. As hydrogen is considered as a promising energy carrier from concerns driven by global warming, the goal of this work was a development and optimization of an integrated modelling and optimization of hydrogen energy network for Texas. To achieve such goal, the hydrogen energy network formulation based on Mixed Integer Linear Programming (MILP) was performed.

In the hydrogen energy network, five raw materials and three electricity potential sources were introduced, and they highly affected on the technology availability when they are depleted. Hydrogen was produced from technologies such as SMR, coal and biomass gasification, and alkaline/PEM/solid oxide electrolysis. The produced hydrogen was compressed or liquefied to be ready for use. The produced hydrogen was sold at $5/kg, and could be transported from one region to other through tube trailers, tanker trucks, tube railcars, and tank railcars to maximize the profit and meet hydrogen demand.

Lastly, some possible scenarios were tested such as discounting electricity price scenarios and limiting raw material availability. When electricity price was reduced, there were technology transitions from SMR to the electrolysis at some geographical regions. Additionally, the electricity price discount triggered an increase in hydrogen autonomy of each geographical region as it decreased the amount of hydrogen transported. When the fossil fuel based raw material availability was gradually reduced over time period according to Horizon 2020, there were increased raw material transportations as the raw materials depleted faster in some geographical regions at certain time periods. The combined scenarios regarding both electricity price and raw material limitation were also tested, and it showed the competence of two technologies, biomass gasification and solid oxide electrolysis, as both required natural gas which was limited.

ACKNOWLEDGEMENTS

I would like to appreciate for my academic supervisor professor Stratos Pistikopoulos that gave me such a great opportunity to develop myself both academically and personally. He provided me endless supports with guidance. Moreover, I would like to thank him that giving me an insight of how to live passionately again.

Additionally, I would like to thank Gerald for guiding and training for the research throughout the whole period. The objective, right target, that you showed me intrigued me hard to keep carry on this program.

Thanks also go to my friends and colleagues and the department faculty and staff for making my time at Texas A&M Energy Institute a great experience.

Finally, special thanks to my family for their amazing supports regardless of my decision. I love you so much for standing there for me and being an anchor of my life.

CONTRIBUTORS AND FUNDING SOURCES

This work was supervised by a dissertation committee consisting of Professor Efstratios N. Pistikopoulos [advisor] and Mahmoud El-Halwagi of the Department of Chemical Engineering and Energy Institute, and Professor Sergiy Butenko of the Department of Industrial and Systems Engineering.

The mathematical formula introduced for Appendix B was provided by Professor Efstratios N. Pistikopoulos and was published in 2011. All other work conducted for this dissertation was completed by the student independently.

There are no outside funding contributions to acknowledge related to the research and compilation of this document.

TABLE OF CONTENTS

LIST OF FIGURES

Page

LIST OF TABLES

Page

1. INTRODUCTION

1.1. Problem Statement

Global warming driven by greenhouse gas (GHG) emissions and urban air pollution has been on the rise. Such concerns having been triggered an energy transition from conventional energy, a major contributor to GHG emission, to alternative energy that is more sustainable. Indeed, alternative energy infrastructures having been continuously suggested to meet both the environmental factors and world energy demand And they showed both could be met by efficient use of renewable energy sources such as wind, solar, and biomass (Li et al., 2008; Liu et al., 2007). An energy transition from the use of fossil fuel to hydrogen is one feasible direction as hydrogen can be produced from renewable sources. Hydrogen is a carbon-free energy carrier with high energy content and low GHG emissions for its energy cycle (Adamson and Pearson, 2000; Hugo et al., 2005). Studies in Figure 1.1 show the projected increase in the number of vehicles and their respective energy source which consequentially show the necessity of hydrogen infrastructural development (National Academy of Engineering et al., 2004).

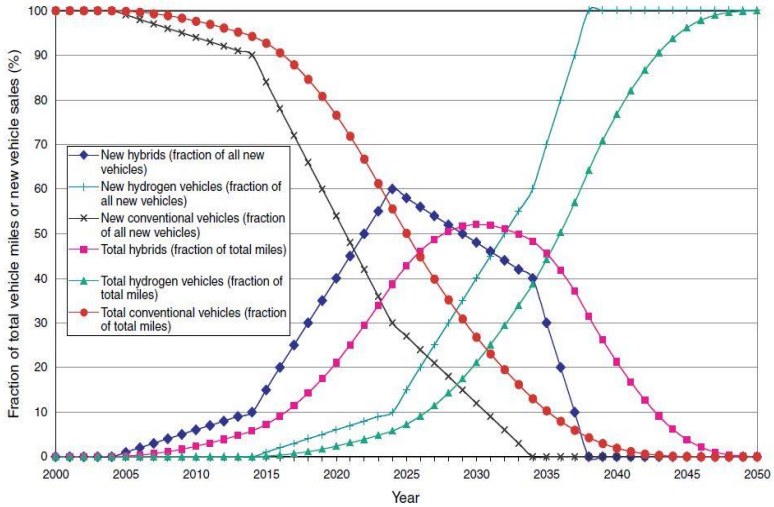

Figure 1.1. Optimistic market scenario regarding a fraction of vehicle sales in the United States (National Academy of Engineering et al., 2004).

There are some challenges with hydrogen infrastructural development, especially as regards optimum hydrogen pathway amid various uncertainties. Uncertainties, such as transportation structure and plant production type between centralized and decentralized production, are hard to be incorporated in the hydrogen infrastructural development (Kim et al., 2008). Additionally, introducing new energy infrastructure may require huge initial capital costs and poor initial period returns so commercial breakthrough for new fueling infrastructure is also required. One approach to reducing high initial capital cost could be the use of already existing infrastructures used for conventional energy infrastructure to hydrogen one. Existing electricity and conventional energy grids can also be utilized to produce hydrogen. Such these methods can relieve huge initial capital costs (Hugo et al., 2005).

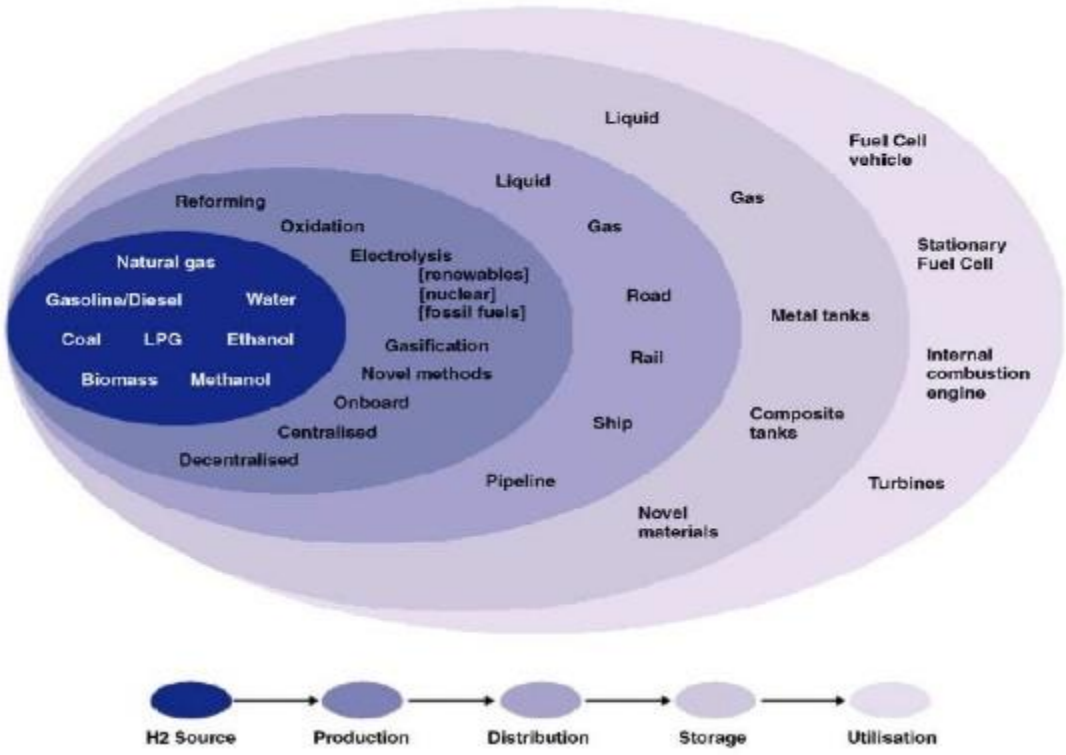

Figure 1.2. Potentially possible technologies within hydrogen infrastructure (Taken from BP hydrogen website)

As illustrated in Figure 1.2 above, hydrogen can be produced from a variety of energy sources. These energy sources including raw materials are converted to hydrogen in different phases through a variety of techniques. Then the hydrogen is stored and transported via feasible options. Specifically, common transportation units such as tube trailer, tube railcar, and pipeline are used for gaseous hydrogen. Tank truck, tank railcar are mostly used to transport liquefied hydrogen. Different network structures are formulated based on the characteristics of geographical cells and their market status by each scenario, and each structure is optimized to have the best solution which satisfies the objective function. Strategic hydrogen infrastructural development requires a great deal of planning because it is affected by market instability and other uncertainties (Kim and Moon, 2008; Li et al., 2008). A mathematical planning tool developed for optimization of chemical centers in UK is used for the integrated hydrogen pathway that is economically viable and sustainable (Liu et al., 2011).

1.2. Objectives

The main objective of this thesis is development and optimization of an integrated supply chain network for the hydrogen infrastructural development in Texas using the tools used for previous studies. The objective could be achieved by doing the followings:

- Formulation of a hydrogen superstructure network using Mixed Integer Linear Programming (MILP) optimization including both continuous and discrete choices of decision variables.
- Scenario studies of hydrogen infrastructure network which reflect possible future governmental policies.
- Environmental impact assessment of the hydrogen infrastructure network through multi-objective optimization.

2. LITERATURE REVIEW

2.1. Literature Review of General Technologies Applied

In the development of hydrogen infrastructural, the types of technology used plays an important role in the structure of the optimal solution. Technologies including steam reforming, electrolysis, partial oxidation, and catalytic cracking reaction are used to produce hydrogen. Among these options, the steam reforming of fossil fuel and water electrolysis with Direct Current (DC) are the most commonly used technologies for hydrogen production. For the steam reforming process, fuels such as methane, methanol, ethanol, and natural gas are used. During steam reforming process, a reaction occurs between the supplied fuel and high temperature, high pressure steam within a reformer (García and Laborde, 1991).

The electrolysis of water is one of the most promising methods to produce hydrogen based on renewable energy source. Two types of electrolysis, Proton Exchange Membrane (PEM) and alkaline electrolyte solution, are most commonly used (Turner et al., 2008). In PEM water electrolysis, water is split into oxygen, protons, and electrons by voltage which is normally higher than the thermo-neutral voltage (Barbir, 2005). Subsequently hydrogen protons pass through the membrane to reach cathode, and the protons are combined with electrons to form hydrogen. In alkaline water electrolysis, two electrodes placed within an electrolyte solution composed of potassium hydroxide or sodium hydroxide (Hu, 2000). The solution transports hydroxide ions to the anode and hydrogen ion to the cathode. Electrons flow from anode to cathode simultaneously to produce hydrogen through combination of hydrogen ions and electrons. Some renewable energy sources, such as wind power and solar power, could be used for both methods because they require electricity to produce hydrogen. However, alkaline water electrolysis is more suitable for real hydrogen infrastructure because most real infrastructures are needed huge hydrogen plants to satisfy the increasing hydrogen demand of region, city, and nation. Additionally,

PEM method is more suitable for localized small scale hydrogen production. A PEM flow diagram is described in Figure 2.1 (Manabe et al., 2013).

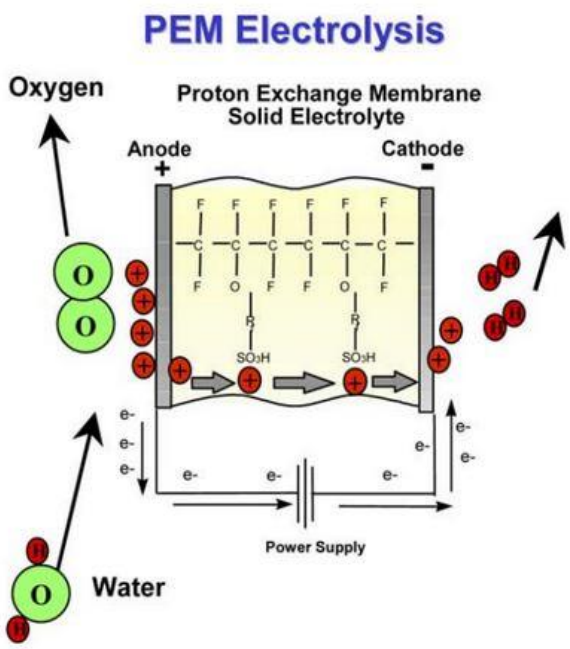

Figure 2.1. Schematic representation of PEM water electrolysis (Manabe et al., 2013).

2.2. Hydrogen Facilities

Hydrogen station in the city of Burbank shows a specific scenario of how hydrogen infrastructure could be realized for vehicles. The hydrogen station is located in Burbank, California, and hydrogen is produced from a natural gas reformer with 108 kg/day capacity. A primary energy source, natural gas, is supplied using 60 psi pressure pipeline for natural gas reformation. Then the produced hydrogen is purified to 99.99% through pressure swing adsorption system with 200 psi. The pure hydrogen is compressed to 435 bar by two diaphragm compressors, each with 2.1 kg/hr capacity, to be stored in hydrogen storage. The hydrogen is fueled at 350 bars for the vehicles with low minimum required pressure

for fueling (< 350 bars). A fact that the hydrogen is fueled to vehicles using pressure difference justifies hydraulic booster compressor with 50 kg/hr capacity which increases the discharge pressure from 350 bars up to 875 bars, and this compressor allows even the vehicle with high minimum required pressure (> 350 bars) to fuel it. In this system, hydrogen is cooled down before it is dispensed into the vehicle because the temperature hugely affects dispensing rate. In this system, hydrogen with chiller at -20 ℃ has fuel dispensing rate of 1.75 kg/min while hydrogen without chiller has 0.25 kg/min. With this hydrogen infrastructure, the Burbank station dispenses average 120 kg hydrogen per month to fuel 41 Fuel Cell Vehicles (FCVs) (Abele, 2015).

Hydrogen station in the city of Santa Monica also has an on-site hydrogen generation infrastructure. The station uses PEM electrolyser for hydrogen production, and it has a capacity of 12 kg/day. Then the produced hydrogen is compressed to 480 bars by diaphragm compressor, and stored into three storages with 52.5 kg capacity. The hydrogen is dispensed at 350 bars. One feature in this system compromises osmosis water treatment, and this system prevents mineral formation on the proton membrane surface. This makes the PEM system more efficient under small on-site hydrogen production. The infrastructure also contains water cooling system and control panel which boosts hydrogen dispensing rate and prevents unexpected malfunction of the system (Abele, 2015).

Another hydrogen infrastructure is in California State University, Los Angeles (CSULA). Hydrogen is produced from HySTAT^{TM}30 alkaline water electrolyzer at 60 kg/day. The produced hydrogen is stored in three storage tanks which have 60kg total capacity at 350 bars. There are compressors compress hydrogen to 350/700 bars using PDC diaphragm and Hydro-Pac Intensifiers respectively. And hydrogen chiller maintains the hydrogen temperature as -20°C for fast hydrogen dispense. Utility support facilities, such as cooling water system and water treatment system, are used to remove generated heat from compressors and to produce deionized water for electrolyzer water feed (Abele, 2015).

Hydrogen production based on wind power is also used for Wind-Hydrogen-Diesel Energy project of Nalcor Energy in Ramea Island, Canada, as shown below in Figure 2.2. Wind power, primary energy source, produces electricity to be used for alkaline water electrolyser to produce hydrogen. The system is mainly composed of hydrogen storage tanks, and ICE electricity generator, alkaline water electrolyser with 162 kW power input, 27 Nm^3/hr capacity and 50% efficiency. Then the produced hydrogen is stored in the tank with 1000 m^3 at 16.2 bars. The stored hydrogen is used for producing electricity when it is needed. Electricity generator for this infrastructure is ICE type with an input power of 250 kW. In addition, there is Energy Management System (EMS) that perform automatic control of infrastructure components, such as wind turbines, alkaline water electrolyser, and electricity generator. The EMS is modelled to prevent possible dangers or unexpected accidents (Gahleitner, 2013).

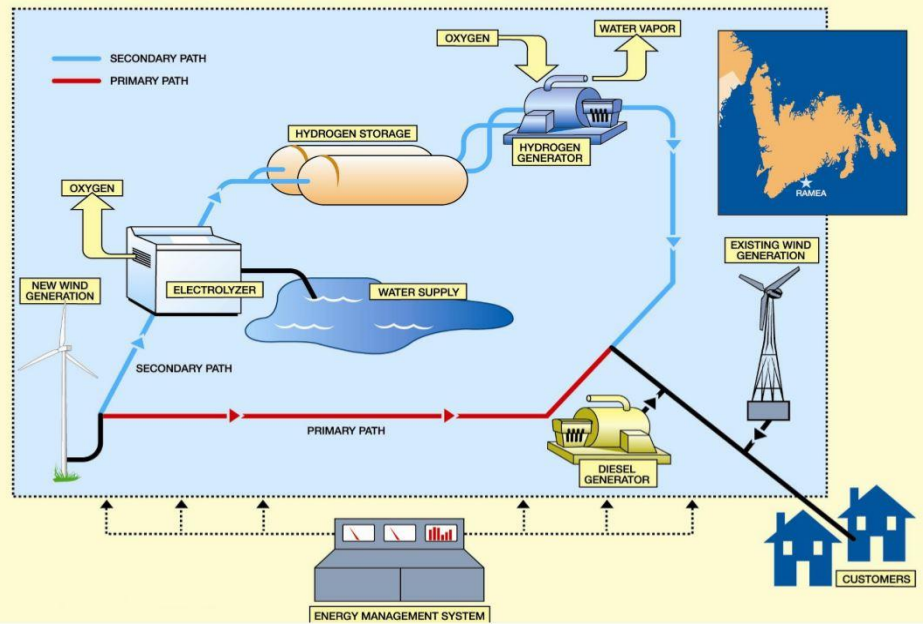

Figure 2.2. Wind-Hydrogen-Diesel energy system in Ramea Island, Canada.

H2Herten application center has one of the most representative hydrogen infrastructure. It is located in Herten, Germany, and produces hydrogen using electricity from wind power and alkaline water electrolysis. In this infrastructure, hydrogen is used for an intermediate

energy storage to ensure continuity of energy supply amid production and demand variabilities. The infrastructure is mainly composed of alkaline water electrolyser, PEMFC, compressor, battery and hydrogen storage. Electricity produced from wind facilities is delivered to alkaline electrolyser with 152 kW power input, 30 Nm^3/hr capacity, and 70% efficiency to produce hydrogen. Then the hydrogen is compressed from 5 bar to 50 bars by the compressor with 30 Nm^3/hr capacity. The compressed hydrogen is stored in the hydrogen storage tank of 22m high, and it can store 5300 Nm^3 or 470 kg of hydrogen. The compressed hydrogen could be used for both producing electricity through PEMFC with input power of 50 kW and delivered to hydrogen fueling station through pipeline or truck delivery. In addition, the compressed hydrogen is also used for ICE with electricity generator to generate electricity. The overall plant efficiency is between 58% and 70%, and it is affected by the amount of heat loss during the process (Gahleitner, 2013; Huss, 2013).

2.3. Hydrogen Infrastructure

Grietus Mulder et al. proposed a hydrogen pathways and infrastructure for European society. They mainly focused on engine efficiency of already existing Internal Combusting Engine (ICE) and Fuel Cell (FC) engine depends on the energy source. They also focused on the emission of carbon dioxide related those kinds of vehicles. The reference case includes the conventional use of gasoline with ICE. In the publication, there were 18 hydrogen pathways. The energy sources used for this study were wind, natural gas, hydropower, hard coal, and oil. Some technologies such as reforming, electrolysis, partial oxidation, gasification, and liquefaction were also used to produce hydrogen. For the distribution of energy source or hydrogen, pipeline, truck vessels, pressure vessels, storage quantity, and storage material were considered. This paper shows a comparison between old-already-existing-car and new-hybrid-car. For the old fuel cell car, the efficiency is not remarkable although it is still way more efficient than the car with gasoline. Specifically, the fuel cell car needed 4.6 kWh of primary energy for 1.64 kWh. But the car with gasoline

needed 6.3 kWh of primary energy only for 1.15 kWh. This shows that the old version fuel cell car already has 2 times better efficiency than the gasoline car. For hybrid cars, fuel cell car only needed 3.4 kWh of primary energy for 1.65 kWh. And the gasoline car needed 4.0 kWh of primary energy for 1.15 kWh. Efficiency for both cases increased but it still shows that the fuel cell car has much higher efficiency than gasoline car. The author suggested two hydrogen penetration scenarios, Top-down and Bottom-top scenarios. The top-down scenario includes hydrogen is made from primary energy sources, and the hydrogen is used to produce electricity in the stationary sector. Even, co-production of hydrogen and electricity would be possible in electric power plants. In this hydrogen production part, the author assumed more hydrogen will be produced from fossil fuels with natural gas, hard coal, and residual oil. To transport the produced hydrogen, the author suggested half liquid phase and half gaseous form. Although such this rough estimation, the assumed hydrogen pathways occur only 50% of the reference carbon dioxide emissions. This is possible with the carbon capture system of production and distribution companies. However, it cannot affect the carbon dioxide emission of the transport sector with truck. And the author emphasized the importance of the hydrogen handling part of transport sector because it can cancel all emission gains derived from reducing carbon dioxide. The author prefers compressed gaseous hydrogen to liquefied hydrogen. To sum up, the hydrogen pathway can be more efficient than the original pathway for conventional energy sources when the pathway comes with fuel cell. And the carbon dioxide capture system and appropriate storage for that gas will highly contribute to the reduction of carbon dioxide (Mulder et al., 2007).

A hydrogen infrastructure is designed and optimized by Zheng Li et al. The model is based on China. In the hydrogen infrastructure, natural gas, coal, biomass, and electricity from renewable sources were used for primary energy sources. And hydrogen production technologies, such as natural gas compression, SMR, gasification, and liquefaction were used. Transportation units, such as pipeline, tank, tube trailer, gas & liquid dispensing units, and electric network units were used to distribute the produced hydrogen. A

superstructure that compromises all units is shown below in Figure 2.3. For the optimization, multi-objective MILP was used, and it includes maximization of Net Present Value (NPV) and minimization of Well-to-Wheel Green House Gas (WTW GHG) emissions as their objective functions. A goal of such MILP problem with both equality and inequality constraints is finding a set of Pareto Optimal solutions, which is a set of supply chain strategies. Such Pareto Optimal solutions cannot be improved without any partial worsening of existing objective targets.

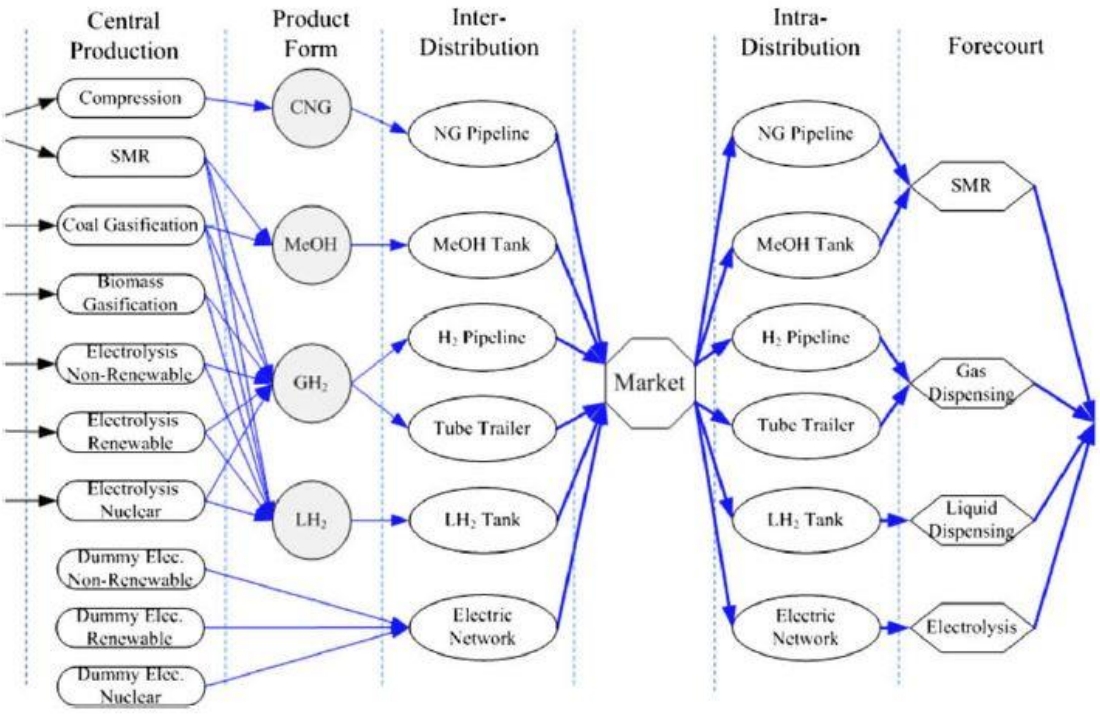

Figure 2.3. Hydrogen superstructure for the China case study (Li et al., 2008).

The author suggested two Pareto Optimal curves for both scenarios, one with MeOH (Scenario A) and the other without MeOH (Scenario B). The scenario A implies that the MeOH works as an intermediate energy carrier and used in distributed on-site spots. The scenario B does not care about the intermediate energy carrier. In that scenario, hydrogen is directly produced from both centralized plant and distributed spots. The two Pareto Optimal curves show the sets of optimal trade-off results between the two objective

functions, and the scenario A shows the bigger economically feasible regions based on higher NPV than the scenario B at same WTW GHG emissions. Two other Pareto Optimal curves including sensitivity analysis regarding hydrogen price are also described, and the curves show that the relationship between hydrogen price and NPV is linear. It represents that the NPV increases when hydrogen price increase, and vice versa for the reverse case (Li et al., 2008).

Jiyong Kim et al. suggested the hydrogen supply chain under demand uncertainty in South Korea. The authors mainly compared efficiency of centralized and decentralized hydrogen production. In this case study, primary energy sources such as coal, natural gas, nuclear energy, biomass, wind, and solar are used. To produce hydrogen, SMR, gasification, liquefaction and electrolysis technologies were used. To transport the produced hydrogen, tanker truck, tube trailer, and pipeline were considered. There are 7 possible infrastructure scenarios which are combined with production, storage, and distribution methods. And each scenario is tested its feasibility to satisfy the demand of each region in South Korea. To measure the demand of each region in South Korea, Long-range Energy Alternatives Planning (LEAP) system is used. It helped to account how energy is consumed, converted, and produced in each region. Additionally, because of the Btu tax which regulates the amount of carbon dioxide, reduction of carbon dioxide is also an issue for this study based on minimizing both capital costs and operating costs. Because of extremely high population density in some regions of South Korea, especially in some regions, building hydrogen production plant is infeasible under the aspect of minimizing capital costs. So the authors suggest building those facilities in adjacent region then transport hydrogen to those high population density areas. What is more, construction of hydrogen pipeline for transportation is not feasible for South Korea because of its geographical region, and truck delivery looked more feasible for this case study. For this case study, although SMR takes more costs than electrolysis, it can have bigger capacity, and it means the truck does not have to travel a lot. This aspect also could be combined with the preference of liquefied hydrogen than compressed gaseous hydrogen with same reason. The final network

structure of liquefied hydrogen production via production and transportation units is shown below in Figure 2.4.

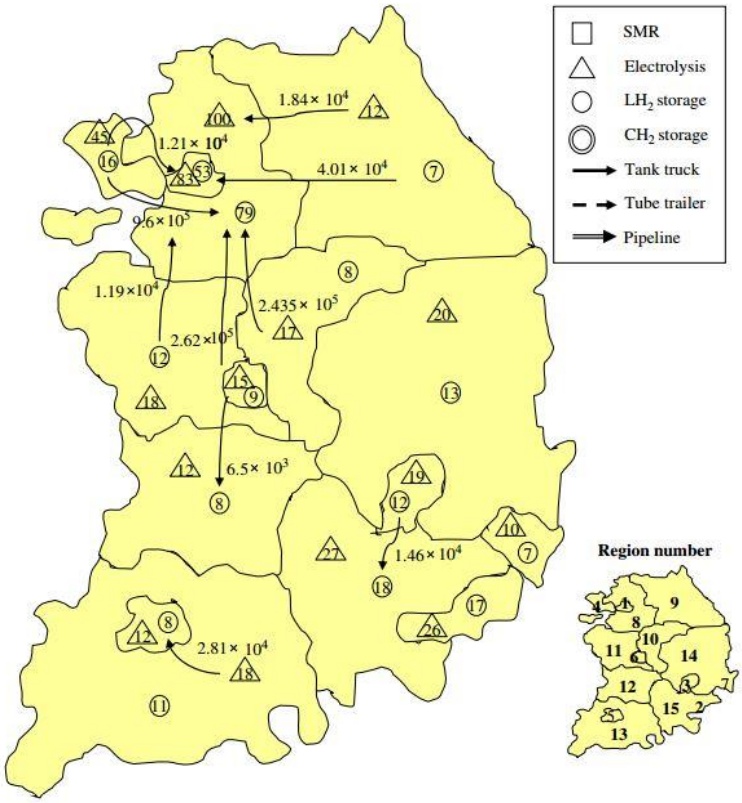

Figure 2.4. Network structure of liquefied hydrogen produced via production and transportation units (Kim et al., 2008).

Furthermore, because of uncertainty, this scenario may have some extra costs including some Btu tax and miscellaneous costs come from unexpected situation. However, this scenario could be preferred based on the aspect of geological feature of South Korea, economical aspect, and environmental aspect. Lastly, this conclusion was possible because there was an assumption that technology progress ratio is 85% now. Because it is not expected that the technologies will experience tremendous development, the hydrogen infrastructure mentioned above is promising (Kim et al., 2008).

For the same target area, the infrastructure is optimized again by multi-objective MILP. The objective functions are consist of the minimization of the total network cost and the

maximization of safety level. To determine the strategy, possible incident criterions for hydrogen activities are normalized, then quantified to calculate the risk size based on the consequence of incidents and their frequency. From such multi-objective optimization, a set of pareto optimal solutions are determined and used for a decision-making curve, and it is presented in Figure 2.5 below. The decision-making curve shows a trend of increasing total daily cost when the total relative risk is decreasing (Kim and Moon, 2008).

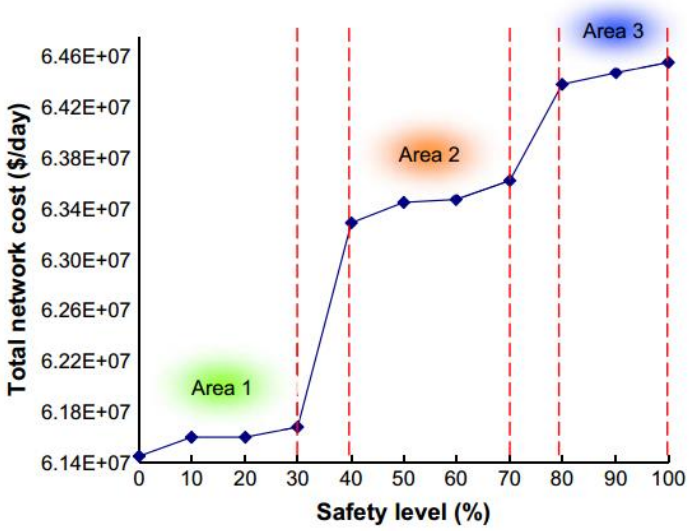

Figure 2.5. Decision-making curve (Kim and Moon, 2008).

As California has been known worldwide for its strict environmental policies, Michael A. Nicholas et al. suggested detailed analysis of California hydrogen highway network for future energy distribution. In this paper, hydrogen station availability is a key factor of the network. The hydrogen station availability contains the travel time of customers to get reach to the nearest hydrogen fuel station. It affects the number of stations required for each region, which means capital costs. The author used regional refueling profiles of a few regions of California as the model's parameters and it is shown below in Table 2.1.

Table 2.1. Regional refueling profiles in California case study

Area	Population in Urban Center	Urban Area (mi^2)	Urban Density (people/mi^2)	Avg. Tract Size (mi)	Number of Urban Stations	Number of People per Station	Avg. Minutes to Closest Station
LA	14,340,402	2,645	5,421	0.9	3,355	4,274	1.60
SF	5,474,575	1,111	4,927	0.96	1,246	4,394	1.72
SD	2,538,862	606	4,189	1.1	572	4,439	2.20
SAC	1,247,224	331	3,786	1.21	304	4,103	2.24

From their analysis, regional variations among the targeted regions should not be neglected because those factors can change the optimal results. Specific road, station, and population distribution could be varied for each region from the generalized data. Normally, decision of how many stations should be located is done based on the population density of the region. To compare the percentage of stations between two regions, it is necessary to check the population density is relatively constant in both two regions because it can show how the other variance, such as road distribution, can affect to the number of required stations. The author also suggested the issue of travel time to the station. There is a trend that population denser region takes less time than the region with less population to get to the station, when the number of stations are same for both regions. (Nicholas and Ogden, 2006).

S.K. Kamarudin et al. suggested the optimization of hydrogen infrastructure in Peninsular Malaysia. To measure energy demand, the authors used two methods. The first one used total vehicle numbers and average total distance traveled. And the second one was an investigation of current gasoline and diesel supply from surveys on local stations in Peninsular Malaysia. The second method showed more realistic scenarios so it was used for the optimization of the hydrogen infrastructure. The hydrogen demand for the second method was 2,666,983 kg/day. In this infrastructure, natural gas was used as the primary energy source because it had the smallest facility fixed cost than any other energy sources, such as biomass and coal gasification, and water electrolysis. Natural gas was reformed through steam reformation method to produce hydrogen. Then the produced hydrogen was delivered via tanker trucks to achieve the minimum cost. In this study, liquid hydrogen

was selected because it can minimize the number of travel required for transportation, so the total cost was also minimized. Specifically, the liquefied hydrogen production cost ($1.52/kg$H_2$) was much higher than the one of compressed hydrogen ($0.8/ kg$H_2$). However, transportation cost for compressed hydrogen ($0.39/kg$H_2$) was almost 10 times more expensive than the one for liquefied hydrogen ($0.04/kg$H_2$) (Kamarudin et al., 2009).

D.Joffe et al. did a hydrogen infrastructure modelling for buses in London. In this infrastructure, SMR and electrolysis are mainly used. However, SMR requires a minimum of 30% constant load to prevent mechanical damage so it should not be used until there is sufficient hydrogen demand to meet 30% minimum load. Operability of electrolyzers is highly affected by the electricity prices and it is desirable to be used during the nighttime since electricity price at night is cheaper than the peak-time price. As a result, bus refueling based on electrolyzers would also occur during nighttime to minimize the storage cost through fueling right after the hydrogen is produced. Bus refueling based on SMR will occur when there is sufficient hydrogen demand, and it is required to produce hydrogen constantly without shutting it down because it takes a long time to shut it down, and it can get some damage from shutting down the process. Once SMR is operated, it can give some economic benefits but buses should visit the station both day and night to minimize the storage costs. To decide the spots for stations, some factors such as total number of buses and distances that will be driven, and storage availability for each station should be considered (Joffe et al., 2004).

A fuel infrastructure pathway regarding technology transition of hydrogen production in Norway was suggested by Christoph Stiller et al. They generated hydrogen demand scenarios and station networks based on Geographical Information System (GIS) until 2050. Specifically, they predicted that hydrogen produced as by-product of existing plants of current technology mainly used for their infrastructure until 2020. However, the main hydrogen production method would be NG SMR and electrolysis when hydrogen demand increases. Such technology transition is described below in Table 2.2. The NG SMR will be composed of central NG SMR (67,000 t/a) and onsite NG SMR (120,480 t/a), and electrolysis also composed of central electrolysis (580 t/a) and onsite electrolysis

(16,120,480 t/a). NG SMR will more suitable for highly populated regions and onsite electrolysis is for sparsely populated regions. Hydrogen will be produced and delivered only as a gaseous form to satisfy the assumption, that all data is based on HyWays project which only used gaseous hydrogen. Delivery method will also be changed from trailer (0.45 t/trailer) for initial stages to pipeline (12", 7200 t/a) for later states. WTW GHG emissions changes from 63 g/km to 32 g/km by 2050, which is not promising. This is because the infrastructure will mainly use natural gas for its energy source without carbon capture. It is highly anticipated that the amount of emission will be decreased if it is with a carbon capture technology (Stiller et al., 2010).

Table 2.2. Technology transition over time for hydrogen production

Technology	2010	2015	2020	2025	2030	2035	2040	2045	2050
Electrolysis	2%	7%	24%	10%	90%	90%	22%	42%	60%
NG-SMR	0%	0%	0%	80%	78%	83%	73%	55%	37%
By-product hydrogen	98%	93%	76%	10%	13%	8%	5%	4%	3%
Biomass gasification	0%	0%	0%	0%	0%	0%	0%	0%	0%

Wen Feng et al. suggested a hydrogen infrastructure for fuel cell vehicles in Beijing, China. They suggested 11 feasible plans based on their current production, storage, and distribution technologies. Then they figured out best scenarios for energy efficiency, environmental impacts, and economic performances. For this case study, China uses coal as its primary energy source to produce electricity. Ironically, huge amount of pollutant generated when hydrogen is produced from electrolysis because the electrolyzer consumes electricity made from coal. Specifically, it causes pollutants (63 kg pollutants/kg H2) from electrolysis under view of the whole life cycle from electricity production to hydrogen production. So electrolysis is excluded from an optimized environmental performance scenario. Instead, the scenario composed of NGSR, pipeline, and gaseous hydrogen shows best environmental performance as 16 kg pollutants/kg H2. And the scenarios composed of coal gasification, pipeline/truck delivery, and gaseous hydrogen shows best energy efficiency scenario as 30%/29%. This means these scenarios requires minimum total

energy consumption as low as 166.41/161.68 MJ for 1 kg of hydrogen. The best scenario in economic performance is composed of methanol synthesis from natural gas, truck delivery, and methanol reforming onboard. It is because this scenario has low capital, operating, and management costs which can overcome high material costs. This scenario shows $2.11/kgH2. However, the scenario composed of coal gasification, truck delivery, and gaseous hydrogen also shows values close to optimum, $2.12/kgH2. This cheap hydrogen price is driven by low capital costs through truck delivery, not pipeline construction. To summarize, the best hydrogen infrastructure scenario for China is composed of coal gasification, truck delivery, and gaseous hydrogen. This result could be possible from extremely cheap coal price in China as it is the biggest coal production country (Feng et al., 2004).

Shane Stephens-Romero et al. demonstrated a novel assessment methodology of hydrogen infrastructure deployment. To produce hydrogen, they considered SMR, electrolysis from renewable sources, petroleum coke, coal gasification for a centralized system. And SMR, High temperature fuel cell (HTFC) cogeneration with natural gas, electrolysis from both grid and renewable sources are considered for distributed system. Options for hydrogen distribution were truck delivery of tube trailer/liquid tanker, and pipeline. The author assumed hydrogen will be dispensed as liquefied hydrogen or 140/350/700 bars of gaseous hydrogen. There are 5 infrastructure scenarios divided by time frame from 2015 to 2016. In 2015, early stage, NG SMR is used for centralized hydrogen production and NG SMR, HTFC cogeneration, electrolysis using grid/renewables are used for distributed production system. In this stage, hydrogen is mostly distributed using tanker trucks after hydrogen is liquefied. But the hydrogen is mostly dispensed as a pressurized gas under 350/700 bars. There are two scenarios for 2030, which weighted fossil fuel and renewables respectively. In this scenario, weight on NG SMR is decreased but the usage of petroleum coke is increased, such as 20% weighted for weighted fossil fuel scenario and 10% for renewable scenario. Hydrogen is dispensed as pressurized gas form although it is distributed through tanker trucks after liquefaction. There are also two scenarios for 2060, and they contain reduction of NG SMR and petroleum coke usage but an increase of coal gasification. In

specific, weighted fossil fuel scenario has 30% coal gasification and 10% coal gasification for renewables. Hydrogen is distributed as 40% tanker truck after liquefaction and 60% gaseous hydrogen pipelines, and it is dispensed only 140/350 bars of the pressurized gas form. The author suggested that those 5 scenarios show much less pollutant emissions than conventional vehicles. Specifically, the fossil fuel weighted and renewable weighted scenarios yield 64.2% and 70.2% GHG emissions reduction except for SOx by 2060 respectively. In fact, emission of SOx is increased, and this is because of the increased amount of petroleum coke usage. The usage of tanker truck also contributes to the SOx emissions. The author also discussed water consumption for each hydrogen production technology. He mentioned petroleum coke gasification and coal gasification require 17.9 gals water/kgH_2 and 24.2 gals water/kgH_2 respectively. However, NG SMR and electrolysis require only 6.3 gals water/kgH_2 and around 3 gals water/kgH_2. This factor highly supports author's observation which the hydrogen infrastructure relies heavily on renewable sources for optimal results. Additionally pipeline distribution method can help pollutant emissions under environmental aspect. However, increasing the usage of petroleum coke and coal would contribute to high pollutant emissions during the process so carbon capture should be considered to realize those sources (Stephens-Romero and Samuelsen, 2009).

A near-term hydrogen infrastructure including economic analysis was suggested by Tim Brown et al. for California. They suggested a detailed economical hydrogen infrastructure for fuel cell vehicle in California. There are 18 existing hydrogen stations, and they get hydrogen from the centralized SMR facilities. Authors suggest 3 possible scenarios, 1. Additional 50 liquefied or gaseous hydrogen stations, 2. Additional 50 liquefied hydrogen stations, and 3. Additional 50 gaseous hydrogen stations. Each scenario is analyzed depends on FCV deployment rate. The FCV deployment rates based on historic HEV sales are shown below in Figure 2.6.

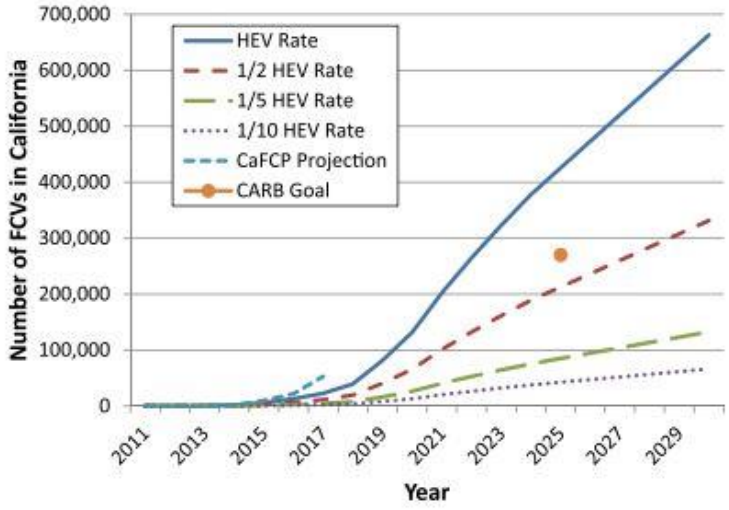

Figure 2.6. FCV deployment rates based on historic HEV sales (Brown et al., 2013).

Scenario 2 evaluated that it is unlikely possible because it requires large capital costs with relatively low and slow throughput. And scenario 3 is also evaluated as unlikely possible because it is expected that it will have the lowest potential profits because of high fixed operation and management cost and relatively low delivery capacity (400kg H_2/day) than liquefied hydrogen delivery capacity (800kgH2/day). The scenarios are based on the assumptions that liquefied hydrogen station has $2 MM capital costs, 400kgH2/day dispensing capacity, $0.1 MM/yr operating and maintenance costs, and gaseous hydrogen station has $1 MM capital costs, 180kgH_2/day dispensing capacity, $0.1 MM/yr operating and maintenance costs. For the realistic plan, scenario 1, shows that the hydrogen infrastructure is still can be profitable although it has FCV deployment rate as only 20% of historic Hybrid electric vehicle (HEV). Specifically, the scenario requires $64.5 MM total financial supports until 2021 for its initial stage preparation, such as building other 50 hydrogen stations. However, it shows the infrastructure can be profitable from 2019, when nearly all hydrogen stations are profitable. Additionally, the total potential profit for this scenario is $125.4 MM until 2028. The total 68 hydrogen stations show that this hydrogen infrastructure is eventually profitable with FCV deployment rate as low as 10%.

However, hydrogen cost gap occurred among stations because different transportation costs depends on delivery distance. The cost range is \$7.77/kg H_2 to \$19.14/kg H_2, and this means a hydrogen station network design is critical for the financial success of this model (Brown et al., 2013).

Maria del Mar Arxer et al. showed Helcules project which contributes to hydrogen infrastructure. The goals for this project are 1.Evaluate an integration of industrial electrolyser in an intermittent energy generating environment, 2.Increase standard pressure of industrial hydrogen storage up to 400 bars through setting uninterrupted electricity supply basis for electrolysis plant and hydrogen compressor, 3.Design hydrogen dispenser to achieve fast refueling and availability for any demand, and 4. Design a simple, safe, and reliable hydrogen refuel operating system. To achieve the goals, the project contains a series of operational modules connected to a high pressure storage tank to dispense hydrogen at 350 bars. So hydrogen generation and vehicle refueling could be performed quickly. To achieve 400 bars of hydrogen storage, hydrogen station will be designed with compression system to dispense hydrogen faster. A control panel will be added to the hydrogen station to activate the whole process, and the control panel will be composed of microcontrollers, emergency stoppage device, valves, circuit breakers, and start-up devices. This infrastructure will mainly be operated by photovoltaic energy and water, and those sources are expected to provide more than 100kWe which is needed to generate 1kg H_2/hr at 400 bars. The water electrolyzer is expected to have 70% efficiency when it is continuously operated, and its energy consumption would be at most 5.25kWhN/m^3. Hydrogen production cost from photovoltaic energy is expected to be \$3.13 N/m3. To calculate hydrogen production cost from water electrolysis, other factors will be discussed such as water quantity, quality, purification costs, and water losses through purification process (Arxer and Martínez Calleja, 2007).

Brian Casey Langford et al. showed a medium sized transit agency for the fuel transition from conventional to hydrogen in Knoxville Area Transit. This infrastructure had planned to supply hydrogen fuel for its bus transit. Hydrogen produced through NG SMR and electrolysis with the cost of \$4.17~\$4.82/kg H_2 and \$6.61~\$6.66/kg H_2 respectively. The infrastructure requires maximum conversion of 132 bus fleets from conventional technology to hydrogen one. Total hydrogen storage capacity required to satisfy the demand is 1184 kg. Based on the assumption that each bus will be refueled on average every three days, the infrastructure will require 6.6, 3.3, and 2.2 hr/day of refueling for 1,2, and 3 dispenser cases. Their Geographical information system (GIS) shows that location of hydrogen station is also crucial because it can promote technology, supply, and demand access to hydrogen. Specifically, this infrastructure can provide ten-mile-radius-access to 86% to the Knox County population. The strategic zones used for this infrastructure is described below in Figure 2.7 (Langford and Cherry, 2012).

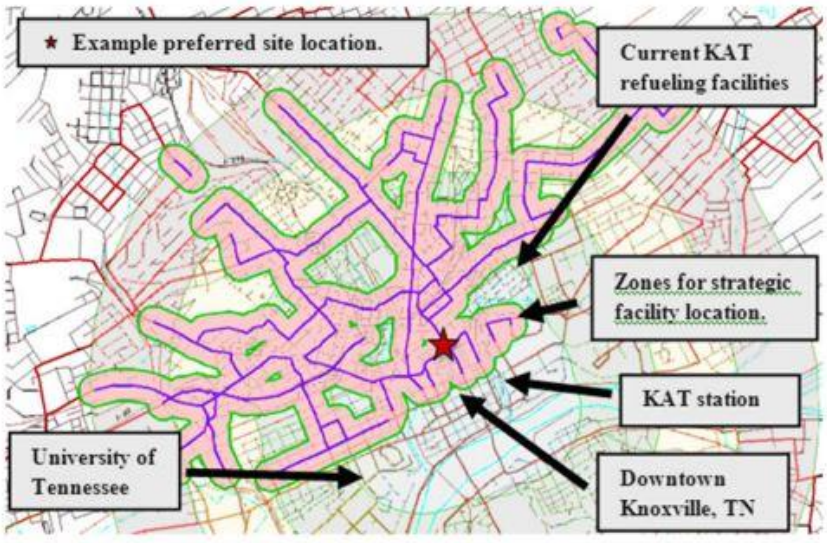

Figure 2.7. Strategic locations of refueling stations (Langford and Cherry, 2012).

Jenn-Jiang Hwang suggested a hydrogen pathways for fuel cell vehicles in Taiwan. The author showed six hydrogen pathways including different technologies using both renewable and non-renewable energy sources, such as natural gas SMR, corn ethanol SMR, alkaline water electrolyzer using grid electricity or solar electricity, and coal gasification with/without carbon sequestration. Among those pathways, electrolyzer using solar electricity method requires a minimum energy, 70MJ/kg H_2, to produce hydrogen with 63.3% process efficiency. Although NG SMR method also shows similar required minimum energy level, 90MH/kg H_2, it has 15 kg GHG/kg H_2 emissions while solar electricity based electrolyzer has only 0.2 kgGHG/kg H_2 emissions, and it has lower efficiency, 56.3% than the solar electricity method. It is evaluated that corn ethanol SMR method is not promising because of high energy requirement, 335 MJ/kg H_2, and high GHG emissions, 17 kgGHG/kg H_2, with only 26.6% efficiency. However, coal gasification could be considered as a competitor of solar energy method because it also shows low-level energy requirement, 120 MJ/kg H_2, and low GHG emissions, 6 kgGHG/kg H_2 although it has relatively low process efficiency of 50.5%. Hydrogen cost from each pathway shows if they are feasible or not. Among the six pathways, only NG SMR method could reach to the hydrogen threshold cost region, \$2~\$4/gal H_2. It is expected that hydrogen cost from NG SMR method will be slightly lower than \$4/gal H_2 at 2011. In the case of alkaline water electrolyzers and corn ethanol SMR, their cheapest hydrogen cost is around \$4.8 and \$4.4/gal H_2, but they can contribute to decreasing the pollutant emissions. As a result, the author says NG SMR is suitable for the initial FCV stages because it can produce cost-competitive hydrogen. After initial stages, technology transition from NG SMR to water electrolyzer or corn ethanol SMR should be considered to make an impact on GHG emissions. Coal gasification is excluded from the candidates because it requires very high feedstock preparation cost so WTW energy consumption is too high (>7000 Btu/mile) (Hwang, 2013).

I. Bartolozzi et al. explained hydrogen infrastructure in Tuscany, Italy, and its environmental impacts through a comparison between fuel cell vehicles (FCV), battery electric vehicles (BEV), and internal combustion engine vehicles (ICEV). In the

infrastructure, wind and biomass sources were used to produce hydrogen by electrolysis or direct separation of hydrogen from biomass gasification syngas. CML2000 method was used to evaluate the environmental impact of each technology through analyzing 10 categories, such as abiotic depletion, acidification, eutrophication, global warming, ozone layer depletion, human toxicity, freshwater aquatic eco-toxicity, marine aquatic eco-toxicity, terrestrial eco-toxicity, and photochemical oxidation. The impact assessment results based on CML2000 method is explained below in Table 2.3. The symbol B, W, IT, BE, WE, and BS stand for biomass, wind, Italian electricity mix, electrolysis supplied with biomass gasification, electrolysis supplied with wind electricity, and direct separation in biomass gasification respectively.

Table 2.3. Impact assessment results based on CML2000 method (Bartolozzi et al., 2013)

Impact category	Units	BEV_B	BEV_W	BEV_IT	FC_BE	FC_WE	FC_IT	ICE_BS
Abiotic depletion	kg Sb eq	0.17	0.19	0.27	0.36	0.23	0.67	0.38
Acidification	kg SO2 eq	0.19	0.16	0.21	0.42	0.19	0.49	0.25
Eutrophication	kg PO4 eq	0.1	0.09	0.10	0.12	0.057	0.12	0.08
Global warming	kg CO2 eq	22.07	24.24	35.65	53.32	33.77	96.38	50.60
Ozone layer depletion	kg CFC-11 eq	1.78E-05	1.84E-05	1.86E-05	1.38E-04	1.35E-04	1.40E-04	2.04E-05
Human toxicity	kg 1,4-DB eq	68.66	66.62	69.79	53.71	41.54	57.28	40.85
Fresh water aquatic eco-toxicity	kg 1,4-DB eq	23.24	21.90	24.13	20.89	14.63	23.69	13.09
Marine aquatic eco-toxicity	kg 1,4-DB eq	56382.3	53214.7	58685.3	43554.7	29006.2	50859.2	28719.2
Terrestrial eco-toxicity	kg 1,4-DB eq	0.22	0.22	0.29	0.26	0.19	0.47	0.26
Photochemical oxidation	kg C2H4 eq	-0.014	0.008	0.01	0.056	0.009	0.021	0.006

Based on the CML2000 method, BEV with electricity from biomass gasification, the wind, and existing electricity mix showed that BEV is less harmful than FCV. Additionally, BEV cases require less non-renewable fossil energy use than FCV and ICEV for the whole process. These results comes from the facts that the hydrogen production technology from renewable energy still has low efficiency, and BEV scenario does not require storage and distribution phase. Such no need for storage and distribution facility heavily contributed to BEV scenario has better environmental performance (Bartolozzi et al., 2013).

3. SUPPLY CHAIN NETWORK DESCRIPTION FOR TEXAS CASE STUDY

3.1. Background

Texas, the biggest state in the United States except for Alaska, has the biggest carbon dioxide emissions among the states. From EIA database, The total carbon dioxide emissions from Texas was 642.0 million metric tons in 2014. This is not only because numbers of conventional plants, but also a lot of carbon dioxide comes from the conventional internal combustion engine vehicle (ICEV). Such data triggers some concerns related to global warming and accelerates the needs of energy transition from gasoline to more sustainable energy.

Table 3.1. Total carbon dioxide emissions by state (Taken from EIA website)

Rank	State	Total carbon dioxide emissions (MM tons)
1	Texas	642
2	California	358
3	Pennsylvania	245
4	Illinois	234
5	Ohio	232
6	Florida	228
7	Louisiana	218
8	Indiana	207
9	New York	170
10	Michigan	163

Currently, hydrogen is highly considered as a promising alternative energy source to contribute to the global warming problems. Hydrogen is a carbon-free energy source, and

it has extremely low greenhouse gas emissions throughout its energy cycle (Hu, 2000; Li et al., 2008).And, it is even highly anticipated to be mainly used for transportation industry including fuel cell vehicles (FCVs) in near future terms instead of currently existing ICEVs, especially with a combination of government programs (Cannon, 1994).

3.2. Problem Formulation

The hydrogen energy network modeling problem in this study could be formulated as given conditions and objective to be determined through optimization process as below:

- Given
    - Time horizon
    - Geographical locations
    - Hydrogen demand over a given time horizon
    - Investment cost
    - Technologies
    - Capacity constraints
    - Environmental constraints

- Objective that determines the optimum configuration that
    - Maximize the net present value (NPV)
    - Minimize the environmental impact
    - Maximize the NPV and minimize the environmental impact simultaneously

The objective of this study is to formulate the hydrogen energy network of Texas and find the optimal point that minimizes both total cost and environmental impact. Such this energy network could be modelled through Mixed Integer Linear Programming (MILP)

including both continuous and discrete choices of decision variables. The information for the given conditions is described in the later part of this chapter, and the methods used for the optimization would be introduced in the next chapter, supply chain network optimization and operation strategy.

3.3. Hydrogen Energy Network Superstructure

For this study, four raw materials, biomass, coal, natural gas, and water are used to produce hydrogen with the electricity comes from hydro power, solar power, and wind power. The final products, compressed hydrogen or liquefied hydrogen, are produced from ten technologies including five hydrogen production methods and two post processes. The five hydrogen production methods consist of steam methane reforming (SMR), biomass gasification (BG), coal gasification (CG), alkaline/polymer electrolyte membrane (PEM) electrolysis (APE), and solid oxide electrolysis (SOE). Two post processes consist of hydrogen compression to 700 bars and hydrogen liquefaction. As the superstructure considers both gaseous and non-gaseous substances, four transportation units are considered, such as tube trailer, tanker truck, tube railcar, and tank railcar. Among the transportation units, tube trailers and tube railcars are used to transport gaseous substances. Reversely, tanker trucks and tank railcars are used to transport non-gaseous substances over the Texas regions. To measure the degree of GHG emissions, three waste components, carbon dioxide, methane, and nitrogen oxide, are considered in this study. The components were not transported to other sub-regions, but just vented when the hydrogen is produced from each sub-regions. Both compressed and liquefied hydrogen are sold at $5/kg ratio for the whole time periods. Explanation of the mathematical model structure and techniques used is described in Appendix B.

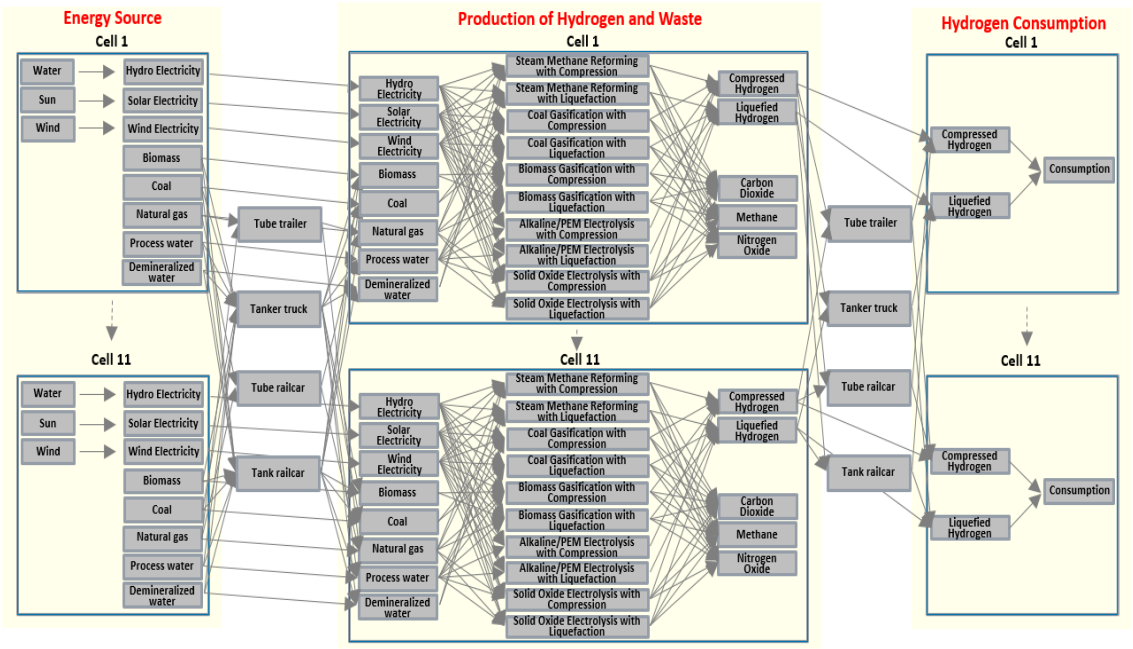

Figure 3.1. Hydrogen energy network superstructure

3.4. Time Horizon

This supply chain network has a time horizon consists of 8 periods. The time horizon starts from 2015 and lasts until 2055. Each period has 5 years respectively. For each time period, the model decided a strategy regarding the operational options based on hydrogen demand, expansion or shrinkage of production capacity, technology availability, total costs, GHG emissions, and NPV.

3.5. Geographical Areas

3.5.1. Population Projections in Cells

Geographically, Texas has 254 counties. However, the geographical areas had simplified to 11 cells through merging adjacent counties as most of the counties have had small-

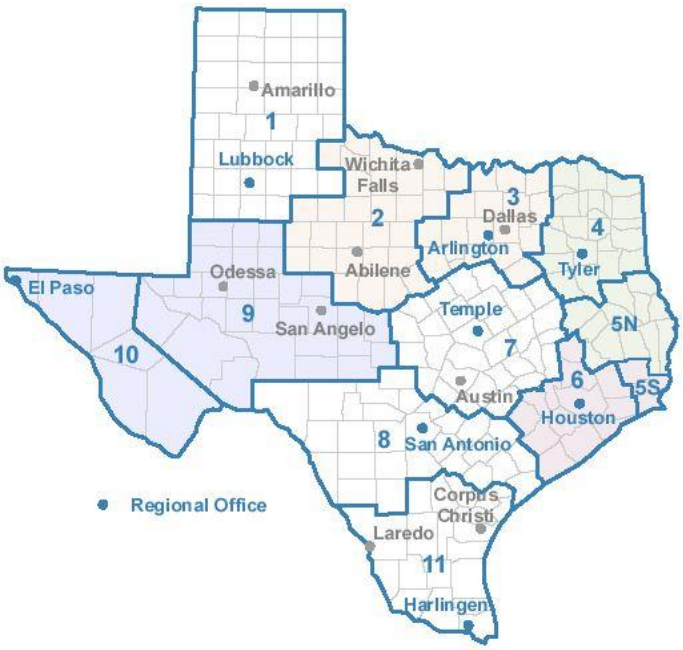

Figure 3.2. Assigned geographical areas for this case study. (Taken from Texas Department of State Health Service: https://www.dshs.texas.gov/chs/info/info_txco.shtm)

population, less than 100,000. A figure for the assigned geographical areas for this study is shown above in Figure 3.2. The population projection of each cell had been estimated through the tool named "Texas Population Projection by Migration Scenario Data". The tool measures expected population of each cell based on both 2000-2010 Texas migration ratio and natural phenomena, such as births and deaths. Additionally, it also classifies the number of people by age, sex, and ethnicity throughout time periods. The projected population for each cell over time periods is described below in Table 3.2 (Texas State Data Center et al., 2014).

Table 3.2. Projected population of each cell over time

Cell	2015	2020	2025	2030	2035	2040	2045	2050
i1	861,081	942,285	999,906	1,060,766	1,122,212	1,184,026	1,248,747	1,318,027
i2	558,838	579,760	593,434	605,376	614,386	620,354	624,662	628,489
i3	7,922,450	8,262,583	9,223,446	10,350,467	11,652,101	13,142,957	14,849,119	16,817,756
i4	1,175,101	1,237,949	1,307,615	1,380,440	1,454,396	1,531,382	1,616,456	1,715,397
i5	779,391	836,526	873,647	911,083	946,905	981,402	1,016,701	1,056,522
i6	6,895,132	7,591,647	8,483,669	9,466,708	10,540,101	11,712,202	12,996,660	14,416,642
i7	3,283,634	3,758,358	4,222,430	4,722,791	5,270,225	5,883,251	6,576,542	7,356,230
i8	2,765,627	3,149,310	3,443,804	3,743,990	4,028,264	4,307,984	4,579,759	4,847,021
i9	566,784	642,563	679,719	717,040	752,739	786,097	817,569	848,479
i10	845,333	980,456	1,063,374	1,142,673	1,215,074	1,281,526	1,342,874	1,398,989
i11	2,362,179	2,560,541	2,808,263	3,053,750	3,295,852	3,524,715	3,747,076	3,965,745

3.5.2 Vehicle Commuter Ratio

A comprehensive analysis of Texas' urban streets and highway performance was conducted based on both "Urban Mobility Scorecard" of Texas A&M Transportation Institute and Federal Highway Administration (Schrank et al., 2015). The score was measured by population group size, a number of auto commuters, freeway and arterial street vehicle mileages for ten representative Texas' cities, such as Austin, Beaumont, Brownsville, Corpus Christi, Dallas-Fort Worth-Arlington, El Paso, Houston, Laredo, Mc Allen, and San Antonio.

The vehicle commuter ratio for each area was calculated by dividing the number of auto commuters by the whole population of each area. The average ratios throughout 1982 and 2014 for all areas are shown below, and there is a trend depends on the population of each area. In specific, higher population area showed lower vehicle commuter ratio, and it was analyzed that other units, especially bus system, contribute to this trend. Reversely, smaller population area showed a bit higher vehicle commuter ratio as such areas rarely have alternative public transportation units.

To simplify the model, the average value from all ten regions was assumed as 0.45 or 45%, and it means 45% of total population was assumed as vehicle commuters with his or her own vehicle. The Table 3.3, below describes the data used for the calculation of vehicle commuter ratio, and the following table, Table 3.4 shows the number of commuters for each cell over time.

Table 3.3. Vehicle commuter ratio of reference regions

Area	Classification	Lowest ratio	Highest ratio	Average
Beaumont	Small	39.5%	54.2%	46.8%
Brownsville	Small	39.0%	53.3%	46.2%
Corpus Christi	Small	38.8%	51.5%	45.1%
Laredo	Small	38.9%	51.8%	45.4%
El Paso	Medium	39.6%	51.1%	45.3%
McAllen	Medium	40.0%	51.8%	45.9%
Austin	Large	37.8%	47.0%	42.4%
San Antonio	Large	37.9%	51.1%	44.5%
Dallas-Fort Worth-Arlington	Very large	40.0%	46.9%	43.4%
Houston	Very large	44.4%	48.2%	46.3%

Table 3.4. Number of commuters of each cell over time

Cell	2015	2020	2025	2030	2035	2040	2045	2050
i1	387,486	424,028	449,958	477,345	504,995	532,812	561,936	593,112
i2	251,477	260,892	267,045	272,419	276,474	279,159	281,098	282,820
i3	3,565,103	3,718,162	4,150,551	4,657,710	5,243,445	5,914,331	6,682,104	7,567,990
i4	528,795	557,077	588,427	621,198	654,478	689,122	727,405	771,929
i5	350,726	376,437	393,141	409,987	426,107	441,631	457,515	475,435
i6	3,102,809	3,416,241	3,817,651	4,260,019	4,743,045	5,270,491	5,848,497	6,487,489
i7	1,477,635	1,691,261	1,900,094	2,125,256	2,371,601	2,647,463	2,959,444	3,310,304
i8	1,244,532	1,417,190	1,549,712	1,684,796	1,812,719	1,938,593	2,060,892	2,181,160
i9	255,053	289,153	305,874	322,668	338,733	353,744	367,906	381,816
i10	380,400	441,205	478,518	514,203	546,783	576,687	604,293	629,545
i11	1,062,981	1,152,243	1,263,718	1,374,188	1,483,133	1,586,122	1,686,184	1,784,585

3.5.3. Distance between Cells

Distance between two cells is an important parameter as it has big impact on the transportation cost. For this case study, the cities close to center of each cell are selected, and those cities are used to measure the distance between two cells. The Table 3.5 below shows the distance among 11 cells for this study. The tool named "Google Maps" is used to estimate distance in miles based on the zip code of those representative cities.

Table 3.5. Distance between two cells (in miles)

City, County	ZIP CODE		i1	i2	i3	i4	i5	i6	i7	i8	i9	i10	i11
Wayside, Armstrong county	79094	**i1**	60	264	349	471	598	601	443	486	298	424	653
Albany, Shackelford county	76430	**i2**	264	60	137	263	372	364	206	270	213	372	437
Colleyville, Tarrant county	76034	**i3**	349	137	60	139	249	275	151	281	322	496	446
Big Sandy, Upshur county	75755	**i4**	471	263	139	60	153	228	204	332	448	623	499
Woodville, Tyler county	75979	**i5**	598	372	249	153	60	110	195	291	478	725	381
Houston, Harris county	77005	**i6**	601	364	275	228	110	60	155	196	437	614	273
Rogers, Bell county	76569	**i7**	443	206	151	204	195	155	60	152	294	483	310
San Antonio, Bexar county	78202	**i8**	486	270	281	332	291	196	152	60	259	423	171
Big Lake, Reagan county	76932	**i9**	298	213	322	448	478	437	294	259	60	210	426
Fort Davis, Jeff Davis county	79734	**i10**	424	372	496	623	725	614	483	423	210	60	533
Falfurrias, Brooks county	78355	**i11**	653	437	446	499	381	273	310	171	426	533	60

3.6. Hydrogen Demand Projection

Hydrogen demand projection from 2015 to 2050 had been performed by Energy Information Administration (EIA) (EIA, 2017a). The allocation of Texas hydrogen demand ratio is estimated by the ratio of registered vehicles in Texas to the number of registered vehicles in the United States (Elaine et al., 2017; Jeremiah, 2015). Based on the EIA's hydrogen demand projection, the Texas' hydrogen demand until 2055 was

estimated through the assumption of a hydrogen demand at each time spot lasts for five years. The Figure 3.3 below shows both estimated Texas' hydrogen demand projection until 2050 based on EIA's data, and the estimated step-shaped hydrogen demand for the case study simulation. Additionally, the hydrogen demand of each cell was also projected throughout the time periods by the number of commuters estimated for each time spot. The overall Texas' hydrogen demand had been increased rapidly over time although it is observed that the cells with large population showed faster hydrogen demand increase, and the cells with small population showed slower demand increase. So, it is firmly believed that the infrastructure penetration speed would be more accelerated over time, especially in farther future. The figure of hydrogen demand of each cell over time is shown below in Figure 3.4.

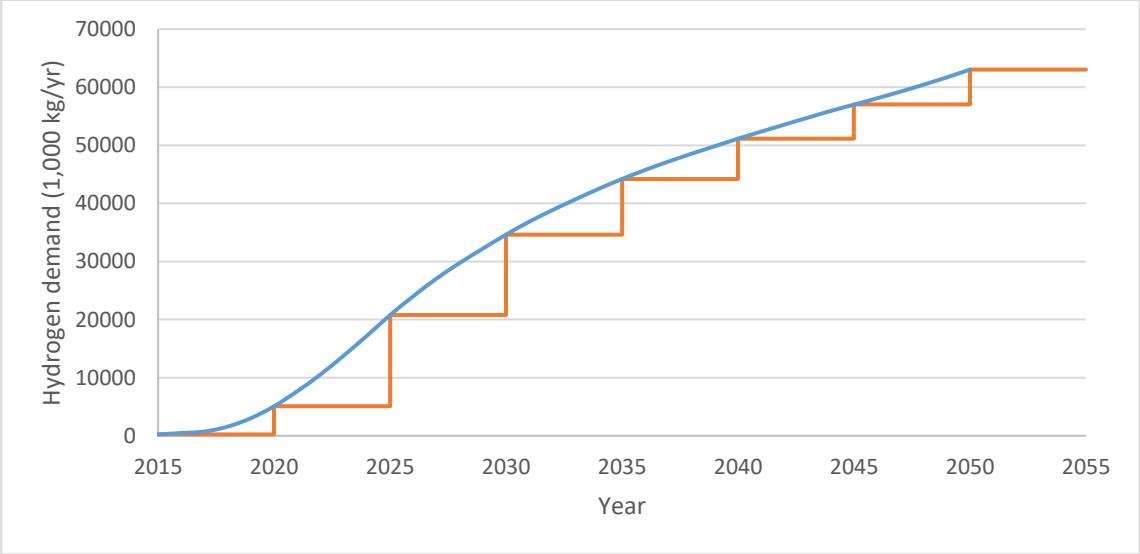

Figure 3.3. Hydrogen demand projection in Texas until 2050.

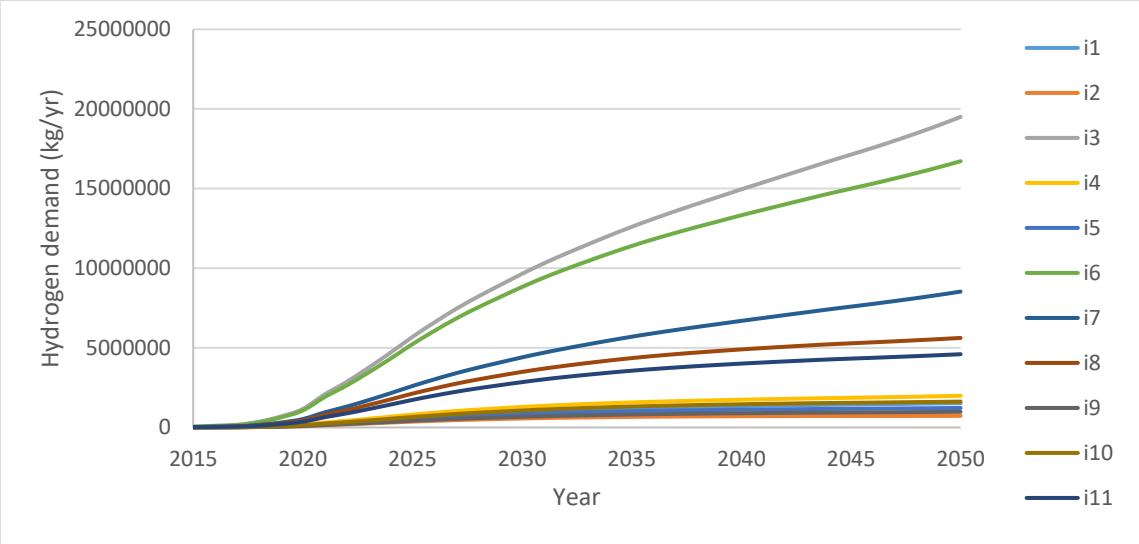

Figure 3.4. Hydrogen demand projection of each cell until 2050.

3.7. Resource Capacity for Cells

3.7.1. Raw Material Capacity

To produce hydrogen, the raw materials are demanded by five hydrogen production methods. The maximum potentially extractable capacity of each raw material source is classified by its geographical origin. The parameters regarding maximum raw material capacity are taken from U.S. Energy Information Administration (EIA), as presented below in Table 3.6. The capacities for both process water and demineralized water are assumed as infinite (EIA, 2017b).

Table 3.6. Maximum extractable raw materials for each cell

Cell	Biomass (kg/day)	Coal (kg/day)	Natural gas (kg/day)	Process water (kg/day)	Demineralized water (kg/day)
i1	158229.4325	0	0	INF	INF
i2	14090.01957	0	3951139845	INF	INF
i3	96064.73581	0	264744808.9	INF	INF
i4	105747.0841	1089856.751	11440436056	INF	INF
i5	151317.6517	0	2599263236	INF	INF
i6	154391.546	0	22796227389	INF	INF
i7	67972.52446	2150586.614	344267422.1	INF	INF
i8	44739.17808	176700.5088	0	INF	INF
i9	16623.87476	0	931038341.9	INF	INF
i10	10630.13699	0	0	INF	INF
i11	90961.09589	0	0	INF	INF

3.7.2. Electricity Capacity

The electricity used for the Texas case study came from renewable sources, such as hydropower, solar power, and wind power. To prevent an electricity loss during a long distance electricity transmission, it was assumed that the electricity produced in a certain cell only consumed by that certain cell during whole time periods. The potentially generable amount of electricity from each source is classified into each cell level.

Table 3.7. Maximum potentially generable electricity from each source for each cell

Cell	Hydro (kwh/day)	Solar (kwh/day)	Wind (kwh/day)
i1	0	6548023704	5052842640
i2	0	4550974747	3929467680
i3	1771200	162571420	2375989200
i4	0	2583022122	1370571840
i5	2592000	2006362353	1494859320
i6	0	132112580	1011592800
i7	7112880	4260332571	2953437120
i8	1954800	5278126144	2536553880
i9	0	6612703631	4298173200
i10	0	3611799079	641477880
i11	658800	3542237648	3451661640

The parameters regarding each renewable source, hydro energy, solar energy and wind energy are taken from EIA, National Renewable Energy Laboratory (NREL), and AWS Truepower respectively (EIA, 2017b; Lopez et al., 2012; NREL and AWS Truepower, 2010a, 2010b).

3.8. Hydrogen Production Technologies

Ten hydrogen production technologies considered in this case study. Each technology produces compressed or liquefied hydrogen as their final product, and each technology contains one hydrogen production method out of five production methods, and one post process out of two post processes. Additionally, each hydrogen production method requires different raw material and different amount of electricity to produce a final product. The explanation of individual hydrogen production method described below. Post process explanation is located in the next session. The figures and operating conditions for the five hydrogen production methods used in this section are taken from The Hydrogen Analysis (H2A) project of U.S. Department of Energy (DOE, 2015).

3.8.1. Steam Methane Reforming (SMR)

The hydrogen production from SMR has well known to be one of the most efficient and widely used processes with less GHG emissions. The model was based on Aspen Plus® for material and energy balance. The process mainly consists of sulfur guard, steam reformer, water gas shift (WGS) reactors, pressure swing adsorption (PSA), and heat recovery steam generator (HRSG). When the natural gas fed into the system, the guard cleans sulfurs, odorizers, and mercaptans.

Then purified natural gas reacts with steam at the steam reforming process to produce hydrogen. Following WGS process enhances the hydrogen production ratio, and PSA

purifies the produces hydrogen. The maximum hydrogen production capacity is 341,448 kg/day at 42°C and 23.5 atm. The SMR process flow diagram is described in Figure 3.5.

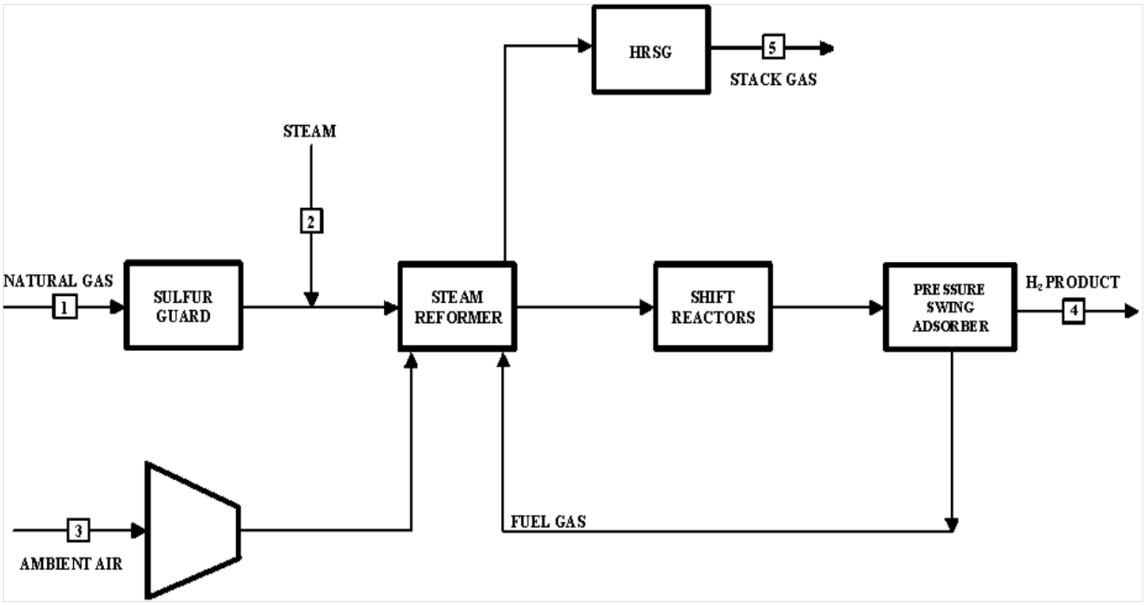

Figure 3.5. SMR process flow diagram for hydrogen production (DOE, 2015).

3.8.2. Coal Gasification (CG)

This CG model used in this study was also taken from The H2A project of U.S. DOE. The hydrogen production process includes conventional gas cooling, commercial shift conversion/acid gas cleanup, commercial sulfuric acid technology, and PSA. In this process, oxygen is firstly produced from air separation unit (ASU) then reacts with coal and water at coal gasifier unit. Then the produced gas reacts with high temperature steam again to enhance the hydrogen production ratio. Following shift converter also contributes to producing extra amount of hydrogen. The produced gas send to the amine to separate sweet gas and acid gas, and only sweet gas is sent to the PSA unit for further purification. The maximum plant output of this process is designed to produce 255,447 kg/day of

hydrogen condition of 21°C and 21 atm. The coal gasification flow diagram is shown below in Figure 3.6.

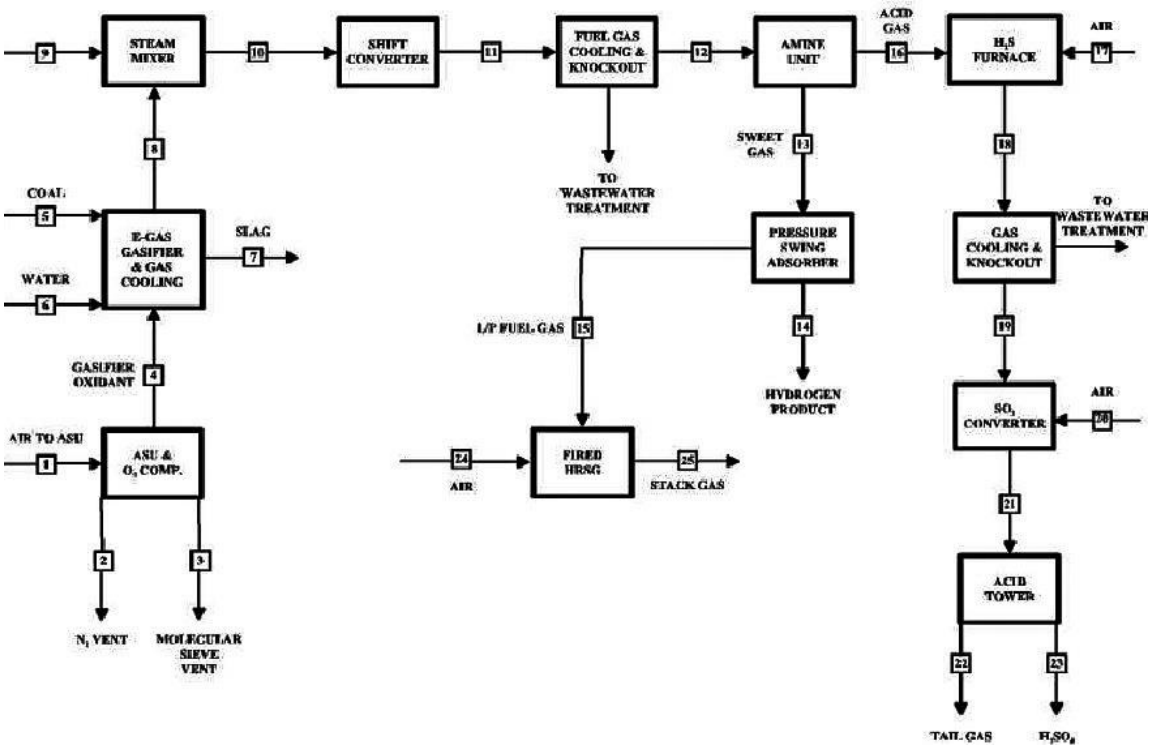

Figure 3.6. Coal gasification process flow diagram for hydrogen production (DOE, 2015).

3.8.3. Biomass Gasification (BG)

The BG process is a promising hydrogen production method as it requires biomass, such as woody waste. The process mainly consists of biomass drying, reforming, purification, steam cycle production, and cooling water system. In this process, when the biomass fed into the system, it is dried from a rotary dryer. The dried mass reacts with steam at the gasifier unit and produces syngas. The produced syngas undergoes purification processes including scrubber unit and catalytic treatment to remove sulfur components. The treated syngas fed into the steam reformer and reacts with steam to produce hydrogen, and extra

amount of hydrogen produced from both high temperature shift (HTS) and low temperature shift (LTS) processes. Then the produced hydrogen is purified through PSA unit to greater than 99.99+%. This process is designed to produce hydrogen up to 139,712 kg/day at the hydrogen condition of 43°C and 69 atm. More detailed process flow diagram is described below in Figure 3.7.

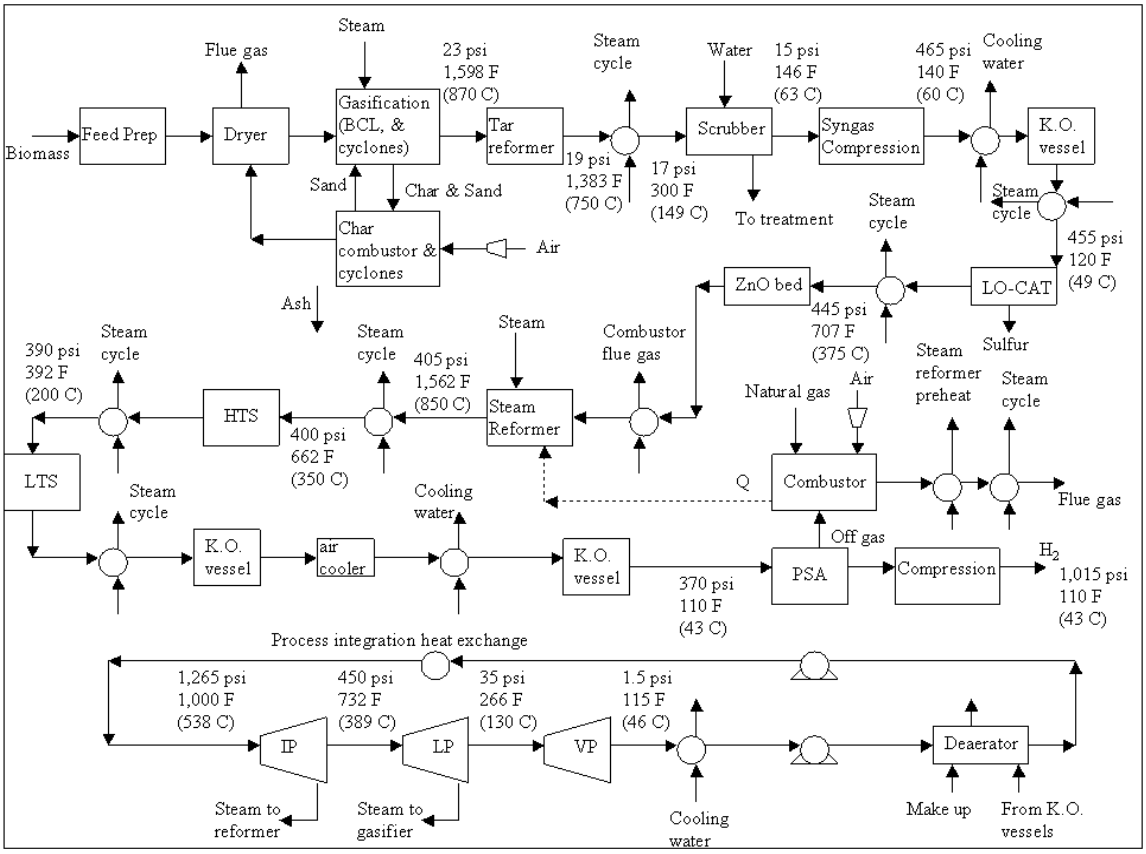

Figure 3.7. Biomass gasification process flow diagram for hydrogen production (DOE, 2015).

3.8.4. Alkaline/PEM Electrolysis (APE)

Electrolysis is one of the promising hydrogen production methods benign to environment because it does not produce any GHG during hydrogen production. The process consists of water management system, power transformer and rectifier, oxygen and hydrogen management system, and electrolyzer. When water and power fed into the process, they produce hydrogen through electrolysis which separates oxygen component and hydrogen component from the fed water. The process is designed to produce hydrogen of 48,500 kg/day maximum ratio, and the produced hydrogen has conditions of 65°C and 30.6 atm. Process flow diagram of this technology is described below in Figure 3.8.

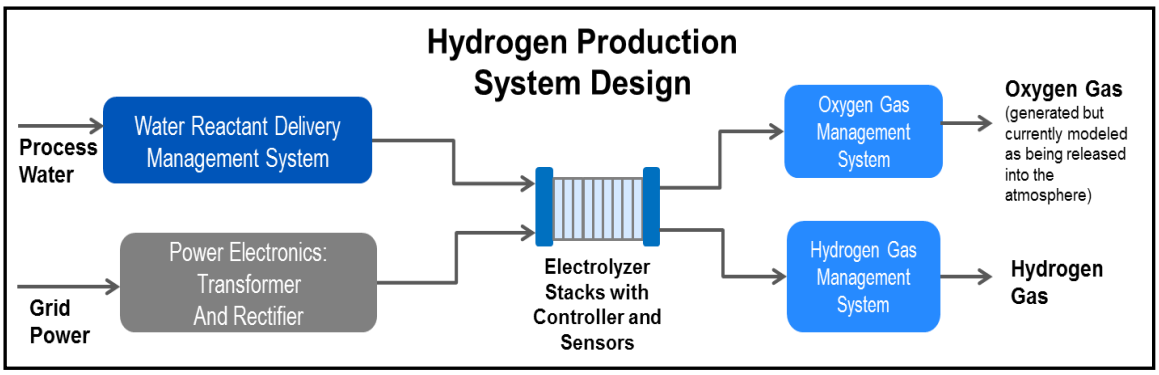

Figure 3.8. Alkaline/PEM electrolysis process flow diagram for hydrogen production (DOE, 2015).

3.8.5. Solid Oxide Electrolysis (SOE)

The SOE model is also taken from H2A project of U.S. DOE as well as other hydrogen production models. The model requires both electricity and thermal energy. Compared to APE, the SOE requires less electricity input but requires thermal energy for a high temperature water electrolysis. The model consists of electrolyzer stacks, furnace, heat exchangers, and separators. During the operation, natural gas fed used to produce thermal energy through the furnace, and the produced heat is used for heating water before it is

fed into the electrolyzer. This model is designed to produce hydrogen at the maximum ratio of 41,220 kg/day, and physical condition of hydrogen flow was 32℃ at 20.4 atm. Figure 3.9 below shows overall process flow diagram.

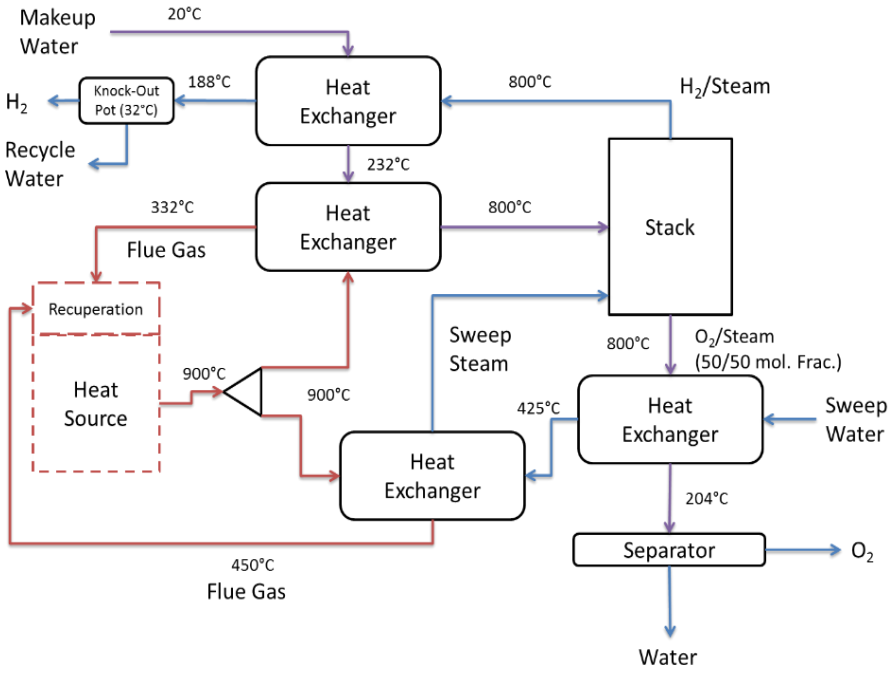

Figure 3.9. Solid oxide electrolysis process flow diagram for hydrogen production (DOE, 2015).

3.9. Post Process

Two post processes, compression and liquefaction, are considered to make hydrogen more appropriate for delivery and ready to sell. Thermodynamic calculation had performed to measure the required amount of energy for each process because of the different physical hydrogen condition from each hydrogen production method.

3.9.1. Hydrogen Compression

The amount of energy needed for hydrogen compression to 700 bar was calculated based on adiabatic gas compression equation including initial and final hydrogen pressure, initial specific volume, and hydrogen specific heat ratio as shown below (Ulf and Baldur, 2003).

$$W = (2.78 \times 10^{-7}) \cdot \left(\frac{k}{k-1}\right) \cdot P_0 \cdot V_0 \cdot \left(\frac{P_1}{P_0}^{\frac{k-1}{k}} - 1\right)$$

Where:

W	[kwh/kg]	=	specific compression work
P_0	[Pa]	=	initial pressure
P_1	[Pa]	=	final pressure
V_0	[m^3/kg]	=	initial specific volume
k		=	specific heat ratio, adiabatic coefficient

For the hydrogen compression, specific heat ratio of 1.41 is used. Based on the equation, the amount of energy required for compress hydrogen up to certain pressure is calculated and plotted below in Figure 3.10, and it shows different energy requirements for each production methods as hydrogen from each method had different physical conditions. Specifically, the amount of energy required to compressed hydrogen from biomass gasification method required only 1.24 kwh/kg H_2, because of the highly pressured output from the production method.

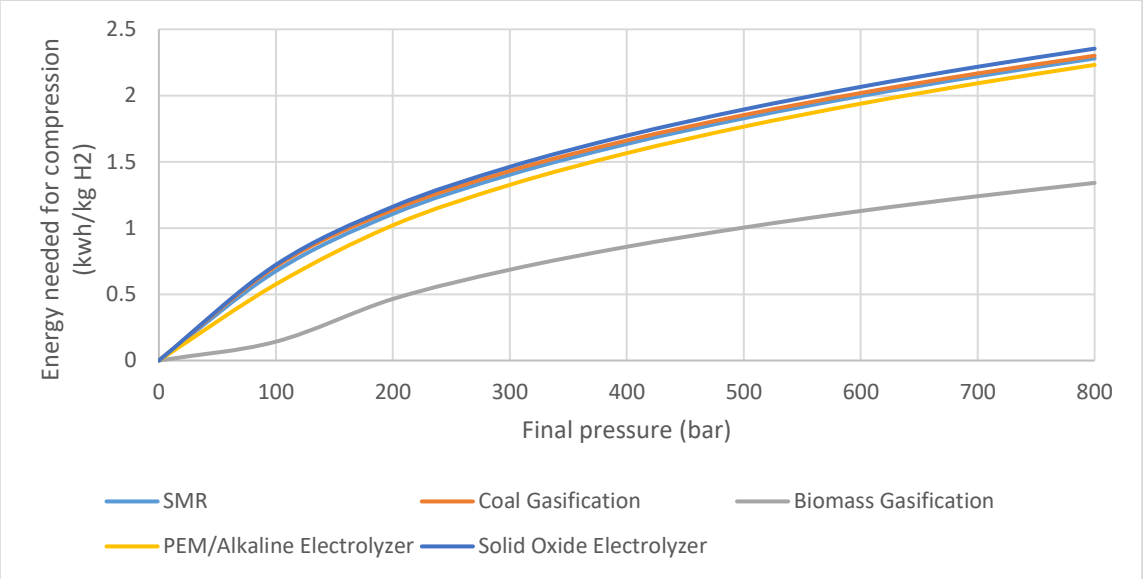

Figure 3.10. Electricity needed for hydrogen compression from production methods.

3.9.2. Hydrogen Liquefaction

The amount of energy required for hydrogen liquefaction was estimated based on typical energy requirements for the hydrogen liquefaction. According to Ulf Bossel et al., the energy required to liquefying hydrogen is related to hydrogen plant capacity, and it could be low as much as 11.11 kWh/kg of hydrogen when plant capacity is big enough (Ulf and Baldur, 2003). However, in this case study, it was assumed that 1 kg of hydrogen could be liquefied using 15.83 kWh/kg of energy, and it represents the plant capacity of 300 kg/hr. The relationship between the energy required with plant capacity is shown below in Figure 3.11.

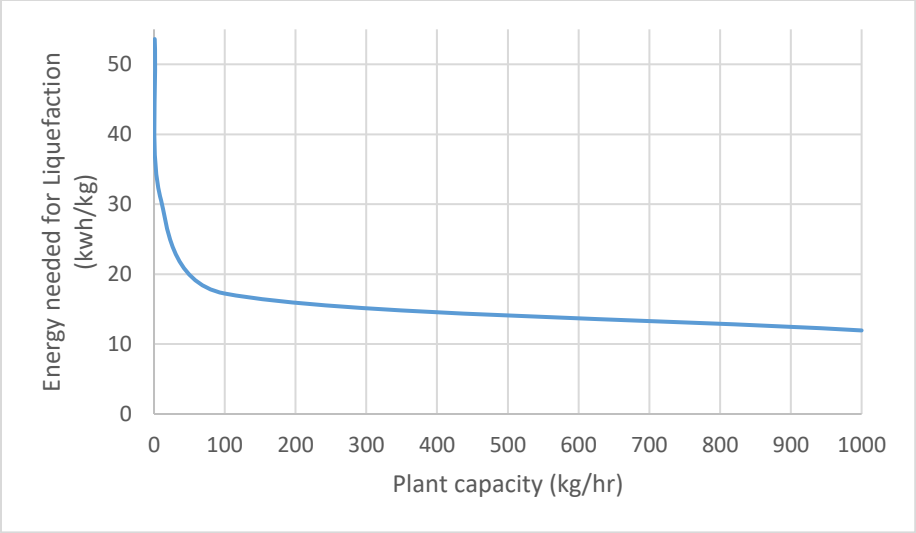

Figure 3.11. Electricity needed for hydrogen liquefaction (Ult and Baldur, 2003).

3.10. Resource Unit Input and Unit Production Cost

As each technology requires different raw materials and energy amounts, different unit hydrogen production cost is measured. The Table 3.8 below shows material costs including both raw materials and electricity. Additionally, a summarized Table 3.9 below compromises amount of raw material and energy needed to produce 1 kg of hydrogen for all technologies and their unit hydrogen production costs (DOE, 2015; EIA, 2017c).

Table 3.8. Material costs

Materials	$/kg or $/kwh
Biomass	0.0858
Coal	0.0413
Natural Gas	0.2320
Process Water	0.0005
Demineralized Water	0.0015
Hydro Electricity	0.0594
Solar Electricity	0.0599
Wind Electricity	0.0469

Table 3.9. Unit resource input and hydrogen unit production costs

Materials	SMR		Coal Gasification		Biomass Gasification		Alkaline/PEM Electrolysis		Solid Oxide Electrolysis	
	Comp	Liq	Comp	Liq	Comp	Liq	Comp	Liq	Comp	Liq
Biomass (kg)	0	0	0	0	13.49	13.49	0	0	0	0
Coal (kg)	0	0	8.508	8.508	0	0	0	0	0	0
Natural gas(kg)	3.86	3.86	0	0	0.146	0.146	0	0	1.19	1.19
Process Water (kg)	0	0	2.98	2.98	1.321	1.321	4.76	4.76	2.378	2.378
Demineralized Water (kg)	3.355	3.355	0	0	0	0	0	0	0	0
Electricity (kwh)	2.146	15.833	2.167	15.833	1.240	15.833	56.393	70.133	39.017	52.633
$/kg hydrogen	**1.001**	**1.643**	**0.454**	**1.095**	**1.250**	**1.935**	**2.647**	**3.292**	**2.107**	**2.746**

3.11. Waste Emissions

3.11.1. GHG Emissions

Three types of wastes including GHGs, such as carbon dioxide, methane, and nitrogen oxide, emitted from both raw material extraction and hydrogen production processes. The Table 3.10 below shows the GHG emission amount from both two processes.

Table 3.10. GHG emission by source extraction and hydrogen production

	Waste produced from raw material extraction for 1kg hydrogen production				
	Biomass	Coal	Natural Gas	Process Water	Demineralized Water
Carbon Dioxide (kg)	-22.91	0.36	1.42	0	0
Methane (kg)	0.00356	0.0266	0.0373	0	0
Nitrogen Oxide (kg)	0.000781	6.97E-06	0.000197	0	0
	Waste produced from 1kg hydrogen production				
	SMR	Coal Gasification	Biomass Gasification	Alkaline/PEM Electrolysis	Solid Oxide Electrolysis
Carbon Dioxide (kg)	9.28	21.42	24.92	0	0
Methane (kg)	0	0	0	0	0
Nitrogen Oxide (kg)	0	0	0	0	0

3.11.2. GHG Tax

Based on the amount of GHG emission from both raw material extraction and hydrogen production process, a tax for such GHG emissions is considered. In the case studies, the tax is assumed as $0.04/kg for all types of GHG emissions. The Table 3.11 below describes the overall tax estimated for 1kg of hydrogen production from five production methods. From the table below, using biomass as a feedstock contributes on reducing the carbon dioxide emissions, and it also contributes to minimizing GHG tax among conventional hydrogen production methods. However, SMR and Coal gasification are still economically feasible hydrogen production methods.

Table 3.11. Overall GHG emission by technology and estimated tax for unit production

	Overall waste produced for 1kg hydrogen production and tax credit									
	SMR		**Coal Gasification**		**Biomass Gasification**		**Alkaline/PEM Electrolysis**		**Solid Oxide Electrolysis**	
Carbon Dioxide (kg)	10.700		21.780		2.010		0		1.420	
Methane (kg)	0.037		0.027		0.004		0		0.037	
Nitrogen Oxide (kg)	1.97E-04		6.97E-06		7.81E-04		0		1.97E-04	
GHG Tax ($/kg)	0.429		0.872		0.081		0		0.058	
GHG Tax + H_2	Comp	Liq	Comp	Liq	Comp	Liq	Comp	Liq	Comp	Liq
Production cost ($/kg)	1.430	2.072	1.326	1.967	2.229	2.914	2.647	3.292	2.165	2.804

3.11.3. Horizon 2020 Project

From the introduction presented in the first chapter, reduction of GHG emission is increasingly demanded by many countries to prevent serious global warming phenomenon through building a low-carbon environment. To cut current pollutant emissions, Europe countries started a project named “Horizon 2020”, and it consists of 22 areas.

One of those 22 areas, Environment and Climate Action, has an objective of achieving sustainable use of raw materials and resource management to build an economy resilient

on proceeded climate change. Such that objective has been reflected in this case study as limiting the amount of fossil fuel allowed to be used for hydrogen production. Specifically, two fossil fuels, coal and natural gas, are limited to be used only 15% of the allowed amount of previous time period for all cells. In year base, as each time period consists of five years, only 68.4% of previous year's fossil fuel amount is allowed to be used for a consecutive year. The Figure 3.12 below describes the total allowable amount of fossil fuels over time.

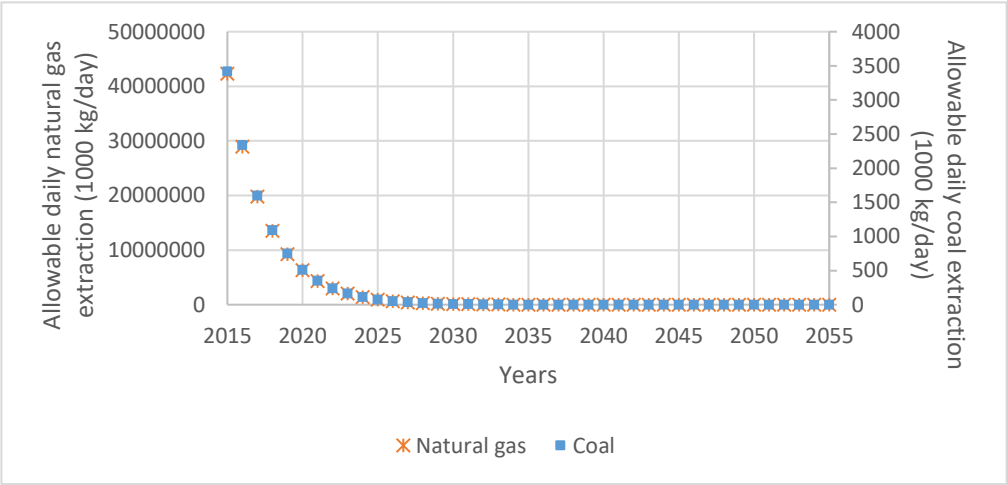

Figure 3.12. Total allowable amount of fossil fuels over time.

3.11.4. Eco-Indicator 99 Methodology

Among numerous environmental impact assessment methods, Eco-Indicator 99 methodology has chosen as it estimates the actual damages based on three categories, such as human health, ecosystem quality, and minerals and fossil resources. Additionally, this method also has an advantage of the usage of normalization and weighting factors because those factors can reflect what has mainly being considered, and at how much degree the pollutants are actually affecting the environment in this study. The procedure consists of four steps including resource/land-use/fate analysis, exposure and effect analysis, damage analysis, and normalization and weighting. General representation of Eco-Indicator 99

methodology is graphically described below with intermediate steps (Mark and Renilde, 2001).

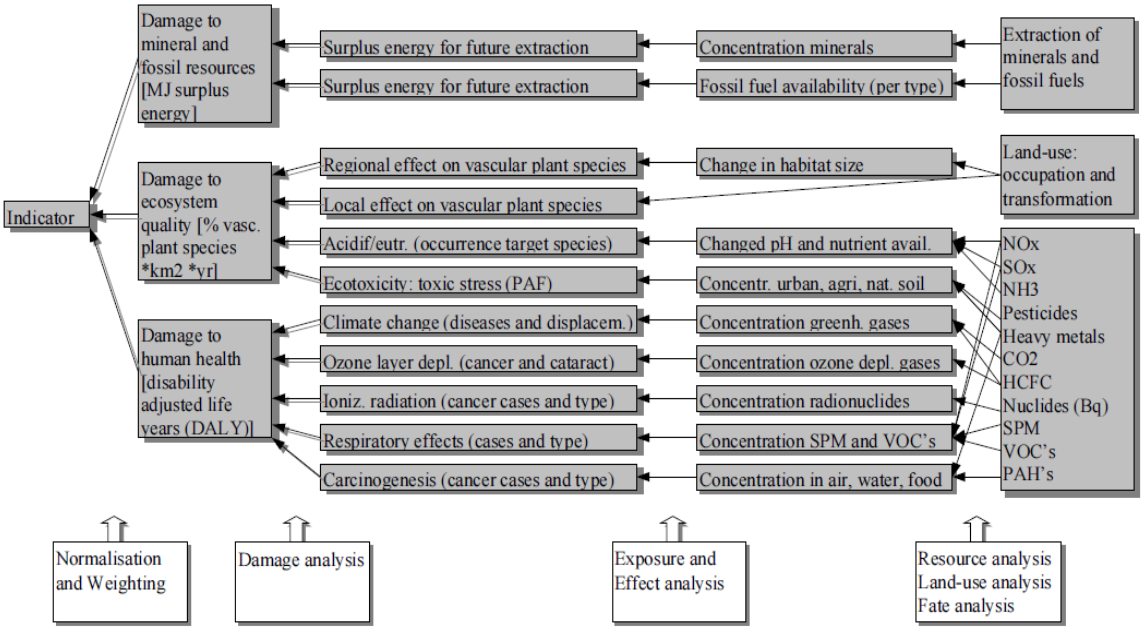

Figure 3.13. General representation of Eco-Indicator 99 Methodology (Mark and Renilde, 2001).

For the case study, ten indicators are considered for the three categories. Human health category includes 1) Carcinogenic effects on humans, 2) Respiratory effects on humans caused by organic substances, 3) Respiratory effects on humans caused by inorganic substances, 4) Damages to human health caused by climate change, 5) Human health effects caused by ionizing radiation, and 6) Human health effects caused by ozone layer depletion. Under Ecosystem quality category, 7) Damage to ecosystem quality caused by ecotoxic emissions, 8) Damage to ecosystem quality caused by the combined effect of acidification and eutrophication are listed. Minerals and fossil fuel category includes both 9) Damage to resources caused by extraction of minerals and 10) Damage to resources

caused by extraction of fossil fuels, to estimate the environmental damage based on raw material extraction.

To quantify the damages, damage factors and normalization factors for the pollutants emitted from this case study, such as carbon dioxide, methane, and nitrogen oxide are taken from Eco-Indicator 99 methodology report. Values for the two factors are shown below in Table 3.12 (Mark and Renilde, 2001). Weighing factor for the categories, such as human health, ecosystem quality, and minerals and fossil fuel are assumed as 0.4, 0.55, and 0.05 respectively. Such assumption represents an importance of each category. Ecosystem quality category has the biggest weighting factor because building an environmentally sustainable infrastructure is very important. The human health category also affected to be important as well. However, the minerals and fossil fuel category has the lowest weight factor because of the abundant potential resources in Texas area. More detailed explanations and mathematical expression for the Eco-Indicator 99 methodology is located in the Appendix B at the end of this paper.

Table 3.12. Damage and normalization factors in the hierarchist perspective (Mark and Renilde, 2001)

Indicators	Carbon dioxide		Methane		Nitrogen oxide		Coal extraction		Natural gas extraction	
	Damage	Norm	Damage	Norm	Damage	Norm	Damage	Norm	Damage	Norm
Carcinogenic	0	0	0	0	0	0	0	0	0	0
Respiratory - Organic	0	0	1.28E-08	8.31E-07	0	0	0	0	0	0
Respiratory - Inorganic	0	0	0	0	8.87E-05	5.76E-03	0	0	0	0
Climage Change	2.10E-07	1.36E-05	4.40E-06	2.86E-04	0	0	0	0	0	0
Ionisation Radiation	0	0	0	0	0	0	0	0	0	0
Ozone Depletion	0	0	0	0	0	0	0	0	0	0
Ecotoxic Emission	0	0	0	0	0	0	0	0	0	0
Acidification & Eutrophication	0	0	0	0	5.713	1.11E-03	0	0	0	0
Depletion of Mineral	0	0	0	0	0	0	0	0	0	0
Depletion of Fossil fuel	0	0	0	0	0	0	0.252	3.00E-05	4.55	5.41E-04

3.12. Capital and Operating Costs

3.12.1. Cost of Hydrogen Production Methods

In many infrastructure studies, the plant capital and operating costs take a big part on NPV estimation. In this case study, the plant capital cost is calculated using reference plant capital cost, reference plant capacity, and actual plant capacity expansion. Plant capital cost of each hydrogen production method is measured by multiplication of reference plant capital cost and an exponential value of plant expansion/reference plant capacity ratio.

The plant fixed operating cost also calculated similarly to the plant capital cost, but it uses reference fixed operating and maintenance (O&M) cost instead of the reference plant capital cost, and plant capacity instead of plant capacity expansion. For both cases, an economy of scale is set to 0.6156 for all technologies, taken from NREL. The reference plant capital cost, reference plant capacity, and reference O&M cost data are taken from the both H2A project of U.S. DOE and NREL, and the data is shown below in Table 3.13. Graphical correlations of plant capital cost vs. plant capacity expansion, and plant fixed O&M cost vs. plant capacity are shown below in Figure 3.14-15 (DOE, 2015). Detailed mathematical equations with explanation are located in Appendix B.

Table 3.13. Reference plant data for hydrogen production methods

Technology	Reference Plant Capital Cost (MM $)	Reference Plant Capacity (kg hydrogen /day)	Fixed O&M Cost ($/kg hydrogen/day)
SMR	225.433	341448	21203
Coal Gasification	452.433	255447	63208
Biomass Gasification	189.124	139712	30064
Alkaline/PEM Electrolyzer	24.446	48500	19546
Solid Oxide Electrolyzer	22.117	41220	14824

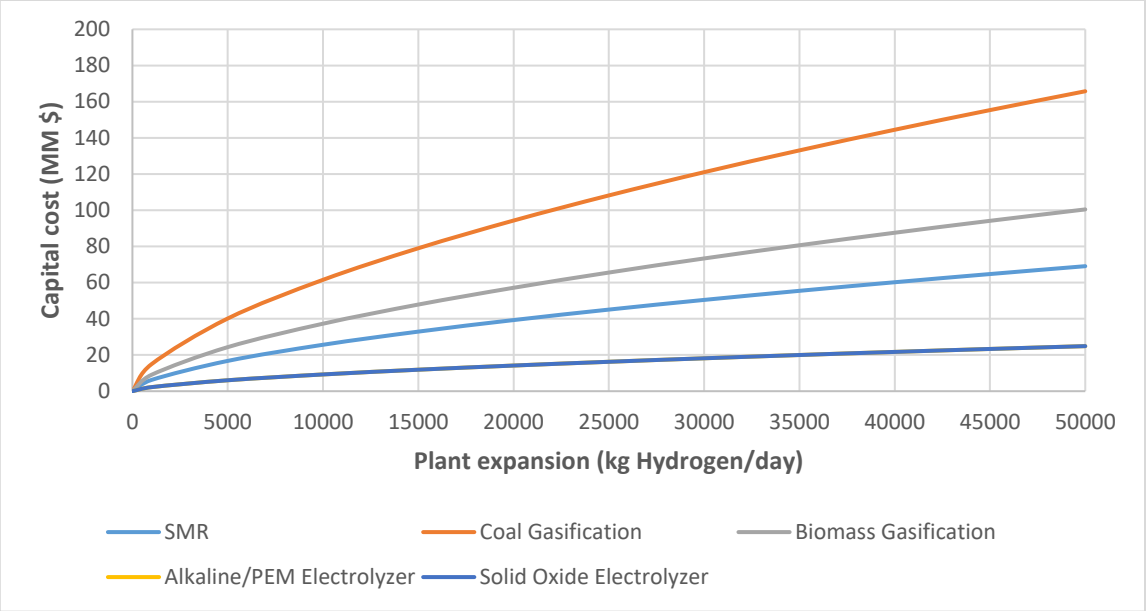

Figure 3.14. Plant capital cost depends on plant expansion.

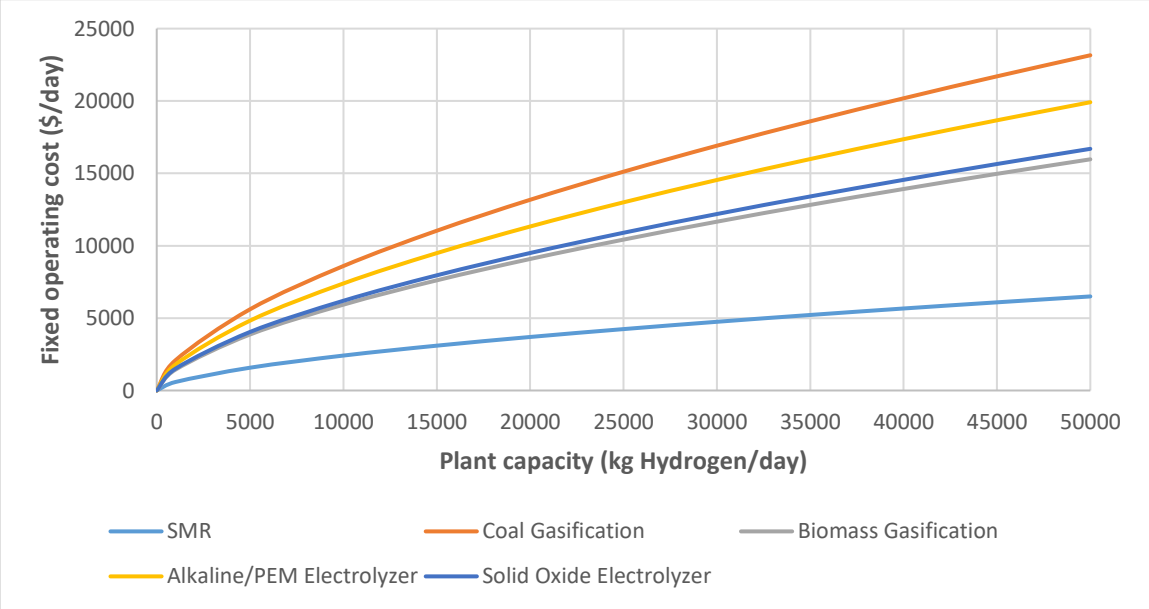

Figure 3.15. Plant fixed operating cost depends on plant capacity.

3.12.2. Cost of Post Processes

From the presented in the chapter 3.8 and 3.9, the hydrogen produced from the five methods has individually different physical conditions. Such this difference affects to the hydrogen compression process, because it is negligible when hydrogen is cooled to the cryogenic temperature during liquefaction process.

To calculate the capital cost for hydrogen compression to 700 bars, equipment capital cost data of NREL was used. Specifically, based on the data regarding compressor size and its capital cost, the compressor size and energy input for unit hydrogen production are used to build a relationship between compressor capital cost and hydrogen production rate. Because of the different conditions from each production methods, different relationship is expected. Following Figure 3.16 below is shows the relationship between compression capital cost and hydrogen processing rate for all five hydrogen with different physical conditions. In the figure below, biomass gasification method shows the lowest compressor capital cost level as it does not require much energy to compress hydrogen up to 700 bars (Wade, 1998).

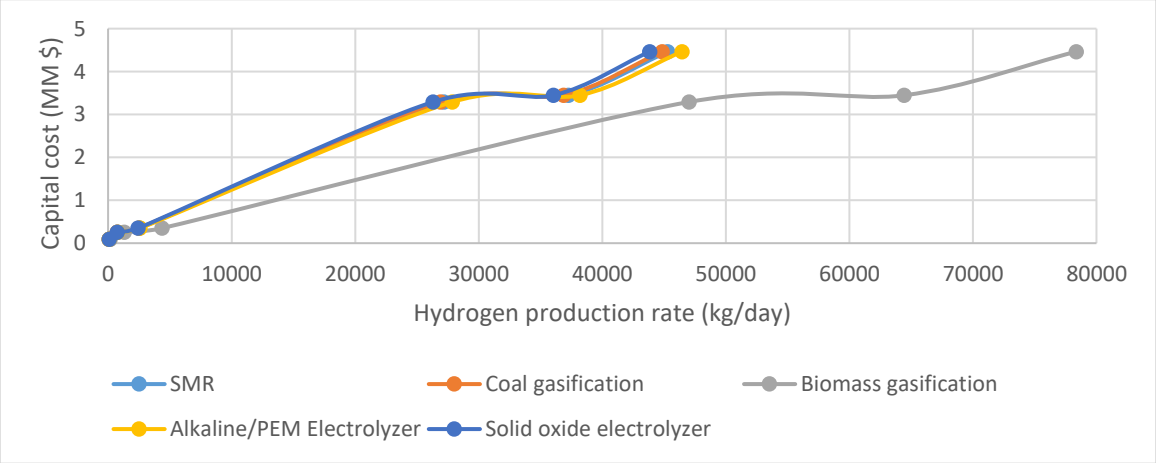

Figure 3.16. Compressor capital cost depends on hydrogen production rate.

The capital cost data for hydrogen liquefaction process is also taken from NREL. As different physical conditions could be neglected for the liquefaction process, the liquefaction capital cost is directly related to the hydrogen production rate, as shown below in Figure 3.17. Although the liquefaction process has a disadvantage of extremely high capital cost, it has an advantage when transportation is needed, because liquid could be transported more efficiently with fewer numbers of transportation units. For the post processes, each variable cost is generated from electricity usage.

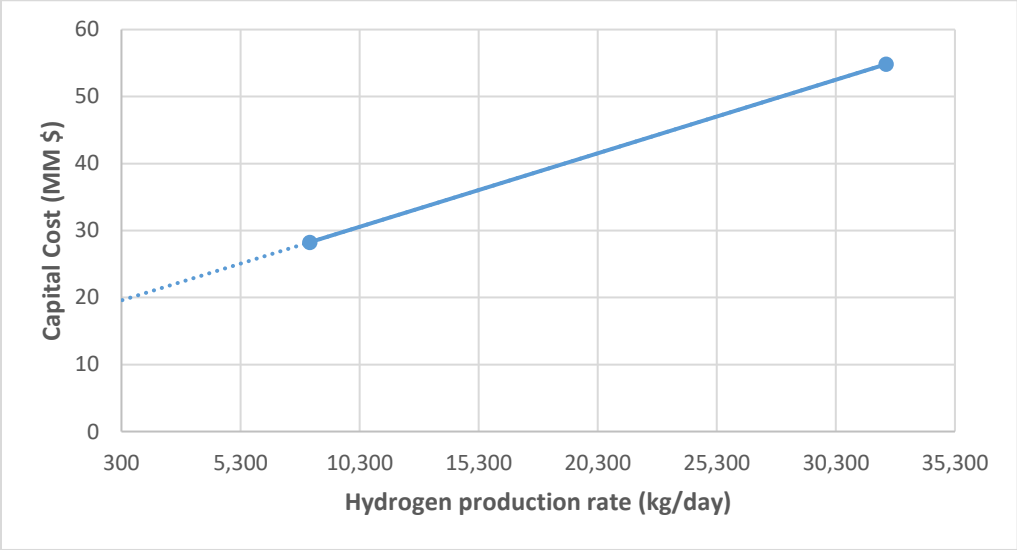

Figure 3.17. Liquefier capital cost depends on hydrogen production rate.

3.13. Transportation

As illustrated on the superstructure, transportation of raw materials and hydrogen occur between two geographical areas. There are four types of transportation units to transport both compressed and liquefied hydrogen, such as tube trailer, tanker truck, tube railcar, and tank railcar. In specific, tube trailer and tube railcar are used to transport gaseous substances, for instance compressed hydrogen and natural gas. Tanker truck and tank

railcar are used to transport non-gaseous substances, such as liquefied hydrogen, biomass and coal. For the transportation units based on cab, such as tanker truck and tube trailer, they have advantages on speed, loading/unloading time, and relatively cheaper unit price. However, they are only able to transport small amount for each trip so a number of transportation units might be required. On the other hand, for the transportation units based on railroad, such as tank railcar and tube railcar, they have advantages on the fuel economy, fuel price, and large transportation capacity. Despite these advantages, those units moves slowly and require longer time for loading/unloading, so expensive driver wage might be required. The parameters for four different transportation types are used for this case study, and they are shown below in Table 3.14 (Almansoori and Shah, 2006). Texas railroad map prepared by Railroad Commission (RRC) of Texas state is also shown in Figure 3.18.

Table 3.14. Transportation parameters (Almansoori and Shah, 2006)

Cost type	**Tube trailer**		**Tanker truck**		**Tube railcar**		**Tank railcar**	
	Raw Material	**CH_2**	**Raw Material**	**LH_2**	**Raw Material**	**CH_2**	**Raw Material**	**LH_2**
Fuel economy (miles/gal)	5.998				9.997			
Fuel price ($/gal)	4.391				1.06			
Speed (miles/hr)	34.176				27.962			
Load/Unload (hr)	2				12			
Driver wage ($/hr)	23				23			
Unit price ($10^3$$/unit)	250	250	350	500	300	300	400	500
Unit capacity (kg/unit)	181	181	4082	4082	454	454	9072	9072

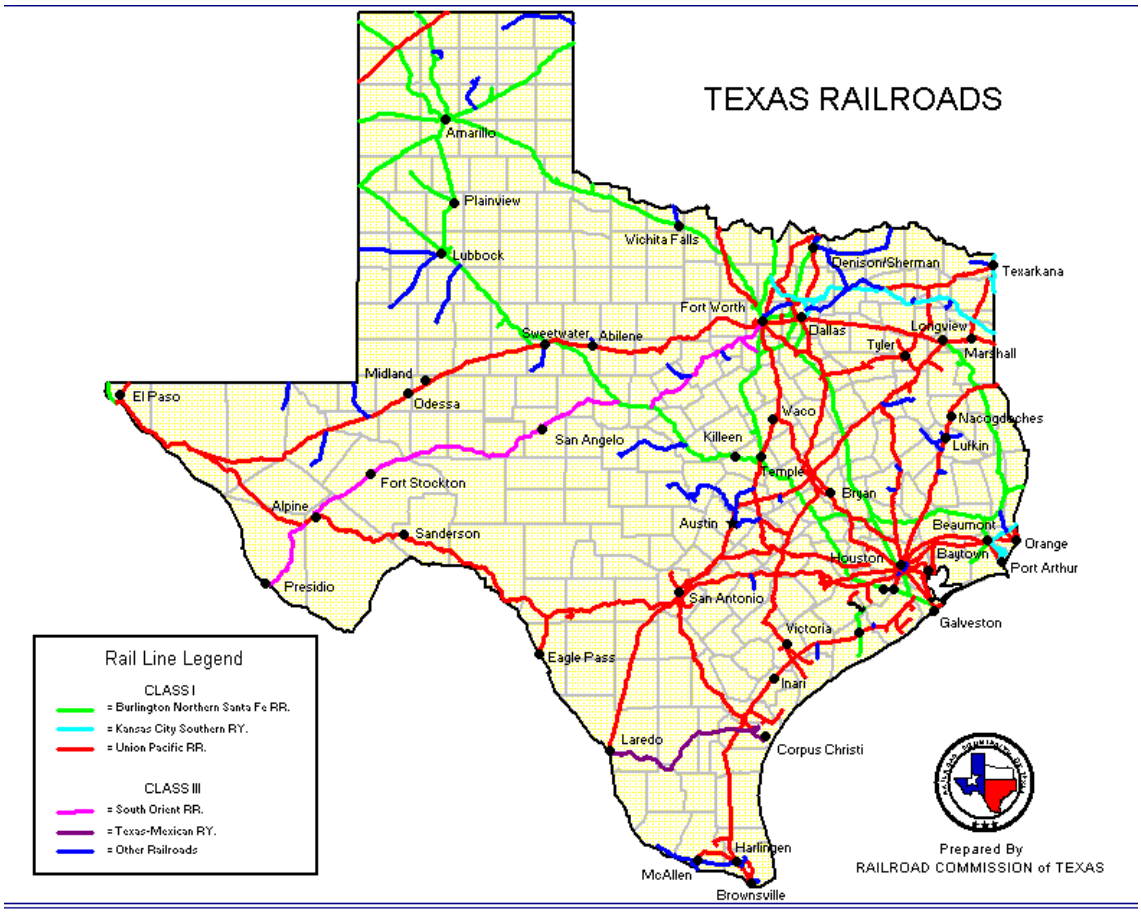

Figure 3.18. Texas railroad map (Taken from Railroad Commission of Texas).

4. SUPPLY CHAIN NETWORK SCENARIOS AND OPTIMIZATION

4.1. Base Scenario

Based on the supply chain network described above, a simulation work has performed with an objective function of maximizing NPV. The optimal configuration of hydrogen supply chain network for the whole time horizon is shown in Figure 4.1. It was anticipated that SMR with compression would mostly dominate the hydrogen production capacity because the technology has both low unit hydrogen production cost and plant capital/operating cost.

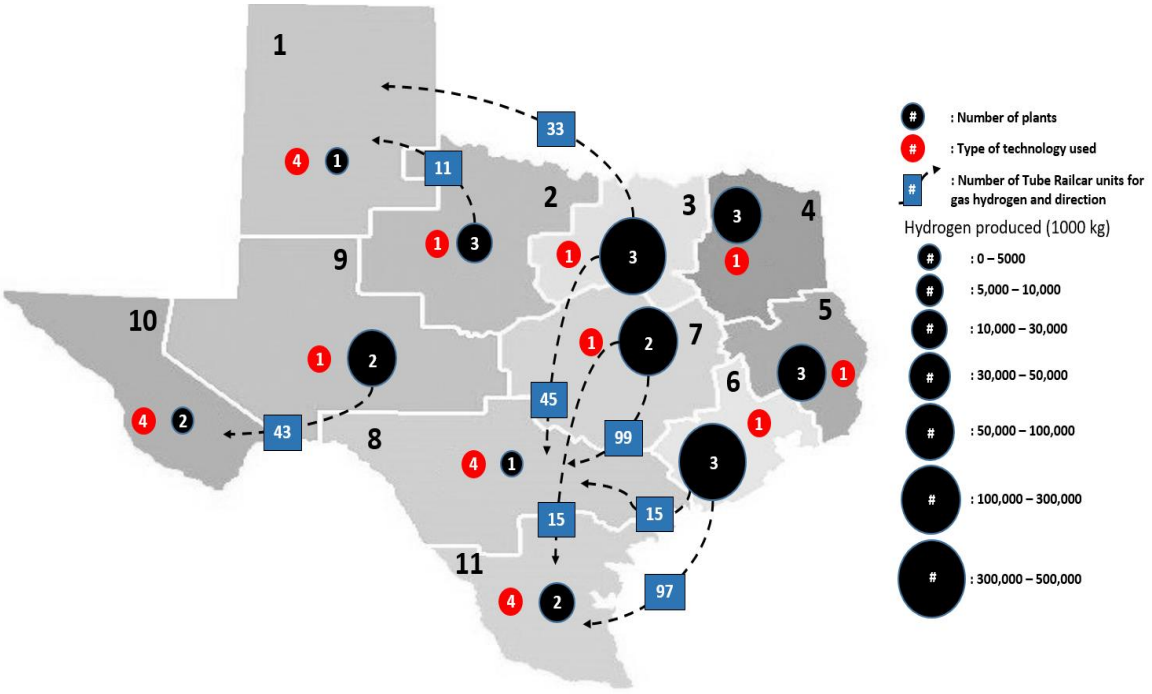

Figure 4.1. Optimal configuration of base scenario for the whole time periods.

During the scenario simulation, the technologies only selected are SMR with compression and alkaline/PEM electrolysis with compression, but mostly SMR with compression is dominantly used to produce hydrogen. Such dominant amount of hydrogen production is concentrated in the cell 3, cell 6, and cell 7, as the cells have high hydrogen demand with resource, natural gas. The cells without natural gas, cell 1, cell 8, cell 10, and cell 11, choose Alkaline/PEM electrolysis to produce hydrogen. Among the four transportation units, the one selected is only tube railcar. The hydrogen production strategy for the whole time periods is shown in Table 4.1.

Table 4.1. Optimal hydrogen production strategy for base scenario

Cell	Technology	Hydrogen production during period (1000 kg)							
		t1	t2	t3	t4	t5	t6	t7	t8
i1	APE	0	0	0	0	106.9	106.9	0	106.9
i2	SMR	19.4	1068.2	2657.7	2821.0	3321.1	3528.9	3603.9	11101.1
i3	SMR	274.9	5798.6	30683.6	68917.3	90327.9	81391.8	92873.4	97513.3
i4	SMR	40.8	868.8	4030.6	6432.7	7861.8	8711.2	9325.8	9946.3
i5	SMR	27.0	587.1	2692.9	4245.5	5118.5	5582.7	5865.7	6126.0
i6	SMR	239.2	6984.9	45050.4	59856.0	73545.8	73253.0	95606.1	96019.4
i7	SMR	113.9	4847.8	13015.1	22007.6	28488.3	70400.8	64364.1	70757.3
i8	APE	0	0	0	46.9	46.9	0	0	0
i9	SMR	19.7	1139.0	5372.9	8312.6	9868.8	11100.1	11345.2	12369.8
i10	APE	0	0	0	353.4	661.5	661.5	661.5	661.5
i11	APE	82.0	139.9	144.7	144.7	993.6	993.6	993.6	10566.1
Total	SMR	734.9	21294.3	103503.1	172592.6	218532.1	253968.5	282984.1	303833.2
	APE	82.0	139.9	144.7	545.1	1809.0	1762.0	1655.1	11334.5

The financial investment values for the base case is summarized in Table 4.2 below. It represents that the total cost is mainly dominated by resource costs, dumping costs, and plant capital costs. The carbon credit comes from extracting biomass is also applied to decrease the dumping costs.

Table 4.2. All costs for the optimal solution for base scenario

Cost type	Cost (10^9 $)
Plant capital cost	4.37
Plant decommissioning cost	0
Plant fixed operating cost	2.04
Plant variable operating cost	1.83
Transport capital cost	0.22
Transport operating cost	3.24
Resource cost	12.22
Dumping cost	5.84
Total	29.77

4.2. Discounted Electricity Price Scenarios

In addition to the based case scenario, the two extra scenarios regarding electricity price change have been performed to check if the electricity price can affect the technology transition from SMR to more renewable technologies including biomass gasification, alkaline/PEM electrolysis or solid oxide electrolysis. The three scenario studies including original electricity price, 15% discounted electricity price, and 30% discounted electricity price are simulated. As shown in Table 4.1, alkaline/PEM electrolysis and solid oxide electrolysis require especially a lot of electricity among hydrogen production methods. So it was expected that the technologies including those two methods more to be chosen to produce hydrogen regardless of hydrogen phase, as the electricity price goes cheaper. The discounted electricity price is described below in Table 4.3.

Table 4.3. Electricity price for discounted electricity price scenarios

Electricity type	0% Discounted	15% Discounted	30% Discounted
Hydro Electricity ($/kwh)	0.0594	0.0505	0.0416
Solar Electricity ($/kwh)	0.0599	0.0509	0.0419
Wind Electricity ($/kwh)	0.0469	0.0399	0.0328

Regardless of the degree of the electricity price discount, the electricity source selected is the 100% wind power, because of the price difference among the sources. And only compressed hydrogen is produced for all scenarios because the hydrogen demand is not big enough to make up the huge capital and operating cost for the liquefaction process. Over the time periods, there is a trend regarding the technology use, specifically more hydrogen is produced from technologies including alkaline/PEM electrolysis and solid oxide electrolysis when electricity price goes down. Specifically in time period 7 with no discount, hydrogen amount from SMR is bigger almost 171 times than the hydrogen from alkaline/PEM electrolysis. However, the ratio decreases to 3.7 for the 30% discount scenario.

For the cells with no natural gas resource, such as cell 1, 8, 10, and 11, select alkaline/PEM electrolysis rather than using SMR with natural gas transported from other cells. And for the cell-3, solid oxide electrolysis appears at time period 8 rather than increasing the SMR capacity. Such trend is described in Table 4.4 – 4.6 below which represent hydrogen production from each cell for the time periods 1, 7, and 8. The tables for other time periods are located in Appendix C. The optimal configuration of hydrogen supply chain network for the eighth time period in 30% discount scenario is shown below in Figure 4.2, which has the biggest hydrogen demand. In the figure, tube railcar is selected to transport the compressed hydrogen, especially for the cells with no natural gas resource. Such this phenomenon is understood that the process including both hydrogen production through SMR and transportation is still relatively cheaper than the cost of expanding alkaline/PEM electrolysis capacity.

From the discounted electricity price scenarios described above, it is obvious that the scenarios represent a possibility of renewable technologies to be used more extensively with the help of the policies regarding electricity price, such as governmental subsidies can cause the electricity price to go down.

Table 4.4. Comparison of optimal hydrogen production strategies for discounted electricity price scenarios at first time period

Time period 1		**Hydrogen production (1000 kg)**		
Cell	**Technology**	**0% Discount**	**15% Discount**	**30% Discount**
i1	APE	0	29.9	29.9
i2	SMR	19.4	19.4	19.4
i3	SMR	274.9	274.9	274.9
i4	SMR	40.8	40.8	40.8
i5	SMR	27.0	27.0	27.0
i6	SMR	239.2	239.2	239.2
i7	SMR	113.9	113.9	113.9
i8	APE	0	0	95.9
i9	SMR	19.7	19.7	19.7
i10	APE	0	29.3	29.3
i11	APE	82.0	82.0	82.0
Total	SMR	734.9	734.9	734.9
	APE	82.0	141.2	237.1
Ratio	SMR / APE	9.0	5.2	3.1

Table 4.5. Comparison of optimal hydrogen production strategies for discounted electricity price scenarios at seventh time period

Time period 7		Hydrogen production (1000 kg)		
Cell	**Technology**	**0% Discount**	**15% Discount**	**30% Discount**
i1	APE	0	3499.5	6735.3
i2	SMR	3603.9	6089.5	4073.0
i3	SMR	92873.4	88983.2	85669.0
i4	SMR	9325.8	9325.8	9325.8
i5	SMR	5865.7	5865.7	5227.7
i6	SMR	95606.1	74981.6	75619.6
i7	SMR	64364.1	54772.1	37942.1
i8	APE	0	9592.0	25593.5
i9	SMR	11345.2	8859.6	6373.9
i10	APE	661.5	3604.7	6090.3
i11	APE	993.6	21618.0	22446.6
Total	SMR	282984.1	248877.5	224231.1
	APE	1655.1	38314.1	60865.7
Ratio	SMR / APE	171.0	6.5	3.7

Table 4.6. Comparison of optimal hydrogen production strategies for discounted electricity price scenarios at eighth time period

Time period 8		Hydrogen production (1000 kg)		
Cell	**Technology**	**0% Discount**	**15% Discount**	**30% Discount**
i1	APE	106.9	0	6813.7
i2	SMR	11101.1	7786.9	4472.7
i3	SMR	97513.3	97513.3	89049.5
	SOE	0	0	8463.8
i4	SMR	9946.3	9946.3	9946.3
i5	SMR	6126.0	6126.0	6126.0
i6	SMR	96019.4	83591.1	85150.6
i7	SMR	70757.3	61165.4	42653.2
i8	APE	0	9592.0	25716.2
i9	SMR	12369.8	9062.4	6576.8
i10	APE	661.5	3968.9	6454.6
i11	APE	10566.1	22994.3	23822.9
Total	SMR	303833.2	275191.4	243975.0
	APE	11334.5	36555.2	62807.3
	SOE	0	0	8463.8
Ratio	SMR /(APE+SOE)	26.8	7.5	3.4

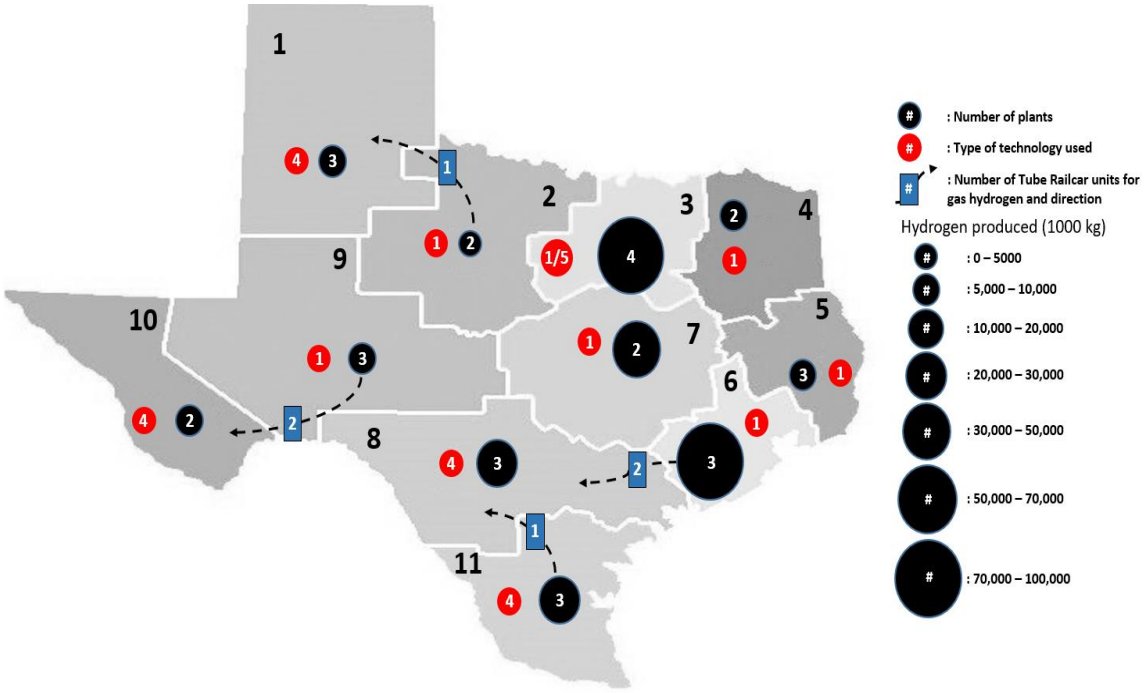

Figure 4.2. Optimal configuration of 30% discounted electricity price scenario for the eighth time period.

4.3. Horizon 2020 Project Scenario

As explained in above chapter 3.11.3, Horizon 2020 project in this case studies represents for limiting the extractable amount of fossil fuels, for example, coal and natural gas every year. It was expected that Horizon 2020 project has an effect of decreasing the capacity of plants with conventional technologies, such as coal gasification and SMR. For each time period, only 15% of previous period's extractable fossil fuel is allowed to be used.

During the scenario simulation, the technologies selected are SMR, biomass gasification, and alkaline/PEM electrolysis, and only compressed hydrogen is produced. Dominant hydrogen is produced from cell 3 and cell 6 through SMR until the middle periods, but a technology transition from SMR to biomass gasification and alkaline/PEM electrolysis starts at the sixth time period because of fossil fuel depletion. As a result, hydrogen is dominantly produced from those technologies at the last time period. Most hydrogen is

still produced from the cells with high demand, but the technology transition affected hydrogen to be produced from sustainable technologies rather than SMR. The hydrogen production data for the whole time periods is shown below in Table 4.7.

Table 4.7. Optimal hydrogen production strategy for original Horizon 2020 scenario

Cell	Technology	Hydrogen production during period (1000 kg)							
		t1	t2	t3	t4	t5	t6	t7	t8
i1	BG	0	0	0	0	4409.0	5675.0	5675.0	5675.0
	APE	0	0	0	0	0	231.8	1529.4	1529.4
i2	SMR	19.4	1068.2	1829.2	2821.0	4978.2	23414.1	21003.4	2449.9
	APE	0	0	0	0	0	0	0	19917.0
i3	SMR	274.9	5798.6	52898.4	53174.8	62985.7	8549.4	470.0	0
	BG	0	0	0	0	0	25269.2	25269.2	25269.2
	APE	0	0	0	0	0	0	20159.4	50034.8
i4	SMR	40.8	868.8	4030.6	6432.7	7861.8	21882.5	31696.7	9241.8
i5	SMR	27.0	587.1	2692.9	4245.5	11746.9	12211.1	12211.1	2099.7
	APE	0	0	0	0	0	0	0	9958.5
i6	SMR	239.2	5327.8	26149.8	75598.5	89288.2	94795.3	94795.3	17346.7
	BG	0	0	0	0	0	0	0	28250.8
	APE	0	0	0	0	0	0	0	29875.4
i7	SMR	113.9	4847.8	13015.1	22007.6	28488.3	12360.3	1854.0	63.5
	APE	0	0	0	0	0	0	16557.4	43418.3
i8	APE	0	0	0	46.9	232.6	10191.1	19793.6	29752.1
i9	SMR	19.7	2796.1	2887.2	8312.6	9040.2	9443.0	4716.8	752.1
	APE	0	0	0	0	0	0	0	4996.1
i10	APE	0	0	0	0	1490.1	1490.1	7747.4	8111.7
i11	APE	82.0	139.9	144.7	144.7	416.3	20050.3	21618.0	21618.0
Total	SMR	734.9	21294.3	103503.1	172592.6	214389.3	182655.5	166747.3	31953.7
	BG	0	0	0	0	4409.0	30944.2	30944.2	59195.0
	APE	82.0	139.9	144.7	191.7	2138.9	31963.1	87405.2	219211.2

The optimal configuration of hydrogen supply chain network for the whole time periods in horizon 2020 project is shown below in Figure 4.3. As the fossil fuels get rarer over time, raw material transportation also happens from the fifth time period. In specific, natural gas is transported via tube railcar from the natural gas rich cell to others to produce hydrogen through SMR. For some cells, such as cell 1, 3, and 6, biomass gasification is also considered, and biomass is transported through tank railcar to satisfy such technology transition.

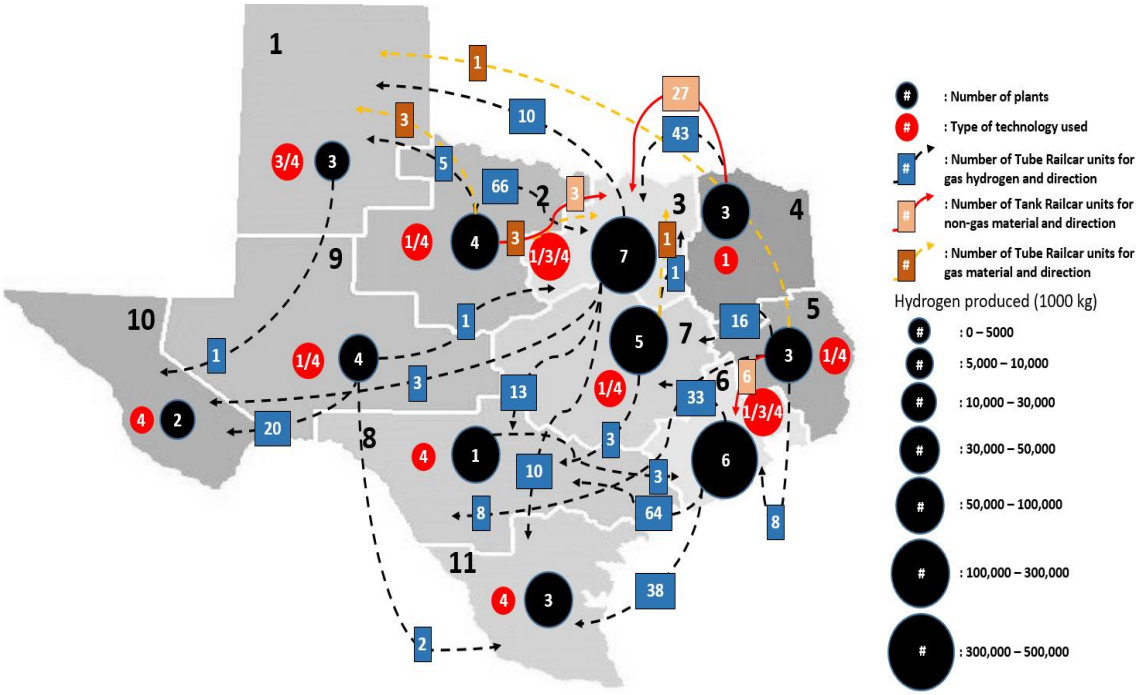

Figure 4.3. Optimal configuration of the original Horizon 2020 scenario for the whole time periods.

Among the hydrogen transportation units, only tube railcar is used. Until the middle periods, the produced hydrogen is mostly transported from the cells with natural gas source to other cells which do not have the source. However, after the middle periods, as much hydrogen starts to be produced from biomass gasification and alkaline/PEM electrolysis, the hydrogen is transported from the cells with high hydrogen demand, such as cell 3, 6, and 7.

4.4. Combined Scenarios

As illustrated in chapter 4.3, limiting the extractable amount of fossil fuels plays an important role in determining the hydrogen production technologies. In this section, two other scenarios regarding both electricity price change and limitation of the amount of fossil fuels to estimate how much degree of technology transition could be achieved. The fossil fuel limitation ratio used for these scenarios is the same ratio of Horizon 2020 project in chapter 4.3, and electricity discount ratio of 15% and 30% are used.

The optimal hydrogen production data for the whole time period is described in Table 4.8. During the scenario simulation, four technologies including SMR, biomass gasification, alkaline/PEM electrolysis, and solid oxide electrolysis are selected only to produce compressed hydrogen. Generally, hydrogen production data shows similar technology selection trend, but it is noticeable that the technology transition from SMR to other sustainable three technologies starts faster than the original Horizon 2020 case discussed in chapter 4.3. It is understood that the cheaper electricity price triggers and accelerates such that transition as the electricity price directly affects the unit hydrogen production costs, especially for the two electrolysis technologies.

More specifically, SMR still shows its hydrogen production dominance up until the fifth time period. However, the quantity of hydrogen produced from SMR is relatively lower than the original Horizon 2020 scenario’s one. Meanwhile the amount of hydrogen produced from alkaline/PEM electrolysis is remarkable compared to its hydrogen

production of the original Horizon 2020 scenario, as its production capacity expands fast even in early time periods, and starts to produce more hydrogen from the seventh time period.

Table 4.8. Optimal hydrogen production strategy for Horizon 2020 with 15% discounted electricity price scenario

Cell	Technology	Hydrogen production during period (1000 kg)							
		t1	t2	t3	t4	t5	t6	t7	t8
i1	APE	29.9	661.3	596.4	2457.4	3580.5	6735.3	7204.4	7642.2
i2	SMR	19.4	406.9	1829.2	5306.6	5806.7	6014.5	6089.5	3191.8
	APE	0	0	0	0	0	0	0	452.3
i3	SMR	274.9	5798.6	30915.7	48231.8	52711.1	8549.4	470.0	116.7
	BG	0	0	0	0	0	25269.2	25269.2	25269.2
	APE	0	0	0	0	1989.1	20910.2	40044.6	57968.5
i4	SMR	40.8	868.8	4030.6	6432.7	16147.3	26260.2	26725.4	8383.2
	APE	0	0	0	0	0	0	0	1563.1
i5	SMR	27.0	587.1	2692.9	4245.5	5118.5	5582.7	5865.7	2099.7
	APE	0	0	0	0	0	0	0	4026.2
i6	SMR	239.2	6984.9	41892.3	60684.6	65636.8	68281.7	73288.9	12674.8
	APE	0	0	0	0	0	0	0	29875.4
	SOE	0	0	0	0	0	0	1692.8	18620.4
i7	SMR	113.9	4294.7	13015.1	22007.6	22007.6	12360.3	1854.0	278.1
	APE	0	0	0	0	8962.6	19158.6	36088.0	42375.1
i8	APE	95.9	553.1	672.5	672.5	10631.0	24505.9	26422.0	48473.2
i9	SMR	19.7	450.9	2095.1	4998.4	4897.5	4471.7	5014.1	752.1
	APE	0	0	0	0	0	0	0	4167.6
i10	APE	29.3	688.1	3277.7	3667.6	5739.6	7289.9	7450.2	8111.7
i11	APE	82.0	139.9	2856.3	14230.1	17815.8	20050.3	21618.0	22994.3
Total	SMR	734.9	19391.9	96470.9	151907.2	172325.5	131520.4	119307.5	27496.4
	BG	0	0	0	0	0	25269.2	25269.2	25269.2
	APE	237.1	2042.3	7402.9	21027.5	48718.5	98650.1	138827.2	227649.6
	SOE	0	0	0	0	0	0	1692.8	18620.4

The optimal configuration of hydrogen supply chain network for the whole time periods during this scenarios is shown below in Figure 4.4. Because of the lack of fossil fuels, natural gas transportation happens from the sixth time period. Additionally, as a part of technology transition, biomass gasification starts to alternate SMR from the sixth time period of cell 3 and produces considerable amount of compressed hydrogen. In this

process, extra needed biomass is transported from other cells which have enough amount of biomass, such as cell 2 and cell 4. In more detail, tube railcar and tank railcar units are used to transport natural gas and biomass, respectively.

To transport hydrogen, the only transportation unit used is tube railcar. One noticeable trend in hydrogen transportation is that it shows much fewer transportation units compared to the original Horizon 2020 scenario. It is understood that the discounted electricity price contributes to each cell's hydrogen security, as it decreases the unit hydrogen production costs.

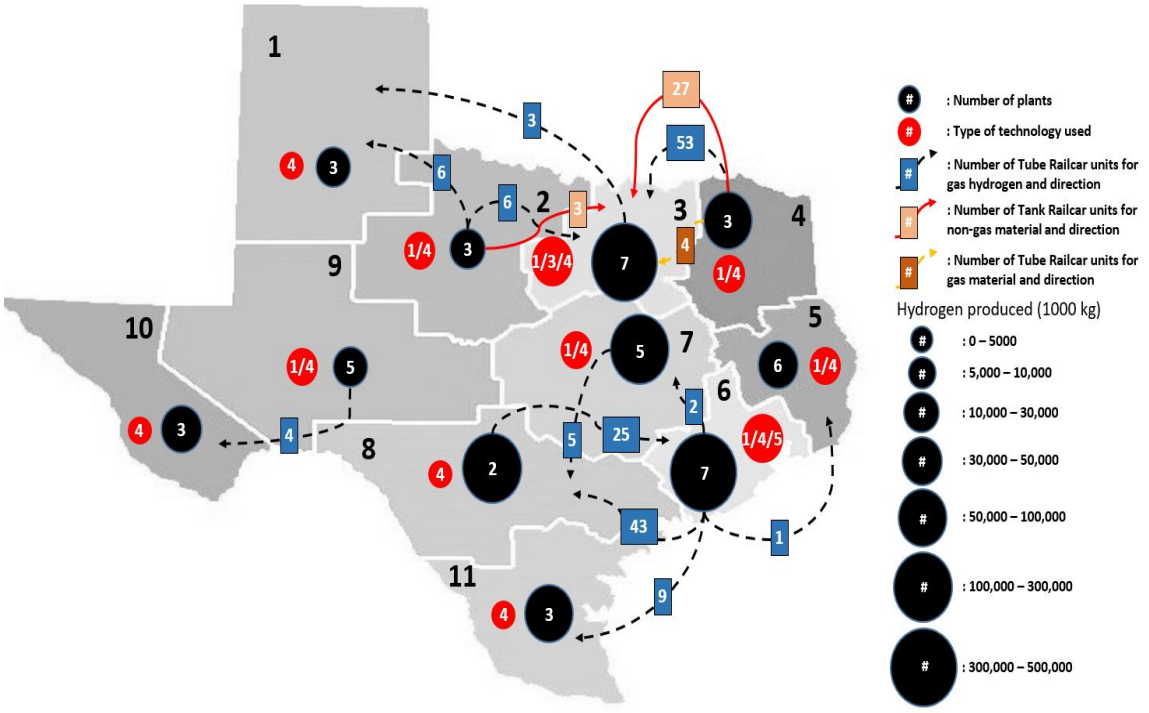

Figure 4.4. Optimal configuration of the 15% discounted electricity price with Horizon 2020 scenario for the whole time periods.

Similar to the Horizon 2020 scenario without electricity price discount, hydrogen is mostly transported from the cells with SMR technology to the cells without it, such as cell 1, 8, 10, and 11, at both early and middle periods. After the periods, hydrogen is mainly transported to the cells with high hydrogen demand, especially for the cell 3 and cell 6.

When the 30% electricity price is applied to the original Horizon 2020 scenario, the hydrogen network shows very similar structure to the 15% electricity price discount scenario, as described in Table 4.9 below. As the previous scenario, only compressed hydrogen is produced from the four technologies, SMR, biomass gasification, alkaline/PEM electrolysis, and solid oxide electrolysis. However, a considerable amount

Table 4.9. Optimal hydrogen production strategy for Horizon 2020 with 30% discounted electricity price scenario

Cell	Technology	Hydrogen production during period (1000 kg)							
		t1	t2	t3	t4	t5	t6	t7	t8
i1	APE	29.9	661.3	596.4	800.3	6066.1	6735.3	7204.4	7642.2
i2	SMR	19.4	406.9	1829.2	2821.0	3321.1	19271.3	19271.3	3191.8
	APE	0	0	0	0	0	0	0	452.3
i3	SMR	274.9	5798.6	41686.9	54860.2	54871.1	9158.2	1078.9	0
	BG	0	0	0	0	0	9171.9	9171.9	9171.9
	APE	0	0	0	0	8114.6	39833.9	59750.9	73692.7
i4	SMR	40.8	868.8	4030.6	6432.7	7861.8	8711.2	9204.4	9204.4
	APE	0	0	0	0	0	0	0	620.5
	SOE	0	0	0	0	0	0	121.5	121.5
i5	SMR	27.0	587.1	2692.9	4245.5	5118.5	5582.7	5865.7	2099.7
	APE	0	0	0	0	0	0	0	4854.8
i6	SMR	239.2	5327.8	26149.8	44113.6	64687.2	67453.1	67453.1	10848.2
	APE	0	0	0	0	0	0	0	29875.4
	SOE	0	0	0	0	0	0	7528.5	24545.0
i7	SMR	113.9	2637.6	13015.1	24680.4	26303.0	12360.3	1709.0	0
	BG	0	0	0	0	0	0	3084.3	3084.3
	APE	0	0	0	0	2185.4	21106.5	33056.6	51976.4
	SOE	0	0	0	0	0	0	92.1	92.1
i8	APE	95.9	2210.2	2329.6	12288.1	14062.4	24505.9	26422.0	28104.2
i9	SMR	19.7	450.9	2095.1	3341.3	4068.9	4471.7	4471.7	752.1
	APE	0	0	0	0	0	0	245.1	4167.6
i10	APE	29.3	688.1	792.1	5324.7	6568.1	7289.9	7747.4	8111.7
i11	APE	82.0	1797.0	8656.1	14230.1	17815.8	20050.3	21618.0	25480.0
Total	SMR	734.9	16077.7	91499.6	140494.6	166231.6	127008.5	109054.0	26096.3
	BG	0	0	0	0	0	9171.9	12256.2	12256.2
	APE	237.1	5356.5	12374.2	32643.1	54812.4	119521.7	156044.5	234977.8
	SOE	0	0	0	0	0	0	7742.1	24758.6

of hydrogen is produced from the two electrolysis technologies, and the amount is bigger than the one from the 15% discount scenario. Simple, the electricity price plays an important role especially in technology transition, as the transition from SMR to electrolysis is more proceeded when more electricity price discount is applied.

It is also observed that there is another technology transition between biomass gasification and solid oxide electrolysis in late time periods, as both technologies require natural gas for their operation. Generally, the solid oxide electrolysis is more preferred when there is enough amount of natural gas, most because of its cheap capital costs. Such trend is observed in cell 4 and cell 6. However, when the extractable amount of natural gas is too much limited over time periods by the Horizon 2020 project, the biomass gasification is more preferred because it requires less amount of natural gas, only 12.3% of the natural gas required for solid oxide electrolysis. Specifically, in cell 3 and cell 7, biomass gasification is selected for their late time periods rather than selecting solid oxide electrolysis with natural gas transportation.

The optimal results of the Horizon 2020 project with 30% discount scenario for the whole time periods are shown in Figure 4.5. The number of total technologies remains as same with the 15% discount scenario, but some technologies, such as biomass gasification and solid oxide electrolysis, are newly introduced to cells, cell 4 and cell 7.

The transportation unit selected for this scenario is only tube railcar for both natural gas and hydrogen. The hydrogen transportation starts from the third time period. Similar to the 15% discount scenario, most of them until middle time periods head for the cells which do not use SMR for hydrogen production. For the late time periods, hydrogen is mainly transported to the cells, with high hydrogen demand as having hydrogen through transportation is preferred rather than increasing the plant production capacity. The natural gas is transported in the eighth time period as an extra amount of natural gas is required for the cell 3 to produce hydrogen from biomass gasification.

Compared to the 15% discount scenario, it is also observed that both raw material and hydrogen security for all cells have been improved because of the decreased number of

transportation units. This represents that each cell utilizes more raw materials and existing plant production capacity existing than other discount scenarios.

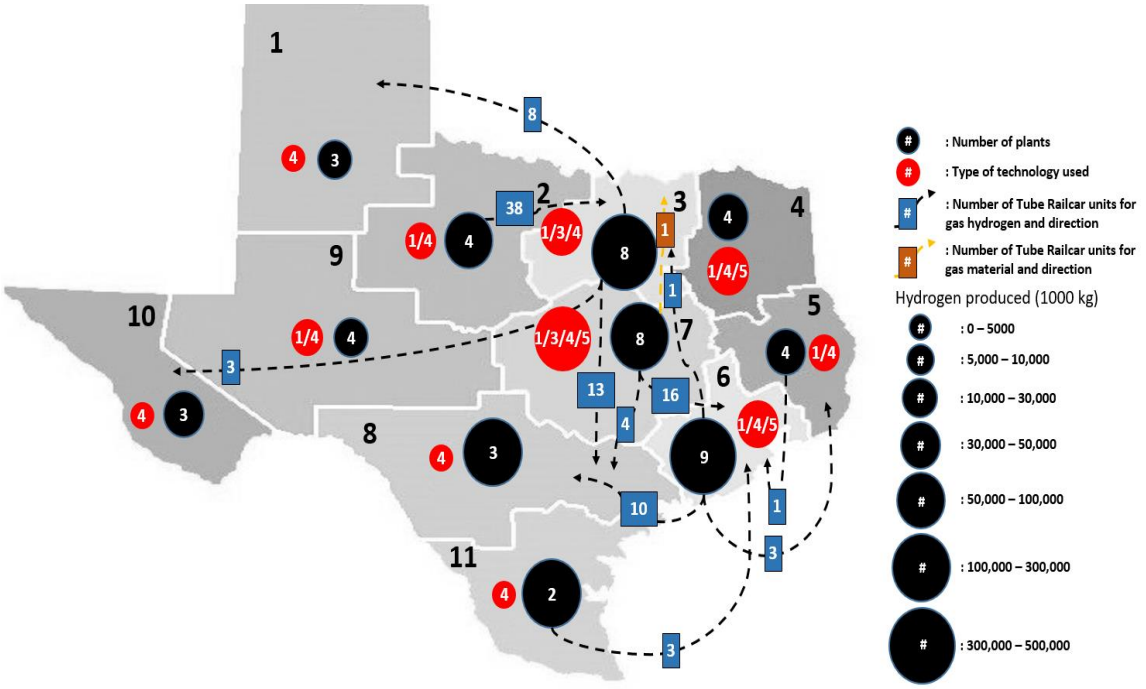

Figure 4.5. Optimal configuration of the 30% electricity price discount with Horizon 2020 scenario for the whole time periods.

4.5. Efficient Set of Solutions for Base Scenario

To reflect the degree of environmental impact described in the chapter 3.11.4 into the supply chain network, the Eco-Indicator 99 methodology is applied to the base case scenarios explained in the chapter 4.1. The goal of this process is to build the best strategy that achieves both maximum NPV and minimum environmental impact. To quantify the environmental impact from multiple indicators at one time, the damage factors, normalization factor, and weighting factor are considered simultaneously. For this

scenario, multi-objective optimization regarding the maximization of NPV and minimization of Eco-Indicator 99 score is performed. The set of Pareto Optimal Solutions is used to build a Pareto curve, which is shown in Figure 4.6.

It suggests a set of trade-off solutions between NPV and Eco-Indicator 99 score. The optimal solution regarding a maximization of NPV has an infrastructural design related to SMR and alkaline/PEM electrolysis for compressed hydrogen production. Meanwhile the optimal solution for a minimization of Eco-Indicator 99 score has an infrastructure that 100% depends on alkaline/PEM electrolysis for compression hydrogen production. The alternative solutions between those two extreme ones show the trade-off trend depends on the environmental constraint. Specifically, NPV moves gently at moderate environmental constraint, because an infrastructure for those optimal solutions is still mainly based on the SMR which has economic advantages origin from cheaper unit production cost. However, NPV moves rapidly at strict environmental constraint because the alternative solutions are more likely to have alkaline/PEM electrolysis rather than SMR. As a result, the alternative solutions lose economic advantages when the environmental constraint gets stricter.

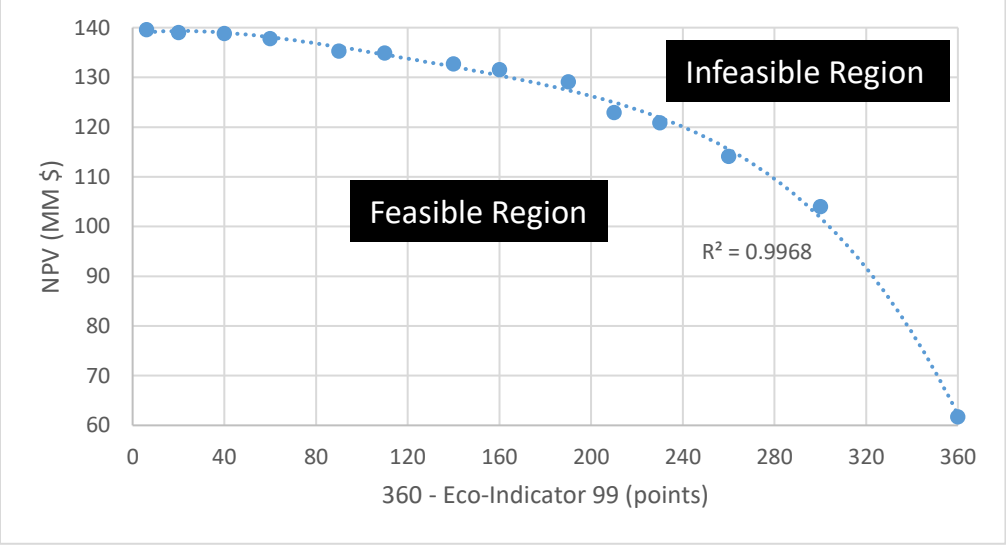

Figure 4.6. Pareto Curve for the base case.

5. CONCLUSION

The main objective of this Master dissertation, development and optimization of an integrated supply chain network for the hydrogen infrastructural development in Texas, was achieved with the MILP modelling, environmental impact assessment through multi-objective optimization. The MILP model was based on the previously cited study, which is explained in Appendix B, while the hydrogen supply chain network optimization was based on the unique parameters of target region which were mainly introduced in chapter 3. The obtained optimal solutions from introduced scenarios were compared to figure out how the operational strategy is changed from the two scenario studies, electricity price change and raw material limitation. Lastly, a set of trade-off solutions, Pareto Optimal solutions, between NPV and environmental constraint was achieved to introduce decision-making curve, which is also called as Pareto curve, for the decision makers. Suggestions for future direction are listed below:

- The use of metal hydride for hydrogen transportation
- The consideration of changing hydrogen selling price
- The consideration of adding CO_2 capture system for the hydrogen production technologies
- The consideration of introducing carbon sequestration instead of ventilation
- The consideration of adding cap-and-trade system among all cells

REFERENCES

Abele, A., 2015. Status of Existing Hydrogen Refueling Stations (No. 600-12-018). California Energy Commission.

Adamson, K.-A., Pearson, P., 2000. Hydrogen and methanol: a comparison of safety, economics, efficiencies and emissions. J. Power Sources 86, 548–555.

Almansoori, A., Shah, N., 2006. Design and Operation of a Future Hydrogen Supply Chain. Chem. Eng. Res. Des. 84, 423–438.

Arxer, M. del M., Martínez Calleja, L.E., 2007. Hercules project: Contributing to the development of the hydrogen infrastructure. J. Power Sources, Scientific Advances in Fuel Cell Systems, Turin, Italy, 13-14 September 2006 171, 224–227.

Barbir, F., 2005. PEM electrolysis for production of hydrogen from renewable energy sources. Sol. Energy, Solar Hydrogen 78, 661–669.

Bartolozzi, I., Rizzi, F., Frey, M., 2013. Comparison between hydrogen and electric vehicles by life cycle assessment: A case study in Tuscany, Italy. Appl. Energy, Sustainable Development of Energy, Water and Environment Systems 101, 103–111.

Brown, T., Schell, L.S., Stephens-Romero, S., Samuelsen, S., 2013. Economic analysis of near-term California hydrogen infrastructure. Int. J. Hydrog. Energy 38, 3846–3857.

Cannon, J.S., 1994. Hydrogen vehicle programs in the U.S.A. Int. J. Hydrog. Energy 19, 905–909.

DOE, 2015. DOE Hydrogen and Fuel Cells Program: DOE H2A Production Analysis. US Department of Energy.

EIA, 2017a. Annual Energy Outlook. US Energy Information Administration.

EIA, 2017b. Texas State Profile and Energy Estimates. US Energy Information Administration.

EIA, 2017c. Levelized Cost and Levelized Avoided Cost of New Generation Resources in the Annual Energy Outlook 2017. US Energy Information Administration.

Elaine, C., Patricia, H., Rolf, S., Michael, S., Long, N., 2017. National Transportation Statistics.

Feng, W., Wang, S., Ni, W., Chen, C., 2004. The future of hydrogen infrastructure for fuel cell vehicles in China and a case of application in Beijing. Int. J. Hydrog. Energy, Fuel Cells 29, 355–367.

Gahleitner, G., 2013. Hydrogen from renewable electricity: An international review of power-to-gas pilot plants for stationary applications. Int. J. Hydrog. Energy 38, 2039–2061.

García, E.Y., Laborde, M.A., 1991. Hydrogen production by the steam reforming of ethanol: Thermodynamic analysis. Int. J. Hydrog. Energy 16, 307–312.

Hu, W., 2000. Electrocatalytic properties of new electrocatalysts for hydrogen evolution in alkaline water electrolysis. Int. J. Hydrog. Energy 25, 111–118.

Hugo, A., Pistikopoulos, E.N., 2005. Environmentally conscious long-range planning and design of supply chain networks. J. Clean. Prod., Recent advances in industrial process optimisationRecent advances in industrial process optimisation 13, 1471–1491.

Hugo, A., Rutter, P., Pistikopoulos, S., Amorelli, A., Zoia, G., 2005. Hydrogen infrastructure strategic planning using multi-objective optimization. Int. J. Hydrog. Energy 30, 1523–1534. doi:10.1016/j.ijhydene.2005.04.017

Huss, A., 2013. Wind power and hydrogen: complementary energy sources for sustainable energy supply. Fuel Cells Bull. 2013, 12–17.

Hwang, J.-J., 2013. Sustainability study of hydrogen pathways for fuel cell vehicle applications. Renew. Sustain. Energy Rev. 19, 220–229.

Jeremiah, K., 2015. Vehicle Titles and Registration Division (VTR) Fiscal Year (FY) 2014.

Joffe, D., Hart, D., Bauen, A., 2004. Modelling of hydrogen infrastructure for vehicle refuelling in London. J. Power Sources, Selected papers presented at the Eighth Grove Fuel Cell Symposium 131, 13–22.

Kamarudin, S.K., Daud, W.R.W., Yaakub, Z., Misron, Z., Anuar, W., Yusuf, N.N.A.N., 2009. Synthesis and optimization of future hydrogen energy infrastructure planning in Peninsular Malaysia. Int. J. Hydrog. Energy 34, 2077–2088.

Kim, J., Lee, Y., Moon, I., 2008. Optimization of a hydrogen supply chain under demand uncertainty. Int. J. Hydrog. Energy 33, 4715–4729.

Kim, J., Moon, I., 2008. Strategic design of hydrogen infrastructure considering cost and safety using multiobjective optimization. Int. J. Hydrog. Energy 33, 5887–5896.

Langford, B.C., Cherry, C., 2012. Transitioning a bus transit fleet to hydrogen fuel: A case study of Knoxville Area Transit. Int. J. Hydrog. Energy, 2010 AIChE Annual Meeting Topical Conference on Hydrogen Production and Storage Special Issue 37, 2635–2643.

Li, Z., Gao, D., Chang, L., Liu, P., Pistikopoulos, E.N., 2008. Hydrogen infrastructure design and optimization: A case study of China. Int. J. Hydrog. Energy 33, 5275–5286.

Liu, P., Gerogiorgis, D.I., Pistikopoulos, E.N., 2007. Modeling and optimization of polygeneration energy systems. Catal. Today, I.A. Vasalos Festschrift 127, 347–359.

Liu, P., Whitaker, A., Pistikopoulos, E.N., Li, Z., 2011. A mixed-integer programming approach to strategic planning of chemical centres: A case study in the UK. Comput. Chem. Eng., Energy & Sustainability 35, 1359–1373.

Lopez, A., Roberts, B., Heimiller, D., Blair, N., Porro, G., 2012. U.S. Renewable Energy Technical Potentials: A GIS-Based Analysis (Technical Report). NREL.

Manabe, A., Kashiwase, M., Hashimoto, T., Hayashida, T., Kato, A., Hirao, K., Shimomura, I., Nagashima, I., 2013. Basic study of alkaline water electrolysis. Electrochimica Acta 100, 249–256.

Mark, G., Renilde, S., 2001. The Eco-indicator 99: a damage oriented method for life cycle assessment, Methodology Report (No. 3rd edition). PRé Consultants.

Mulder, G., Hetland, J., Lenaers, G., 2007. Towards a sustainable hydrogen economy: Hydrogen pathways and infrastructure. Int. J. Hydrog. Energy, EHEC2005 32, 1324–1331.

National Academy of Engineering, National Research Council, Division on Engineering and Physical Sciences, Board on Energy and Environmental Systems, Committee on Alternatives and Strategies for Future Hydrogen Production and Use, 2004. The Hydrogen Economy: Opportunities, Costs, Barriers, and R&D Needs. National Academies Press.

Nicholas, M., Ogden, J., 2006. Detailed Analysis of Urban Station Siting for California Hydrogen Highway Network. Transp. Res. Rec. J. Transp. Res. Board 1983, 121–128.

NREL and AWS Truepower, 2010a. United States - Annual Average Wind Speed at 80m. National Renewable Energy Laboratory (NREL), AWS Truepower.

NREL and AWS Truepower, 2010b. U.S. Wind Capacity Potential (MW) at 80 Meters. National Renewable Energy Laboratory (NREL), AWS Truepower.

Schrank, D., Eisele, B., Lomax, T., Bak, J., 2015. 2015 Urban Mobility Scorecard.

Stephens-Romero, S., Samuelsen, G.S., 2009. Demonstration of a novel assessment methodology for hydrogen infrastructure deployment. Int. J. Hydrog. Energy 34, 628–641.

Stiller, C., Bünger, U., Møller-Holst, S., Svensson, A.M., Espegren, K.A., Nowak, M., 2010. Pathways to a hydrogen fuel infrastructure in Norway. Int. J. Hydrog. Energy, 2008 International Hydrogen Forum (HyForum2008)2008 International Hydrogen 35, 2597–2601.

Texas State Data Center et al., 2014. Projections of the Population of Texas and Counties in Texas by Age, Sec and Race/Ethinicity for 2010-2050. Texas State Data Center, The Office of the State Demographer, The Hobby Center for Public Policy.

Turner, J., Sverdrup, G., Mann, M.K., Maness, P.-C., Kroposki, B., Ghirardi, M., Evans, R.J., Blake, D., 2008. Renewable hydrogen production. Int. J. Energy Res. 32, 379–407.

Ulf, B., Baldur, E., 2003. Energy and the Hydrogen Economy.

Wade, A., 1998. Costs of Storing and Transporting Hydrogen. National Renewable Energy Laboratory.

APPENDIX A

Nomenclature

Binary variables

AE(i,tk,pl,t) 1 if technology *tk* expands for plant *pl* in cell *i* during time period *t*, 0 if not

AS(i,tk,pl,t) 1 if technology *tk* shrinks for plant *pl* in cell *i* during time period *t*, 0 if not

B(i,r,t) 1 if resource *r* is extracted in cell *i* during time period *t*, 0 if not

(i,tk,pl,t,step) Weighing variable for *PCC* and *PFOC*

Fpbin(i,j,tr,p,t) 1 if a flow of product *p* occurs between cell *i* and *j* by mode *tr* during time period *t*, 0 if not

Frbin(i,j,tr,r,t) 1 if a flow of raw material *r* occurs between cell *i* and *j* by mode *tr* during time period *t*, 0 if not

Liq(i,tk,pl,t) 1 if technology tk uses liquefaction for plant *pl* in cell *i* during time period *t*, 0 if not

Transexpbinp(tr,p,t) 1 if the number of transport units of mode *tr* for product *p* expands during time period *t*, 0 if not

Transexpbinr(tr,r,t) 1 if the number of transport units of mode *tr* for raw material *r* expands during time period *t*, 0 if not

Transshrinkbinp(tr,p,t) 1 if the number of transport units of mode *tr* for product *p* shrinks during time period *t*, 0 if not

Transshrinkbinr(tr,r,t) 1 if the number of transport units of mode *tr* for raw material *r* shrinks during time period *t*, 0 if not

Integer variables

NTUexpp(tr,p,t) Number of transport units of mode *tr* used to transport product *p* purchased in time period *t*

NTUexpr(tr,r,t) Number of transport units of mode *tr* used to transport raw material *r* purchased in time period *t*

NTUp(i,j,tr,p,t)	Number of transport units of mode *tr* used to transport product *p* from cell *i* to cell *j* during time period *t*
NTUr(i,j,tr,r,t)	Number of transport units of mode *tr* used to transport raw material *r* from cell *i* to cell *j* during time period *t*
NTUshrinkp(tr,p,t)	Number of transport units of mode *tr* used to transport product *p* sold in time period *t*
NTUshrinkr(tr,r,t)	Number of transport units of mode *tr* used to transport raw material *r* sold in time period *t*

Continuous variables

Capex(t)	Capital expenditure in time period *t*
Consumption(i,p,t)	Mass of product *p* consumed per day in cell *i* during time period *t*
DC(t)	Dumping cost per day during time period *t*
Eco-Indicator 99	Quantified environmental impact score
EI(r,h)	Environmental impact of extraction of raw material *r* for indicator *h*
EI(w,h)	Environmental impact of emission of waste *w* for indicator *h*
Fp(i,j,tr,p,t)	Mass of product *p* flowing per day from cell *i* to cell *j* by mode *tr* during time period *t*
Fr(i,j,tr,r,t)	Mass of raw material *r* flowing per day from cell *i* to cell *j* by mode *tr* during time period *t*
H(h)	Normalized environmental impact for indicator *h*
λ(i,tk,pl,t,step)	Weighing variable for *PCC* and *PFOC*
NPV	Net present value of the entire time horizon
Opex(t)	Operation expenditure in time period *t*
P(i,tk,p,t)	Mass of product *p* produced per day in cell *i* by technology *tk* during time period *t*
PCC(t)	Plant capital cost during time period *t*
PDC(t)	Plant decommissioning cost during time period *t*
PFOC(t)	Plant fixed operating cost during time period *t*

Plantcap(i,tk,pl,t) Available capacity of technology *tk* in plant *pl* in cell *i* during time period *t*

Plantexp(i,tk,pl,t) Amount of capacity expansion of technology *tk* in plant *pl* in cell *i* during time period *t*

Plantshrink(i,tk,pl,t) Amount of capacity shrinkage of technology *tk* in plant *pl* in cell *i* during time period *t*

PR(t) Product revenue per day during time period *t*

Profit(t) Difference between *Sales(t)* and *Opex(t)* during time period *t*

PVOC(t) Plant variable operating cost per day during time period *t*

PW(i,tk,w,t) Mass of waste *w* produced per day by technology *tk* in cell *i* during time period *t*

R(i,r,t) Mass of resource *r* extracted per day from cell *i* during time period *t*

RC(t) Resource cost per day during time period *t*

RE(i,tk,e,t) Amount of electricity *e* used per day by technology *tk* in cell *i* during time period *t*

Sales(t) Product income per day during time period *t*

TCCp(t) Transport capital cost for product during time period *t*

TCCr(t) Transport capital cost for raw material during time period *t*

TDCp(t) Transport decommissioning cost for product during time period *t*

TDCr(t) Transport decommissioning cost for raw material during time period *t*

TOCp(t) Transport operating cost per day for product during time period *t*

TOCr(t) Transport operating cost per day for raw material during time period *t*

Totalprod(i,tk,t) Mass of all products produced per day in cell *i* by technology *tk* during time period *t*

TOTGHG(w) Mass of waste *w* dumped of the entire time horizon

Parameters

Availability(tk) Proportion of time for which technology *tk* is available for production

cp(p) Cost per unit mass of product *p* of the entire time horizon

cr(r) Cost per unit mass of raw material *r* extracted of the entire time horizon

DecmCT Cost per unit of capacity decommissioned for all technologies

Demand(i,t) Mass per day of total products demanded in cell *i* during time period *t*

Dist(i,j) Distance between cell *i* and cell *j*

dr Discount rate

Dumpprice(t,w) Cost per unit mass of waste *w* dumped during time period *t*

Eneeded(tk) Amount of electricity needed by technology *tk*

EPOT(i,e,t) Amount of electricity source *e* generable in cell *i* during time period *t*

$\eta(r,h)$ Normalization factor of extraction of raw material *r* for indicator *h*

$\eta(w,h)$ Normalization factor of emission of waste *w* for indicator *h*

fmax(i,j,tr) Maximum mass that can flow between cell *i* and cell *j* by mode *tr*

fmin(i,j,tr) Minimum mass that can flow between cell *i* and cell *j* by mode *tr*, if a flow occurs

Fuel(tr) Fuel mileage by mode *tr*

Fuelprice(tr) Fuel price by mode *tr*

Nmax(i,r) Maximum mass per day of raw material *r* that can be extracted from cell *i* of the entire time horizon

Nmin(i,r) Minimum mass per day of raw material *r* that can be extracted from cell *i* of the entire time horizon, if any extraction occurs

Omax Maximum number of transport units that can be bought per time period

Omin Minimum number of transport units that can be bought per time period, if any are bought

Ordpy(py) The order of period year *py* within its set

Ordtp(t) The order of time period *t* within its set

Plcap(i,tk,pl,t,z) Set of discrete values that span the range that *Plantcap* can take

Plexp(i,tk,pl,t,l) Set of discrete values that span the range that *Plantexp* can take

Postcap(tk) Post process capital cost coefficient of technology *tk*

Postconst(tk) Post process capital cost constant of technology *tk*

Proratio(tk,p) Fraction of total product mass that is product *p* for technology *tk*

psf Plant size factor

Qmax(tk) Maximum amount of capacity expansion or shrinking for technology *tk* per time period

Qmin(tk) Minimum amount of capacity expansion or shrinking for technology *tk* per time period, if expansion or shrinking occur

Refplantcost(tk) Cost of the reference plant for technology *tk*

Refplantcap(tk) Capacity of the reference plant for technology *tk*

ReffixedOM(tk) Fixed operations and maintenance costs of the reference plant for technology *tk*

Rinp(r,tk) Mass of raw material *r* required by technology *tk* to produce a unit mass of products

Speed(tr) Transportation speed by mode *tr*

$\theta(n,h)$ Weighing factors for indicator *h*

Transunit(tr) Maximum capacity of one transport unit of mode *tr*

tucp(tr,p) Cost to purchase one transport unit of mode *tr* for product *p*

tucr(tr,p) Cost to purchase one transport unit of mode *tr* for raw material *r*

tudcp(tr,p) Cost to decommission one transport unit of mode *tr* for product *p*

tudcr(tr,p) Cost to decommission one transport unit of mode *tr* for raw material *r*

Unitcost(e) Cost to purchase generated electricity by source *e*

$\upsilon(w,h)$ Damage factor of waste *w* for indicator *h*

APPENDIX B

The Mathematical Model based on Mixed Integer Linear Programming (MILP) Formulation

The hydrogen energy network formulation based on MILP is based on the model that previously suggested, and introduced as parts described below (Liu et al., 2011).

B.1. Parametric Domains

The superstructure formulation is introduced in Figure 3.1 previously. It is composed of several sets represent regarding various characteristics of Texas. As explained above, the Texas regions is divided into cells, *i*, to simplify express the geographical area. It is denoted as follows:

$$i \in I \coloneqq \{I_1, I_2, \dots, I_{n_i}\} \tag{1}$$

The product types, *p*, which is required to meet the demand of each cell over time, is denoted as below. The products also could be transported from one cell to others to maximize the hydrogen consumption.

$$p \in P \coloneqq \{P_1, P_2, \dots, P_{n_p}\} \tag{2}$$

The product types introduced in (2) is produced through the technologies denoted as *tk* below to increase profit through meeting the demand required.

$$tk \in TK \coloneqq \{TK_1, TK_2, \dots, TK_{n_{tk}}\} \tag{3}$$

The allowable number of plants of each technology for each cell during each time period, *pl*, is limited to one or more. Such this set allows each technology to produce more hydrogen through extra number of plants if needed.

$$pl \in PL \coloneqq \left\{PL_1, PL_2, \dots, PL_{n_{pl}}\right\} \tag{4}$$

To produce hydrogen through the introduced technologies, a set of raw materials, *r*, is denoted as below. The raw materials mostly represent the major feed stocks of each technology. The raw materials could be transported from one cell to others to maximize hydrogen production in specific cells.

$$r \in R \coloneqq \left\{R_1, R_2, \dots, R_{n_r}\right\} \tag{5}$$

Along with the set of raw materials, a set of electricity sources, *e*, is also denoted as below. It is used for all technologies for the hydrogen production with different amount respectively. Electricity transmission is not considered in this study because of the loss during its transmission.

$$e \in E \coloneqq \left\{E_1, E_2, \dots, E_{n_e}\right\} \tag{6}$$

Waste gas is produced from both raw material extraction and hydrogen production process, denoted by *w*. The waste gas could be carbon dioxide, methane, and nitrogen oxide.

$$w \in W \coloneqq \left\{W_1, W_2, \dots, W_{n_w}\right\} \tag{7}$$

To transport raw materials or hydrogen, the hydrogen infrastructure has transportation units, denoted by *tr*. Each transportation unit can transport either gaseous or non-gaseous substances from one cell to others with different cost and capacity. The number of transportation units represent a degree of material or hydrogen flows among cells.

$$tr \in TR \coloneqq \left\{TR_1, TR_2, \dots, TR_{n_{tr}}\right\} \tag{8}$$

The entire time horizon is consists of several time periods to clearly figure out any trend happens over time. It is denoted by t as follows:

$$t \in T \coloneqq \{T_1, T_2, \dots, T_{n_t}\} \tag{9}$$

Each time period is divided into period years for precise NPV calculation. The period years consist of a number of years denoted as *py* as below:

$$py \in PY \coloneqq \{PY_1, PY_2, \dots, PY_{n_{py}}\} \tag{10}$$

B.2. Objective Function

The model was originally formulated based on MIP, but it has been reformed to MILP. More detailed explanation is located after this section. A nomenclature is listed in previous chapter, Appendix A.

The objective function to maximize the NPV is described below:

$$NPV = \sum_t \sum_{py} \frac{365 \cdot Profit(t)}{(1+dr)^{5\times(ordpt(t)-1)+ordpy(py)-1}} - \sum_t \frac{Capex(t)}{(1+dr)^{5\times(ordpt(t)-1)}} \tag{11}$$

B.3. Economic Constraints

The objective function that represents *NPV* is based on whole time periods based on variables such as *Profit* and *Capex*. The time unit of each variable affects on how the discount rate is applied on the objective equation. For the variable *Profit*, as it has a time unit of day, 365 is multiplied to convert the variable to has a-year-basis. As follows, discounted rate is also applied by a-year-basis. However for *Capex*, as it has a time unit of time period, which is five years, the discount rate is applied by five-year-basis. The discount rate used in this study is 15%. Variable definitions for *Capex*, *Opex*, *Sales*, and *Profit* are shown as follows:

$$Capex(t) = PCC(t) + PDC(t) + TCCr(t) + TCCp(t) + TDCr(t) + \mathrm{TDCp(t)} \quad (12)$$

$$Opex(t) = PFOC(t) + PVOC(t) + RC(t) + TOCr(t) + TOCp(t) + DC(t) \quad (13)$$

$$Sales(t) = PR(t) \quad (14)$$

$$Profit(t) = Sales(t) - Opex(t) \quad (15)$$

Hydrogen consumption for each cell in each time period is constrained not to exceed the hydrogen demand of the time period as follows:

$$\sum_{p} Consumption(i, p, t) \leq Demand(i, t) \quad (16)$$

Correlated to the transportation, raw material and hydrogen flows between two cells, *Fr(i,j,tr,r,t)* and *Fp(i,j,tr,p,t)*, are introduced with a binary variables *Frbin(i,j,tr,r,t)* and *Fpbin(i,j,tr,p,t)*. They work with upper and lower bound of the raw material flow and hydrogen flow, *Fmax(i,j,tr)* and *Fmin(i,j,tr)* respectively, between two cells as follows:

$$Fmin(i,j,tr) \cdot Frbin(i,j,tr,r,t) \leq Fr(i,j,tr,r,t) \leq Fmax(i,j,tr) \cdot Frbin(i,j,tr,r,t) \quad (17)$$

$$Fmin(i,j,tr) \cdot Fpbin(i,j,tr,p,t) \leq Fp(i,j,tr,p,t) \leq Fmax(i,j,tr) \cdot Fpbin(i,j,tr,p,t) \quad (18)$$

The sum of each flow from cell *i* to cell *j* is designed not to exceed the upper bound, *Fmax(i,j,tr)*. Any flow from one cell to itself is constrained not to be possible:

$$\sum_{r} Fr(i,j,tr,r,t) \leq Fmax(i,j,tr) \quad (19)$$

$$\sum_{p} Fp(i,j,tr,p,t) \leq Fmax(i,j,tr) \quad (20)$$

$$Fr(i,i,tr,r,t) = 0 \quad (21)$$

$$Fp(i,i,tr,p,t) = 0 \quad (22)$$

For each hydrogen product, a formulation of mass balance performed including the amount of hydrogen consumed, hydrogen transported from cell *i* to *j*, hydrogen produced, and hydrogen transported from cell *j* to *i*. The LHS represents the outflow and RHS represents the inflow into cell *i*:

$$Consumption(i,p,t) + \sum_{j}\sum_{tr} Fp(i,j,tr,p,t) = \sum_{tk} P(i,tk,p,t) + \sum_{i}\sum_{tr} Fp(j,i,tr,p,t) \quad (23)$$

B.4. Plant Capacity Constraints

Regarding to a capacity of a specific plant with a technology in cell *i* at time period *t*, Plant expansion and Plant shrinkage variables, *Plantexp(i,tk,pl,t)* and *Plantshrink(i,tk,pl,t)* are introduced with two binary variables, *AE(i,tk,pl,t)* and *AS(i,tk,pl,t)*. They work with upper and lower bound of the plant expansion and plant shrinkage, *Qmax(tk)* and *Qmin(tk)* respectively to limit the sudden dramatic increase of any plant:

$$Qmin(tk) \cdot AE(i,tk,pl,t) \leq Plantexp(i,tk,pl,t) \leq Qmax(tk) \cdot AE(i,tk,pl,t) \quad (24)$$

$$Qmin(tk) \cdot AS(i,tk,pl,t) \leq Plantshrink(i,tk,pl,t) \leq Qmax(tk) \cdot AS(i,tk,pl,t) \quad (25)$$

The equation for plant capacity of each time period includes 1) plant capacity of previous time period, 2) plant expansion of current time period, and 3) plant shrinkage of current time period. The capacity change comes from both expansion and shrinkage is applied at the same time period as such change can change production capacity right away:

$$Plantcap(i,tk,pl,t) = Plantcap(i,tk,pl,t-1) + Plantexp(i,tk,pl,t) - Plantshrink(i,tk,pl,t) \quad (26)$$

The all products produced from each technologies in a cell *i*, *Totalprod(i,tk,t)*, has an upper limit composed of plant capacity of each plant with each technology in cell *i* at particular time period and availability, *Availability(tk)*, of each technology:

$$Totalprod(i,tk,t) \leq \sum_{pl} Availability(tk) \cdot Plantcap(i,tk,pl,t) \quad (27)$$

The amount of a specific product produced by each cell, *P(i,tk,p,t)*, depends on both the total production described above and product ratio which specifies the ratio of each product produced as follow:

$$P(i,tk,p,t) = Totalprod(i,tk,t) \cdot Proratio(tk,p) \tag{28}$$

To prevent negative plant capacity, the plant shrinkage cannot exceed the current plant capacity of same plant:

$$Plantshrink(i,tk,pl,t) \leq Plantcap(i,tk,pl,t) \tag{29}$$

The plant capital costs depend on specs of reference plant capital costs, ratio between the degree of plant expansion and reference plant capacity with economies of scale, and costs of post process with coefficient and constant parts as below:

$$\begin{aligned} PCC(t) = \sum_{i}\sum_{pl}\sum_{tk} Refplantcost(tk) \cdot \left(\frac{Plantexp(i,tk,pl,t)}{Refplantcap(tk)}\right)^{psf} \\ + Postcap(tk) \cdot Plantexp(i,tk,pl,t) + Postconst(tk) \\ \cdot Liq(i,tk,pl,t) \end{aligned} \tag{30}$$

And the plant fixed operating cost depends on both specs of reference plant fixed operating costs ratio between the degree of plant capacity and reference plant capacity with economies of scale:

$$PFOC(t) = \sum_{i}\sum_{pl}\sum_{tk} ReffixedOM(tk) \cdot \left(\frac{Plantcap(i,tk,pl,t)}{Refplantcap(tk)}\right)^{psf} \tag{31}$$

As the equations (30) and (31) are non-linear, linearization process is performed through introducing discrete points Plexp(i,tk,pl,t,l) and Plcap(i,tk,pl,t,z), continuous variables λ(i,tk,pl,t,l) and λ(i,tk,pl,t,z), and binary variables δ(i,tk,pl,t,l) and δ(i,tk,pl,t,l) to transform

the process from MIP to MILP (Liu et al., 2007). First, plant capital cost equation is linearized as follow:

$$PCC(t) = \sum_{i}\sum_{pl}\sum_{tk} Refplantcost(tk) \cdot \left(\frac{Plantexp(i,tk,pl,t)}{Refplantcap(tk)}\right)^{psf} + Postcap(tk) \cdot Plantexp(i,tk,pl,t) + Postconst(tk) \cdot Liq(i,tk,pl,t) \tag{32}$$

$$Plantexp(i,tk,pl,t) = \sum_{l} Plexp(i,tk,pl,t,l) \cdot \lambda(i,tk,pl,t,l) \tag{33}$$

$$\sum_{l} \lambda(i,tk,pl,t,l) = 1 \tag{34}$$

$$\lambda(i,tk,pl,t,l) \geq 0 \tag{35}$$

$$\sum_{l=1}^{n-1} \delta(i,tk,pl,t,l) = 1 \tag{36}$$

$$\lambda(i,tk,pl,t,l_1) \leq \delta(i,tk,pl,t,l_1) \tag{37}$$

$$\lambda(i,tk,pl,t,l) \leq \delta(i,tk,pl,t,l-1) + \delta(i,tk,pl,t,l), \qquad l = 2,3,\dots,n-1 \tag{38}$$

$$\lambda(i,tk,pl,t,l) \leq \delta(i,tk,pl,t,l-1) \tag{39}$$

Next, plant fixed operating cost is linearized as below:

$$PFOC(t) = \sum_{i}\sum_{pl}\sum_{tk} RefixedOM(tk) \cdot \left(\frac{Plantcap(i,tk,pl,t)}{Refplantcap(tk)}\right)^{psf} \quad (40)$$

$$Plantcap(i,tk,pl,t) = \sum_{z} Plcap(i,tk,pl,t,z) \cdot \lambda(i,tk,pl,t,z) \quad (41)$$

$$\sum_{z} \lambda(i,tk,pl,t,z) = 1 \quad (42)$$

$$\lambda(i,tk,pl,t,z) \geq 0 \quad (43)$$

$$\sum_{z=1}^{n-1} \delta(i,tk,pl,t,z) = 1 \quad (44)$$

$$\lambda(i,tk,pl,t,z_1) \leq \delta(i,tk,pl,t,z_1) \quad (45)$$

$$\lambda(i,tk,pl,t,z) \leq \delta(i,tk,pl,t,z-1) + \delta(i,tk,pl,t,z), \qquad z = 2,3,\dots,n-1 \quad (46)$$

$$\lambda(i,tk,pl,t,z) \leq \delta(i,tk,pl,t,z-1) \quad (47)$$

Substitution of Eqs. (30) and (31) by Eqs. (32)-(47) makes the model as a whole linear, and makes the problem from MIP to MILP.

The plant variable operating cost, *PVOC(t)*, in this study is based on the amount of electricity generated to produce hydrogen, *RE(i,tk,e,t)*, and unit electricity cost, *Unitcost(e)* as follow:

$$PVOC(t) = \sum_{i}\sum_{tk}\sum_{e} RE(i,tk,e,t) \cdot Unitcost(e) \quad (48)$$

When a particular plant shrinks, plant decommissioning cost occurs depends on the degree of plant shrinkage. The plant decommissioning cost is assumed as $23,000/(kg hydrogen/day).

$$PDC(t) = \sum_{i} \sum_{tk} \sum_{pl} Plantshrink(i, tk, pl, t) \cdot DecmCT \quad (49)$$

In this model, revenue only comes from hydrogen consumption. And it is determined by the degree of hydrogen consumption and hydrogen selling cost. As it was described above, hydrogen price is $5/kg.

$$PR(t) = \sum_{i} \sum_{p} Consumption(i, p, t) \cdot cp(p) \quad (50)$$

B.5. Resource Constraints

Regarding to a raw material extraction in cell *i* at time period *t*, two binary variables, *B(i,r,t)* and *B(i,r,t)* are introduced. They work with upper and lower bound of the raw material extraction, *Nmax(i,r)* and *Nmin(I,r)* respectively to prevent resource over extraction for each cell:

$$Nmin(i, r) \cdot B(i, r, t) \leq R(i, r, t) \leq Nmax(i, r) \cdot B(i, r, t) \quad (51)$$

For the Horizon 2020 scenarios introduced in Chapter 4, equation (51-1) below used instead of equation (51), because extra degree of constraint is applied on raw material extraction:

$$Nmin(i, r) \cdot B(i, r, t) \leq R(i, r, t) \leq Nmax(i, r) \cdot B(i, r, t) \cdot (0.15^{ordtp(t-1)}) \quad (51\text{-}1)$$

For each raw material, a mass balance is formulated by the total hydrogen production, unit resource input, raw material transported from cell *i* to *j*, and raw material transported from cell *j* to *i*. In the equation, LHS represents the outflow and RHS represents the inflow into cell *i*:

$$\sum_{tk} Totalprod(i,tk,t) \cdot Rinp(r,tk) + \sum_{j}\sum_{tr} Fr(i,j,tr,r,t) = R(i,r,t) + \sum_{i}\sum_{tr} Fr(j,i,tr,r,t) \quad (52)$$

The cost for raw material purchase for each time period is calculated through the degree of raw material extraction and unit raw material cost:

$$RC(t) = \sum_{i}\sum_{r} R\,(i,r,t) \cdot cr(r) \quad (53)$$

For each electricity source, an energy balance is formulated by the total hydrogen production, unit energy input, and the amount of energy generated:

$$Totalprod(i,tk,t) \cdot Eneeded(tk) = \sum_{e} RE\,(i,tk,e,t) \quad (54)$$

The sum of electricity generated by each source cannot exceed the daily limit as follow:

$$\sum_{tk} RE\,(i,tk,e,t) \leq EPOT(i,e,t) \quad (55)$$

B.6. Waste Constraints

To measure the amount of waste vented from both raw material extraction and hydrogen production process, the amount of total hydrogen production from each technology and waste production ratio of each technology are used as follow:

$$PW(i,tk,w,t) = Totalprod(i,tk,t) \cdot wasteratio(tk) \tag{56}$$

GHG dumping cost depends on the total amount of pollutants vented from each cell at particular time period and the unit GHG dumping cost. One unit dumping price is applied for all types of pollutants:

$$DC(t) = \sum_{t}\sum_{i}\sum_{w} PW(i,tk,w,t) \cdot Dumpprice(t,w) \tag{57}$$

And such waste amount is classified by each pollutants throughout the cells, technologies, and whole time horizon to measure total GHG amount for the scenario as below:

$$TOTGHG(w) = \sum_{t}\sum_{i}\sum_{tk} PW(i,tk,w,t) \tag{58}$$

The eco-indicator methodology is applied based on the parameters introduced in Chapter 3 and equations taken from previous studies (Hugo and Pistikopoulos, 2005). A set of ten indicators introduced in previous chapter is mathematically represented as below:

$$\mathrm{h} \in \mathcal{E} \coloneqq \{hh_{ca}, hh_{ro}, hh_{ri}, hh_{cc}, hh_{ir}, hh_{od}, ec_{tx}, ec_{ae}, rd_{mn}, rd_{ff}\}$$

Table A.1. Mathematical representation of Eco-Indicators.

Indicators	**Mathematical representation**
Carcinogenic	hh_{ca}
Respiratory - Organic	hh_{ro}
Respiratory - Inorganic	hh_{ri}
Climage Change	hh_{cc}
Ionisation Radiation	hh_{ir}
Ozone Depletion	hh_{od}
Ecotoxic Emission	ec_{tx}
Acidification and Eutrophication	ec_{ae}
Depletion of Mineral	rd_{mn}
Depletion of Fossil fuel	rd_{ff}

Such indicators are categorized by each main damage categories as below:

$$\text{Human Health:} \quad \text{hh} \in \text{H} \ (\subset \mathcal{E}) \coloneqq \{hh_{ca}, hh_{ro}, hh_{ri}, hh_{cc}, hh_{ir}, hh_{od}\}$$

$$\text{Ecosystem Quality:} \quad \text{eq} \in \text{Q} \ (\subset \mathcal{E}) \coloneqq \{ec_{tx}, ec_{ae}\}$$

$$\text{Resource Depletion:} \quad \text{rd} \in \text{D} \ (\subset \mathcal{E}) \coloneqq \{rd_{mn}, rd_{ff}\}$$

such that,

$$\mathcal{E} = \text{H} \cup \text{Q} \cup \text{D}$$

$$\text{H} \cap \text{Q} = 0; \quad \text{H} \cap \text{D} = 0; \quad \text{Q} \cap \text{D} = 0;$$

The environmental impact of both pollutant emission and raw material extraction for every indicator from the whole process in particular cell and time period is described below:

$$EI(w,h) = \sum_{t} \sum_{i} \sum_{tk} v(w,h) \cdot PW(i,tk,w,t) \tag{59-1}$$

$$EI(r,h) = \sum_{t}\sum_{i} v(r,h) \cdot R(i,r,t) \tag{59-2}$$

The normalization of the environmental impact is based on hierarchist perspective. Normalization factor of each pollutant emission and raw material extraction for every indicator from the whole process in particular cell and time period is described below:

$$H(h) = \sum_{w} \eta(w,h) \cdot EI(w,h) + \sum_{r} \eta(r,h) \cdot EI(r,h) \tag{60}$$

A final score of environmental performance of each strategy could be achieved by applying weighing factors for the three categorized indicators. For simplicity, all indicators are formed a set of normalized categories as follow:

$$n \in N = \{n_{hh}, n_{eq}, n_{rd}\} \tag{61}$$

From the previous chapter, the weighing factors for human health, ecosystem quality, and resource depletion categories are introduced as 0.4, 0.55, and 0.05 respectively.

$$Eco - Indicator\ 99 = \sum_{h}\sum_{n} \theta(n,h) \cdot H(h) \tag{62}$$

B.7. Transportation Constraints

The number of transportation units required for both raw material and product transportation among cells is described with material flow and unit transportation capacity as follows:

$$NTUr(i,j,tr,r,t) \geq \frac{Fr(i,j,tr,r,t)}{Transunit(tr)} \tag{63}$$

$$NTUp(i,j,tr,p,t) \geq \frac{Fp(i,j,tr,p,t)}{Transunit(tr)} \tag{64}$$

Any transportation from one cell to itself is constrained not to be possible as below:

$$NTUr(i,i,tr,r,t) = 0 \tag{65}$$

$$NTUp(i,i,tr,p,t) = 0 \tag{66}$$

Regarding to the expansion and shrinkage of transportation for both raw material and product in time period *t*, two binary variables are introduced. They work with upper and lower bound of the transportation expansion and shrinkage, *Omax* and *Omin* respectively to limit the sudden dramatic increase of the transportation unit in particular period as follows:

$$\begin{aligned} Omin \cdot Transexpbinr(tr,r,t) \leq NTUexpr(tr,r,t) \\ \leq Omax \cdot Transexpbinr(tr,r,t) \end{aligned} \tag{67}$$

$$\begin{aligned} Omin \cdot Transshrinkbinr(tr,r,t) \leq NTUshrinkr(tr,r,t) \\ \leq Omax \cdot Transshrinkbinr(tr,r,t) \end{aligned} \tag{68}$$

$$\begin{aligned} Omin \cdot Transexpbinp(tr,p,t) \leq NTUexpp(tr,p,t) \\ \leq Omax \cdot Transexpbinp(tr,p,t) \end{aligned} \tag{69}$$

$$Omin \cdot Transshrinkbinp(tr,p,t) \leq NTUshrinkp(tr,p,t) \leq Omax \cdot Transshrinkbinp(tr,p,t) \quad (70)$$

The equation for transportation fleet size of each time period includes 1) the transportation fleet size of previous time period, 2) transportation fleet expansion of current time period, and 3) transportation fleet shrinkage of current time period. The fleet size change comes from both expansion and shrinkage is applied at the same time period as such change can change transportation strategy right away:

$$\sum_{i,j} NTUr(i,j,tr,r,t) = \sum_{i,j} NTUr(i,j,tr,r,t-1) + NTUexpr(tr,r,t) + NTUshrinkr(tr,r,t) \quad (71)$$

$$\sum_{i,j} NTUp(i,j,tr,p,t) = \sum_{i,j} NTUp(i,j,tr,p,t-1) + NTUexpp(tr,p,t) + NTUshrinkp(tr,p,t) \quad (72)$$

To prevent negative transportation fleet size, the transportation shrinkage cannot exceed the current transportation fleet size of whole geographical area as follows:

$$NTUshrinkr(tr,r,t) \leq \sum_{i,j} NTUr(i,j,tr,r,t) \quad (73)$$

$$NTUshrinkp(tr,p,t) \leq \sum_{i,j} NTUp(i,j,tr,p,t) \tag{74}$$

The total transportation capital costs for both raw material and product depend on the degree of transportation fleet size expansion and the cost for each transportation unit as below:

$$TCCr(t) = \sum_{tr}\sum_{r} NTUexpr(tr,r,t) \cdot tucr(tr,r) \tag{75}$$

$$TCCp(t) = \sum_{tr}\sum_{p} NTUexpp(tr,p,t) \cdot tucp(tr,p) \tag{76}$$

The total transportation operating costs for both raw material and product depend on the parameters of each transportation types, their numbers in particular time period, distance between cells, transportation speed, fuel economy, load/unload hours, driver wages and fuel price as below:

$$TOCr(t) = \sum_{i,j}\sum_{tr}\sum_{r} NTUr(i,j,tr,r,t) \cdot \left[\left\{\frac{Dist(i,j)}{Speed(tr)} + LUH\right\} \cdot Wage + \frac{Dist(i,j)}{Fuel(tr)} \cdot Fuelprice(tr)\right] \tag{77}$$

$$TOCp(t) = \sum_{i,j}\sum_{tr}\sum_{p} NTUp(i,j,tr,p,t) \cdot \left[\left\{\frac{Dist(i,j)}{Speed(tr)} + LUH\right\} \cdot Wage + \frac{Dist(i,j)}{Fuel(tr)} \cdot Fuelprice(tr)\right] \tag{78}$$

When a particular transportation unit shrinks. the total transportation decommissioning cost occurs depends on the degree of the transportation fleet size shrinkage. The transportation decommissioning cost is assumed as $23,000/unit:

$$TDCr(t) = \sum_{tr} \sum_{r} NTUshrinkr(tr, r, t) \cdot tudcr(tr, r) \tag{79}$$

$$TDCp(t) = \sum_{tr} \sum_{p} NTUshrinkp(tr, p, t) \cdot tudcp(tr, p) \tag{80}$$

B.8. Multi-Objective Optimization

Two objective functions are considered in the formulation, 1) NPV and 2) Environmental performance. The problem statement is the maximization of NPV and minimization of Eco-Indicator 99 score simultaneously as summarized below:

$$\underset{x,y}{Minimize\ U} \begin{Bmatrix} f_1(x,y) = -Net\ Present\ Value \\ f_2(x,y) = Eco\ Indicator\ 99 \end{Bmatrix}$$

$$h(x,y) = 0\ and\ g(x,y) \leq 0 \begin{Bmatrix} Economic\ constraint \\ Plant\ capacity\ constraint \\ Resource\ constraint \\ Waste\ constraint \\ Transportation\ constraint \end{Bmatrix} \tag{81}$$

Where U is the utility function and x,y represent the continuous variables, discrete variables respectively.

APPENDIX C

Optimal Hydrogen Production Strategies for Discounted Electricity Price Scenarios at Multiple Time Periods

Table C.1. Comparison of optimal hydrogen production strategies for discounted electricity price scenarios at second time period

Time period 2		Hydrogen production (1000 kg)		
Cell	**Technology**	**0% Discount**	**15% Discount**	**30% Discount**
i1	APE	0	29.9	661.3
i2	SMR	1068.2	1038.3	406.9
i3	SMR	5798.6	5798.6	5798.6
i4	SMR	868.8	868.8	868.8
i5	SMR	587.1	587.1	587.1
i6	SMR	6984.9	5327.8	5327.8
i7	SMR	4847.8	6504.9	2637.6
i8	APE	0	0	2210.2
i9	SMR	1139.0	450.9	450.9
i10	APE	0	688.1	688.1
i11	APE	139.9	139.9	1797.0
Overall	SMR	21294.3	20576.4	16077.7
	APE	139.9	857.8	5356.5
Ratio	SMR/APE	152.2	24.0	3.0

Table C.2. Comparison of optimal hydrogen production strategies for discounted electricity price scenarios at third time period

Time period 3		Hydrogen production (1000 kg)		
Cell	**Technology**	**0% Discount**	**15% Discount**	**30% Discount**
i1	APE	0	800.3	3082.1
i2	SMR	2657.7	1038.3	1829.2
i3	SMR	30683.6	32303.0	28430.1
i4	SMR	4030.6	4030.6	4030.6
i5	SMR	2692.9	2692.9	2692.9
i6	SMR	45050.4	45050.4	41063.7
i7	SMR	13015.1	13015.1	13015.1
i8	SMR	0	0	2329.6
i9	SMR	5372.9	4580.8	2095.1
i10	APE	0	792.1	3277.7
i11	APE	144.7	370.6	2027.7
Overall	SMR	103503.1	102711.1	93156.7
	APE	144.7	1962.9	10717.1
Ratio	SMR/APE	715.2	52.3	8.7

Table C.3. Comparison of optimal hydrogen production strategies for discounted electricity price scenarios at fourth time period

Time period 4		Hydrogen production (1000 kg)		
Cell	**Technology**	**0% Discount**	**15% Discount**	**30% Discount**
i1	APE	0	1094.8	3285.9
i2	SMR	2821.0	6135.2	2821.0
i3	SMR	68917.3	49060.3	60660.0
i4	SMR	6432.7	6432.7	6432.7
i5	SMR	4245.5	4245.5	3417.0
i6	SMR	59856.0	61513.1	46599.2
i7	SMR	22007.6	22007.6	22007.6
i8	SMR	46.9	46.9	5846.8
i9	SMR	8312.6	7484.1	3341.3
i10	APE	353.4	1182.0	5324.7
i11	APE	144.7	14230.1	13401.5
Overall	SMR	172592.6	156878.5	145278.8
	APE	545.1	16553.8	27858.9
Ratio	SMR/APE	316.7	9.5	5.2

Table C.4. Comparison of optimal hydrogen production strategies for discounted electricity price scenarios at fifth time period

Time period 5		Hydrogen production (1000 kg)		
Cell	**Technology**	**0% Discount**	**15% Discount**	**30% Discount**
i1	APE	106.9	29.9	29.9
i2	SMR	3321.1	5806.7	3321.1
i3	SMR	90327.9	62985.7	66900.5
i4	SMR	7861.8	7861.8	6432.7
i5	SMR	5118.5	5118.5	5118.5
i6	SMR	73545.8	61946.1	61946.1
i7	SMR	28488.3	47545.0	33459.6
i8	SMR	46.9	232.6	15975.0
i9	SMR	9868.8	7383.1	4897.5
i10	APE	661.5	3253.9	5739.6
i11	APE	993.6	17815.8	13673.1
Overall	SMR	218532.1	198646.9	182075.9
	APE	1809.0	21332.2	35417.5
Ratio	SMR/APE	120.8	9.3	5.1

Table C.5. Comparison of optimal hydrogen production strategies for discounted electricity price scenarios at sixth time period

Time period 6		Hydrogen production (1000 kg)		
Cell	**Technology**	**0% Discount**	**15% Discount**	**30% Discount**
i1	APE	106.9	1404.5	6735.3
i2	SMR	3528.9	6014.5	3528.9
i3	SMR	81391.8	77918.2	74763.4
i4	SMR	8711.2	8711.2	8711.2
i5	SMR	5582.7	5582.7	5118.5
i6	SMR	73253.0	66624.6	75619.6
i7	SMR	70400.8	50615.1	35952.4
i8	SMR	0	9592.0	15975.0
i9	SMR	11100.1	8507.7	6022.1
i10	APE	661.5	3253.9	5739.6
i11	APE	993.6	17815.8	15664.8
Overall	SMR	253968.5	223974.0	209716.0
	APE	1762.0	32066.2	44114.6
Ratio	SMR/APE	144.1	7.0	4.8